

**INTERNATIONAL COUNCIL OF  
SCIENTIFIC UNIONS**

**WORLD METEOROLOGICAL  
ORGANIZATION**

**WORLD CLIMATE RESEARCH PROGRAMME**

**INTERNATIONAL SATELLITE CLOUD CLIMATOLOGY PROJECT  
(ISCCP)**

**DOCUMENTATION OF NEW CLOUD DATASETS**

**January 1996**

**INTERNATIONAL SATELLITE CLOUD CLIMATOLOGY PROJECT  
(ISCCP)**

**DOCUMENTATION OF NEW CLOUD DATASETS**

**Prepared by**

**William B. Rossow**

**NASA Goddard Space Flight Center  
Institute for Space Studies**

**and**

**Alison W. Walker  
Diane E. Beuschel  
Miriam D. Roiter**

**Science Systems and Application Inc. at  
NASA Goddard Institute for Space Studies**

**January 1996**

# TABLE OF CONTENTS

Page No.

1.	INTRODUCTION .....	1
1.1.	PROJECT OVERVIEW .....	1
1.2.	SUMMARY OF CHANGES .....	2
1.3.	DATA PRODUCTS .....	3
1.4.	CONTACTS FOR ASSISTANCE AND DATA ORDERS .....	5
2.	DATA USER'S GUIDE .....	7
2.1.	D2 DATA (MONTHLY, 280 KM EQUAL-AREA GRID) .....	7
2.1.1.	ARCHIVE TAPE LAYOUT .....	7
2.1.2.	HEADER FILE CONTENTS .....	7
2.1.3.	DATA FILE CONTENTS .....	10
2.2.	D1 DATA (3-HOURLY, 280 KM EQUAL-AREA GRID) .....	16
2.2.1.	ARCHIVE TAPE LAYOUT .....	16
2.2.2.	HEADER FILE CONTENTS .....	16
2.2.3.	DATA FILE CONTENTS .....	19
2.3.	DX DATA (3-HOURLY, 30 KM SAMPLED IMAGE PIXELS) .....	27
2.3.1.	ARCHIVE TAPE LAYOUT .....	27
2.3.2.	HEADER FILE CONTENTS .....	27
2.3.3.	DATA FILE CONTENTS .....	27
2.3.4.	READ SOFTWARE .....	32
2.4.	CONVERSION TABLES FOR PHYSICAL VALUES .....	33
2.5.	CODE DEFINITION TABLES .....	34

3.	DATA PRODUCT DESCRIPTION .....	43
3.1.	GRIDDED PRODUCTS ANALYSIS (STAGE D1 AND D2) .....	43
3.1.1.	MAP GRID DEFINITIONS .....	43
3.1.2.	VARIABLE DEFINITIONS .....	45
3.1.3.	CLOUD TYPE DEFINITIONS .....	47
3.1.4.	SPATIAL AVERAGING .....	49
3.1.5.	MERGING RESULTS FROM SEVERAL SATELLITES .....	50
3.1.6.	TIME AVERAGING .....	52
3.1.7.	ADJUSTMENTS .....	52
3.2.	PIXEL LEVEL ANALYSIS (STAGE DX) .....	55
3.2.1.	OVERVIEW .....	55
3.2.2.	MAP PROJECTIONS .....	56
3.2.3.	VARIABLE DEFINITIONS .....	58
3.2.4.	CLOUD DETECTION .....	60
3.2.4.1.	FIRST CLEAR SKY RADIANCES .....	60
3.2.4.2.	FIRST CLOUD DETECTION THRESHOLDS .....	69
3.2.4.3.	FINAL CLEAR SKY RADIANCES .....	69
3.2.4.4.	FINAL THRESHOLDS .....	72
3.2.5.	RADIATIVE TRANSFER MODEL ANALYSIS .....	73
3.2.5.1.	RADIANCE MODEL DESCRIPTIONS .....	75
3.2.5.2.	CLEAR RETRIEVALS .....	83
3.2.5.3.	CLOUD RETRIEVALS .....	84
4.	ISCCP PROJECT INFORMATION .....	88
4.1.	DATA PROCESSING STRATEGY .....	88
4.2.	VALIDATION STRATEGY .....	89
4.3.	ISCCP WORKING GROUP ON DATA MANAGEMENT .....	90
4.4.	SUMMARY OF PROJECT PHASES .....	92
5.	REFERENCES .....	93
5.1.	GENERAL .....	93
5.2.	PROJECT DOCUMENTS .....	97

6.	APPENDICES .....	98
6.1.	TOVS ATMOSPHERE GRIDDED DATA PRODUCT (TV) .....	98
6.1.1.	OVERVIEW .....	98
6.1.2.	ARCHIVE TAPE LAYOUT .....	99
6.1.3.	HEADER FILE CONTENTS .....	99
6.1.4.	DATA FILE CONTENTS .....	101
6.1.5.	VARIABLE DEFINITIONS .....	103
6.1.6.	SPATIAL RESOLUTION AND COVERAGE .....	104
6.1.7.	VERTICAL PROFILES .....	106
6.1.8.	TIME AVERAGING .....	107
6.2.	ICE/SNOW DATA PRODUCT (IS) .....	108
6.2.1.	OVERVIEW .....	108
6.2.2.	ARCHIVE TAPE LAYOUT .....	109
6.2.3.	HEADER FILE CONTENTS .....	109
6.2.4.	DATA FILE CONTENTS .....	111
6.2.5.	MAP GRID DEFINITIONS .....	112
6.2.6.	VARIABLE DEFINITIONS .....	113
6.2.7.	TIME RESOLUTION AND COVERAGE .....	113
6.2.8.	MERGING ICE AND SNOW DATASETS .....	113

## LIST OF TABLES

Page No.

Table 2.1.1. D2 Archive Tape Layout. . . . .	7
Table 2.1.2. Table of Contents Layout. . . . .	8
Table 2.1.3. Ancillary Data Table Layout. . . . .	9
Table 2.1.4. D2 Data Record Prefix Layout. . . . .	11
Table 2.1.5. D2 Data Map Grid Cell Layout. . . . .	11
Table 2.2.1. D1 Archive Tape Layout . . . . .	16
Table 2.2.2. Table of Contents Layout. . . . .	17
Table 2.2.3. Ancillary Data Table Layout. . . . .	18
Table 2.2.4. D1 Data Record Prefix Layout. . . . .	20
Table 2.2.5. D1 Data Map Grid Cell Layout. . . . .	20
Table 2.3.1. DX Archive Tape Layout. . . . .	27
Table 2.3.2. Table of Contents Layout. . . . .	27
Table 2.3.3. DX Data Header Record Layout. . . . .	28
Table 2.3.4. DX Data Record Layout. . . . .	29
Table 2.3.5. DX Data Section Layouts. . . . .	30
Table 2.5.1. Satellite Identification (ID) Codes and ID Names. . . . .	34
Table 2.5.2. Satellite Position Codes. . . . .	35
Table 2.5.3. Vegetation Type Codes . . . . .	35
Table 2.5.4. Variable Abbreviations and Physical Units. . . . .	36
Table 2.5.5. Cloud Detection Threshold Codes and Threshold Categories. . . . .	37
Table 2.5.6. Land/Water/Coast Codes . . . . .	38
Table 2.5.7. Cloud Types . . . . .	38
Table 2.5.8. TOVS Atmospheric Data Origin Code. . . . .	40
Table 2.5.9. DX Satellite Type Codes and Geographic Sectors. . . . .	40
Table 2.5.10. Ice/Snow Codes. . . . .	40
Table 2.5.11. Equal-Area Map Grid. . . . .	41
Table 2.5.12. ISCCP Tape Designator . . . . .	42
Table 3.1.1. PC Categories Used to Define Cloud Types. . . . .	48
Table 3.1.2. TAU Categories Used to Define Cloud Types. . . . .	48
Table 3.2.1. Surface Types Used in Clear Sky Analysis. . . . .	61
Table 3.2.2. Radiance Difference Values Used in IR Clear Sky Composite Tests. . . . .	66
Table 3.2.3. First Cloud Detection Threshold Values. . . . .	69
Table 3.2.4. Final Cloud Detection Threshold Values. . . . .	73
Table 4.1.1. ISCCP Data Management Commitments. . . . .	89
Table 4.3.1. Working Group on Data Management. . . . .	91

Table 6.1.1. TV Archive Tape Layout. . . . .	99
Table 6.1.2. Table of Contents layout. . . . .	99
Table 6.1.3. Ancillary Data Table Layout. . . . .	100
Table 6.1.4. TV Data Record Prefix Layout. . . . .	102
Table 6.1.5. TV Data Map Grid Cell Layout. . . . .	102
Table 6.1.6. NOAA Code Values in TV Data Record. . . . .	104
Table 6.2.1. IS Archive Tape Layout. . . . .	109
Table 6.2.2. Table of Contents Layout. . . . .	110
Table 6.2.3. Ancillary Data Table Layout. . . . .	110
Table 6.2.4. IS Data Record Prefix Layout. . . . .	112
Table 6.2.5. Ice/Snow Cover Classification Codes. . . . .	113

# 1. INTRODUCTION

## 1.1. PROJECT OVERVIEW

The International Satellite Cloud Climatology Project (ISCCP), the first project of the World Climate Research Program (WCRP), was established in 1982 (WMO-35 1982, Schiffer and Rossow 1983):

- (i) To produce a global, reduced resolution, calibrated and normalized radiance dataset containing basic information on the properties of the atmosphere from which cloud parameters can be derived.
- (ii) To stimulate and coordinate basic research on techniques for inferring the physical properties of clouds from the condensed radiance dataset and to apply the resulting algorithms to derive and validate a global cloud climatology for improving the parameterization of clouds in climate models.
- (iii) To promote research using ISCCP data that contributes to improved understanding of the Earth's radiation budget and hydrological cycle.

Since 1983 an international group of institutions (Section 4.1) has collected and analyzed satellite radiance measurements from up to five geostationary and two polar orbiting satellites to infer the global distribution of cloud properties and their diurnal, seasonal and interannual variations. The primary focus of the first phase of the project (1983 - 1995) was the elucidation of the role of clouds in the radiation budget (top of the atmosphere and surface). In the second phase of the project (1995 onwards) the analysis also concerns improving understanding of clouds in the global hydrological cycle.

The ISCCP analysis combines satellite-measured radiances (Stage B3 data, Schiffer and Rossow 1985, Rossow *et al.* 1987) with the TOVS atmospheric temperature-humidity (TV data, Section 6.1) and ice/snow (IS data, Section 6.2) correlative datasets to obtain information about clouds and the surface. The analysis method first determines the presence or absence of clouds in each individual image pixel and retrieves the radiometric properties of the cloud for each cloudy pixel and of the surface for each clear pixel. The pixel analysis is performed separately for each satellite radiance dataset and the results reported in the Stage DX data product (Sections 2.3 and 3.2), which has a nominal resolution of 30 km and 3 hr. The Stage D1 product is produced by summarizing the pixel-level results every 3 hours on an equal-area map grid with 280 km resolution and merging the results from separate satellites with the TV and IS datasets to produce global coverage at each time (Sections 2.2 and 3.1). The Stage D2 data product is produced by averaging the Stage D1 data over each month, first in each of eight 3-hour time intervals individually and then over all eight time intervals (Sections 2.1 and 3.1).

The first version of ISCCP cloud products, the C-series, covered the period from July 1983 through June 1991. On-going research indicated that a number of improvements and refinements of the analysis and reported statistics were possible. These changes have been implemented for processing of data in the period beyond June 1991; all older data will be re-processed into the newer version. This document describes the new cloud climatology data products produced by ISCCP (D-series), along with revised versions of the two correlative datasets (TOVS Atmospheric and Ice/Snow data).



## 1.2. SUMMARY OF CHANGES

Highlights of differences between the C-series and D-series cloud products are as follows.

### Radiance Calibrations

- Revised VIS and IR calibrations to eliminate spurious changes between different reference polar orbiters (Brest *et al.* 1996)
- Revised normalizations of geostationary satellite calibrations to eliminate occasional short-term deviations (Brest *et al.* 1996)

### Cloud Detection

- Improved cirrus detection over land by lowering IR threshold from 6 K to 4 K
- Improved polar cloud detection over ice and snow surfaces by lowering VIS threshold from 0.12 to 0.06 and by using threshold test on 3.7  $\mu\text{m}$  radiances
- Improved detection of low clouds at high latitudes by changing to VIS reflectance threshold test

### Radiative Model

- Improved treatment of cold (top temperature < 260 K) clouds by using ice polycrystal scattering phase function to retrieve optical thickness and top temperature
- Improved retrieval of cloud optical thicknesses over ice and snow surfaces using 3.7  $\mu\text{m}$  radiances
- Improved retrieval of cloud top temperatures by including effects of IR scattering
- Improved retrieval of surface and cloud top temperatures by adopting new treatment of water vapor continuum absorption in IR

### Gridded Product Contents

- Better resolved variations of optically thicker clouds by adding 6th optical thickness category
- Added correct cloud water path parameter
- Reported actual average values of cloud top temperature, pressure, optical thickness and water path for each of nine cloud types defined by cloud top pressure and optical thickness in the 3-hourly dataset
- Reported separate cloud properties for liquid and ice forms of low and middle-level clouds
- Provided conversion of cloud top pressures to cloud top heights above mean sea level based on atmospheric temperature profile
- Added cloud amount frequency distribution to monthly dataset

### Increase Resolution

- Archived pixel-level cloud products with resolution of 30 km and 3 hr

### 1.3. DATA PRODUCTS

In the first phase of the project, only the gridded, 3-hourly (Stage C1) and monthly (Stage C2) datasets were made available (Rossow and Schiffer 1991, Rossow et al. 1991). These datasets cover the period from July 1983 through June 1991. In the second phase of the project, new versions of these two gridded products are being made available, called Stage D1 (3-hourly) and Stage D2 (monthly), as well as a "pixel-level" product (Stage DX). These products will cover the time period from July 1983 through June 1991 and beyond.

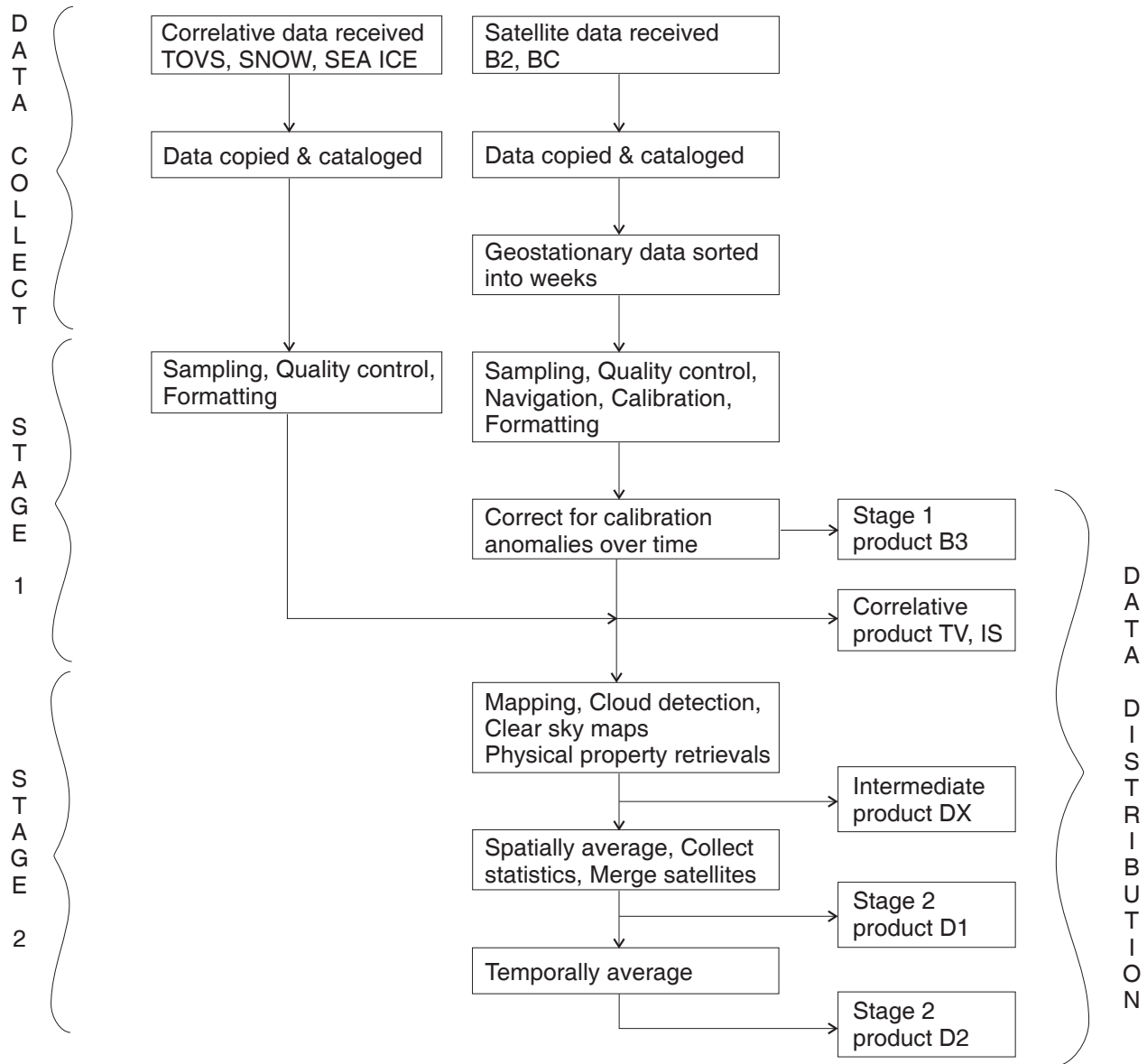


**Figure 1.1.** Schematic of ISCCP data processing and data products.

**Reduced Resolution Radiance Data (B3)**

Resolution: 4-7 km pixel at 30 km interval, 3 hr, individual satellites  
Volume: 1.1 Gbyte per data month for global coverage  
Contents: Radiances with calibration and navigation appended; uniform format for all satellites

**Calibration Table Dataset (BT)**

Resolution: 3 hr, individual satellites  
Volume: 0.9 Gbyte per data year  
Contents: Updated calibration tables for B3 dataset

**Pixel-Level Cloud Product (CX -- not available publically)**

Resolution: 30 km mapped pixels, 3 hr, individual satellites  
Volume: 3.4 Gbyte per data month for global coverage  
Contents: Calibrated radiances and viewing geometry, cloud detection results, cloud and surface properties from radiative analysis

**Pixel-Level Cloud Product - Revised Analysis (DX)**

Resolution: 30 km mapped pixels, 3 hr, individual satellites  
Volume: 5 Gbyte per data month for global coverage  
Contents: Calibrated radiances and viewing geometry, cloud detection results, cloud and surface properties from radiative analysis

**Gridded Cloud Product (C1)**

Resolution: 280 km equal-area grid, 3 hr, global  
Volume: 216 Mbyte per data month  
Contents: Spatial averages of CX quantities and statistical summaries; satellites are merged into global grid; atmosphere and surface properties from TOVS appended

**Gridded Cloud Product - Revised Analysis (D1)**

Resolution: 280 km equal-area grid, 3 hr, global  
Volume: 320 Mbyte per data month  
Contents: Spatial averages of DX quantities and statistical summaries, including properties of cloud types; satellites are merged into global grid; atmosphere and surface properties from TOVS appended

**Climatological Summary Product (C2)**

Resolution: 280 km equal-area grid, monthly, global  
Volume: 4 Mbyte per data month  
Contents: Monthly average C1 quantities including mean diurnal cycle; distribution and properties of total cloudiness and cloud types

**Climatological Summary Product (D2)**

Resolution: 280 km equal-area grid, monthly, global  
Volume: 7.5 Mbyte per data month  
Contents: Monthly average D1 quantities including mean diurnal cycle; distribution and properties of total cloudiness and cloud types

#### 1.4. CONTACTS FOR ASSISTANCE AND DATA ORDERS

All of the ISCCP datasets are **produced** by the

ISCCP Global Processing Center  
NASA Goddard Space Flight Center  
Institute for Space Studies  
2880 Broadway  
New York, NY 10025  
USA

For **technical** questions concerning data formats and software, contact

Alison W. Walker	Phone: 212-678-5542
Science Systems and Application Inc. at	FAX: 212-678-5552
NASA Goddard Institute for Space Studies	e-mail: <a href="mailto:alison@giss.nasa.gov">alison@giss.nasa.gov</a>
2880 Broadway	
New York, NY 10025	

For **scientific** questions about the cloud data products, contact

Dr. William B. Rossow	Phone: 212-678-5567
NASA Goddard Institute for Space Studies	FAX: 212-678-5662
2880 Broadway	e-mail: <a href="mailto:clwbr@giss.nasa.gov">clwbr@giss.nasa.gov</a>
New York, NY 10025	

General **questions and comments** can be e-mailed to

**[isccp@giss.nasa.gov](mailto:isccp@giss.nasa.gov)**

The **ISCCP Home Page** provides more information about the ISCCP organization and data products, sample data and browse images, software, documentation and errata, radiance calibrations, current project status, and data availability. The World Wide Web URL is:

**<http://isccp.giss.nasa.gov>**

All ISCCP data products (except Stage DX data) are **available from**

ISCCP Central Archives  
NOAA/NESDIS/NCDC  
Climate Services Division/  
Satellite Services Branch  
FOB3, Room G233  
Suitland, MD 20233

Phone: 704-271-4800 (option #5)  
FAX: 704-271-4876  
e-mail: [satorder@ncdc.noaa.gov](mailto:satorder@ncdc.noaa.gov)

All ISCCP data products (including Stage DX data) are also **available from** the EOS Distributed Active Archive Center at

User and Data Services  
Langley DAAC  
Mail Stop 157B  
NASA Langley Research Center  
Hampton, VA 23681-0001

Phone: 804-864-8656  
FAX: 804-864-9807  
e-mail: [userserv@eosdis.larc.nasa.gov](mailto:userserv@eosdis.larc.nasa.gov)  
telnet: [eosdis.larc.nasa.gov](telnet://eosdis.larc.nasa.gov)  
(logon ims, password larcims)

## 2. DATA USER'S GUIDE

### 2.1. D2 DATA (MONTHLY, 280 KM EQUAL-AREA GRID)

#### 2.1.1. ARCHIVE TAPE LAYOUT

Each D2 archive tape has 5 header files, followed by a variable number of data files depending on how many months are archived (usually one year per tape). Data are arranged chronologically. Nine files are written for each month, representing the hour-monthly mean for each 3-hour time interval (from UTC 00 to UTC 21) followed by the overall monthly mean. Thus for one year, there are  $12 \times 9 = 108$  data files on the tape.

**Table 2.1.1. D2 Archive Tape Layout.**

FILE	CONTENTS	FORMAT	RECORD LENGTH (BYTES)
1	README file	ASCII	80
2	Table of Contents	ASCII	80
3	Read Software	ASCII	80
4	Ancillary Data Table	ASCII	80
5	Adjustment Coefficients	ASCII	80
6-end	D2 Cloud Data	Binary	13000

*Note: The GPC produces archive tapes using IBM standard label format which means that there are label records written before and after each file on the tape. On IBM systems, these labels provide information to the operating system about the name and format of the file and will appear transparent to the user. On non-IBM systems these label records will appear as extra short files surrounding each file listed above and should be skipped by the user. The presence or absence of these files depends on which archive supplies tape copies to the user, as they may either provide an exact copy (labels present) or a modified copy (labels absent).*

#### 2.1.2. HEADER FILE CONTENTS

**File 1** is the **README** file that contains ASCII text providing descriptive information about the tape format and contents, similar to what is written in this section. The first line of text (80 bytes) gives the ISCCP tape designator code that identifies the contents and version (Table 2.5.12).

**File 2** is the **Table of Contents** file that lists the date and spatial coverage of each data file on the tape in ASCII columns defined in Table 2.1.2. See Table 2.5.1 for Satellite ID code definitions and Table 2.5.2 for Satellite position definitions.

**Table 2.1.2. Table of Contents Layout.**

COLUMN	DESCRIPTION
1	File number
2	Year (83 - 99)
3	Month (1 - 12)
4	Time UTC (00, 03, 06...21)
5	Fraction (%) of good data
6	Fraction (%) of empty map grid cells
7	Satellite ID for Western Pacific/Australia position
8	Satellite ID for Europe/Africa position
9	Satellite ID for Eastern Pacific position
10	Satellite ID for North/South American position
11	Satellite ID for Indian Ocean/Asia position
12	Satellite ID for Afternoon polar orbit
13	Satellite ID for Morning polar orbit

**File 3** contains a sample **FORTTRAN program** and subroutines for reading, decoding and using D2 data as follows:

Program SAMPLE:	Example of how to use these subroutines
Subroutine D2OPEN:	Open a D2 file and initialize
Subroutine D2READ:	Unpack D2 data for one latitude band into integer count values
Subroutine D2REC:	Used by D2READ to unpack a logical record
Subroutine D2PHYS:	Convert integer counts in latitude band to physical values
Subroutine RDANC:	Read ancillary data file
Subroutine PRINTI:	Print parameter count values for one grid box
Subroutine PRINTR:	Print physical values for one grid box
Subroutine CENTER:	Calculate center longitude/latitude of map grid cell
Subroutine CLDHGT:	Calculate cloud top height in meters
Subroutine EQ2SQ:	Convert equal-area map to equal-angle map
BLOCK DATA:	Conversion tables and equal-area grid information

The programs should work as written on most UNIX systems. For DOS, MacIntosh or VAX systems, the OPEN statement in subroutine D2OPEN may need to be modified.

**File 4** contains the **Ancillary Data Table** that lists characteristics of each map grid cell (see Section 3.1.1) in ASCII columns defined in Table 2.1.3.

**Table 2.1.3. Ancillary Data Table Layout.**

COLUMN	DESCRIPTION
1	ISCCP map grid cell number (1 - 6596)
2	Equal-area latitude index (south-to-north = 1 - 72)
3	Equal-area longitude index (west-to-east, variable up to 144)
4	Western-most equal-angle longitude index (1 - 144)
5	Eastern-most equal-angle longitude index (1 - 144)
6	Map grid cell center latitude in degrees
7	Map grid cell center longitude in degrees
8	Map grid cell area (km <sup>2</sup> )
9	Land cover fraction (%)
10	Mean topographic altitude (m)
11	Vegetation type (see Table 2.5.3)

**File 5** contains the **Adjustment Coefficients** applied to the data for each month (see Section 3.1.7) listed as ASCII text.



### 2.1.3. DATA FILE CONTENTS

Each D2 data file (Figure 2.1) reports 130 variables for each of the 6596 map grid cells in the ISCCP Equal-Area map grid (see Section 3.1.1). Each variable is reported in a single byte representing a coded value from 0-255 (see Sections 2.4 and 3.1.2), so there are 130 bytes in each map grid cell. Each physical record is 13000 bytes in length, consisting of a 130 byte record prefix, followed by up to 99 map grid cells of 130 bytes each. All map grid cells and variables are present, even when data are missing. Missing data are indicated by code values of 255. Contents of the prefix are given in Table 2.1.4 and of each map grid cell in Table 2.1.5.

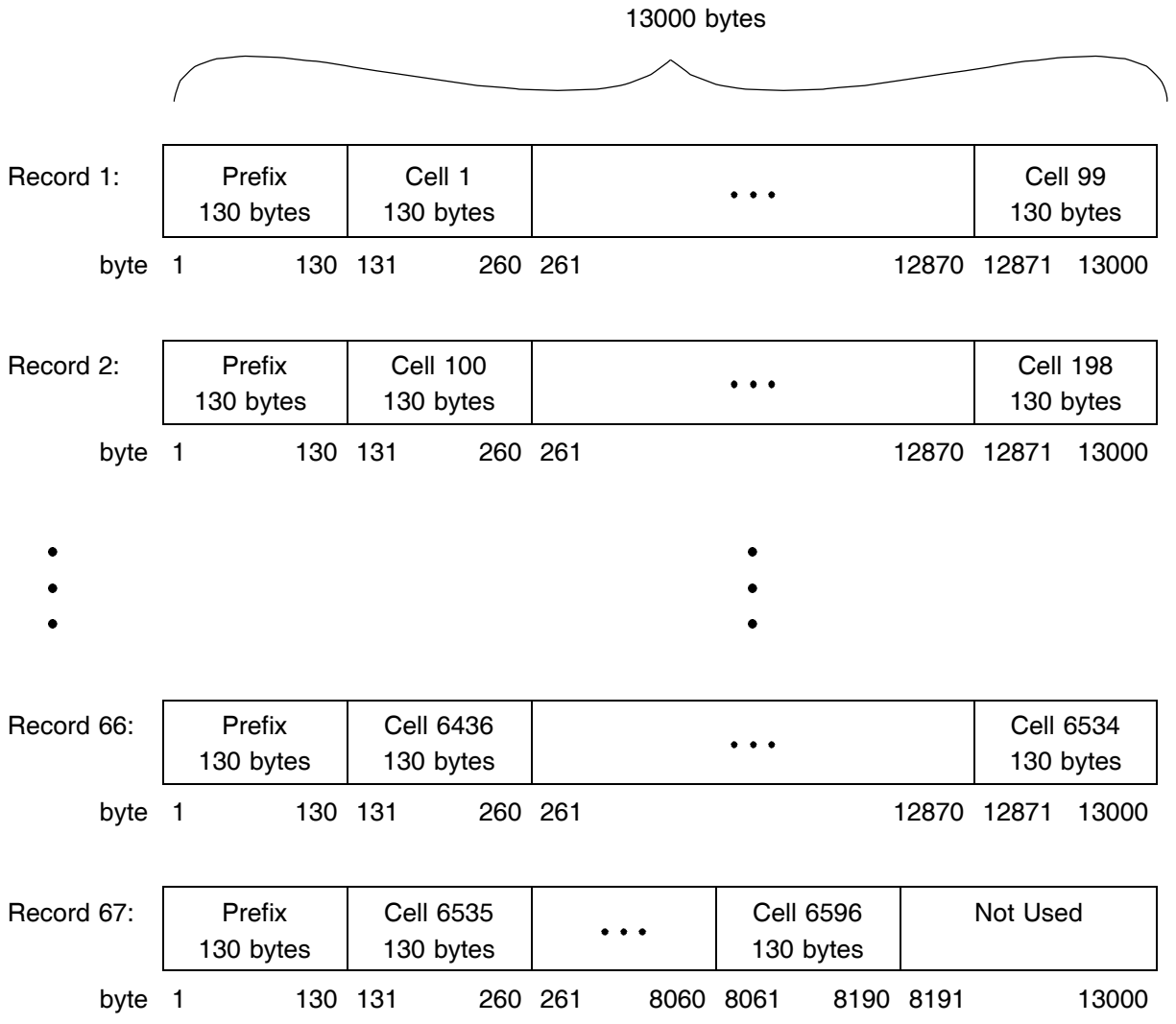


**Figure 2.1.** D2 Data File Layout.

**Table 2.1.4. D2 Data Record Prefix Layout.**

BYTE No.	DESCRIPTION
1	Record number in file (1 - 67)
2	File number on archive tape (5 - 112)
3	Year (83 - 99)
4	Month (1 - 12)
5	<Not used = 255>
6	Time UTC (00, 03, 06, ... 21, 255) where 255 = ALL TIMES
7	Beginning equal-area latitude index in record
8	Beginning equal-area longitude index in record
9	Ending equal-area latitude index in record
10	Ending equal-area longitude index in record
11 - 130	Filled with 255

**Table 2.1.5. D2 Data Map Grid Cell Layout.** (see Table 2.5.4 for definition of abbreviations and units, Table 2.5.5 for definitions of radiance threshold categories and Table 2.5.7 for cloud type definitions). *Note: Variables labeled with "d" are defined only for local daytime and are undefined at night (undefined = 255).*

BYTE No.	DESCRIPTION
MAP GRID CELL IDENTIFICATION	
1	Latitude index (equal-area and equal-angle)
2	Longitude index (equal-area)
3	Western-most longitude index (equal-angle)
4	Eastern-most longitude index (equal-angle)
5	Land/water/coast code (see Table 2.5.6)
6	Number of observations
7	Number of daytime observations
CLOUD AMOUNTS (CA)	
8	Mean cloud amount
9	Mean IR-marginal cloud amount
10	Frequency of mean cloud amount = 0-10%
11	Frequency of mean cloud amount = 10-20%
12	Frequency of mean cloud amount = 20-30%
13	Frequency of mean cloud amount = 30-40%
14	Frequency of mean cloud amount = 40-50%
15	Frequency of mean cloud amount = 50-60%
16	Frequency of mean cloud amount = 60-70%
17	Frequency of mean cloud amount = 70-80%
18	Frequency of mean cloud amount = 80-90%
19	Frequency of mean cloud amount = 90-100%

Continued.

**Table 2.1.5.** (continued).

BYTE No.	DESCRIPTION
MEAN CLOUD TOP PRESSURE (PC)	
20	Mean cloud top pressure
21	Standard deviation of spatial mean over time
22	Time mean of standard deviation over space
MEAN CLOUD TOP TEMPERATURE (TC)	
23	Cloud temperature
24	Standard deviation of spatial mean over time
25	Time mean of standard deviation over space
MEAN CLOUD OPTICAL THICKNESS (TAU)	
26	Mean cloud optical thickness
27	Standard deviation of spatial mean over time
28	Time mean of standard deviation over space
MEAN CLOUD WATER PATH (WP)	
29	Mean cloud water path
30	Standard deviation of spatial mean over time
31	Time mean of standard deviation over space
IR CLOUD TYPES (see Table 2.5.7)	
32	Mean CA for low-level clouds
33	Mean PC for low-level clouds
34	Mean TC for low-level clouds
35	Mean CA for middle-level clouds
36	Mean PC for middle-level clouds
37	Mean TC for middle-level clouds
38	Mean CA for high-level clouds
39	Mean PC for high-level clouds
40	Mean TC for high-level clouds

Continued.

**Table 2.1.5.** (continued).

BYTE No.	DESCRIPTION
VIS/IR/NIR LOW-LEVEL CLOUD TYPES (see Table 2.5.7)	
41d	Mean CA for cloud type 1 = Cumulus, liquid
42d	Mean PC for cloud type 1
43d	Mean TC for cloud type 1
44d	Mean TAU for cloud type 1
45d	Mean WP for cloud type 1
46d	Mean CA for cloud type 2 = Stratocumulus, liquid
47d	Mean PC for cloud type 2
48d	Mean TC for cloud type 2
49d	Mean TAU for cloud type 2
50d	Mean WP for cloud type 2
51d	Mean CA for cloud type 3 = Stratus, liquid
52d	Mean PC for cloud type 3
53d	Mean TC for cloud type 3
54d	Mean TAU for cloud type 3
55d	Mean WP for cloud type 3
56d	Mean CA for cloud type 4 = Cumulus, ice
57d	Mean PC for cloud type 4
58d	Mean TC for cloud type 4
59d	Mean TAU for cloud type 4
60d	Mean WP for cloud type 4
61d	Mean CA for cloud type 5 = Stratocumulus, ice
62d	Mean PC for cloud type 5
63d	Mean TC for cloud type 5
64d	Mean TAU for cloud type 5
65d	Mean WP for cloud type 5
66d	Mean CA for cloud type 6 = Stratus, ice
67d	Mean PC for cloud type 6
68d	Mean TC for cloud type 6
69d	Mean TAU for cloud type 6
70d	Mean WP for cloud type 6

Continued.

**Table 2.1.5.** (continued).

BYTE No.	DESCRIPTION
VIS/IR/NIR MIDDLE-LEVEL CLOUD TYPES (see Table 2.5.7)	
71d	Mean CA for cloud type 7 = Altocumulus, liquid
72d	Mean PC for cloud type 7
73d	Mean TC for cloud type 7
74d	Mean TAU for cloud type 7
75d	Mean WP for cloud type 7
76d	Mean CA for cloud type 8 = Altostratus, liquid
77d	Mean PC for cloud type 8
78d	Mean TC for cloud type 8
79d	Mean TAU for cloud type 8
80d	Mean WP for cloud type 8
81d	Mean CA for cloud type 9 = Nimbostratus, liquid
82d	Mean PC for cloud type 9
83d	Mean TC for cloud type 9
84d	Mean TAU for cloud type 9
85d	Mean WP for cloud type 9
86d	Mean CA for cloud type 10 = Altocumulus, ice
87d	Mean PC for cloud type 10
88d	Mean TC for cloud type 10
89d	Mean TAU for cloud type 10
90d	Mean WP for cloud type 10
91d	Mean CA for cloud type 11 = Altostratus, ice
92d	Mean PC for cloud type 11
93d	Mean TC for cloud type 11
94d	Mean TAU for cloud type 11
95d	Mean WP for cloud type 11
96d	Mean CA for cloud type 12 = Nimbostratus, ice
97d	Mean PC for cloud type 12
98d	Mean TC for cloud type 12
99d	Mean TAU for cloud type 12
100d	Mean WP for cloud type 12

Continued.

**Table 2.1.5.** (continued).

BYTE No.	DESCRIPTION
VIS/IR/NIR HIGH-LEVEL CLOUD TYPES (see Table 2.5.7)	
101d	Mean CA for cloud type 13 = Cirrus
102d	Mean PC for cloud type 13
103d	Mean TC for cloud type 13
104d	Mean TAU for cloud type 13
105d	Mean WP for cloud type 13
106d	Mean CA for cloud type 14 = Cirrostratus
107d	Mean PC for cloud type 14
108d	Mean TC for cloud type 14
109d	Mean TAU for cloud type 14
110d	Mean WP for cloud type 14
111d	Mean CA for cloud type 15 = Deep convective
112d	Mean PC for cloud type 15
113d	Mean TC for cloud type 15
114d	Mean TAU for cloud type 15
115d	Mean WP for cloud type 15
MEAN SURFACE SKIN TEMPERATURE (TS)	
116	Mean TS from clear sky composite
117	Time mean of standard deviation over space
MEAN SURFACE VISIBLE REFLECTANCE (RS)	
118d	Mean RS from clear sky composite
ICE/SNOW COVER	
119	Mean ice/snow cover
TOVS ATMOSPHERIC INFORMATION	
120	Mean Surface pressure (PS)
121	Mean Near-surface air temperature (TSA)
122	Mean Temperature at 740 mb (T)
123	Mean Temperature at 500 mb (T)
124	Mean Temperature at 375 mb (T)
125	Mean Tropopause pressure (PT)
126	Mean Tropopause temperature (TT)
127	Mean Stratosphere temperature at 50 mb (T)
128	Mean Precipitable water for 1000-680 mb (PW)
129	Mean Precipitable water for 680-310 mb (PW)
130	Mean Ozone column abundance (O3)

*Note:* In addition, cloud top heights in meters are calculated in the D2READ program provided.

## 2.2. D1 DATA (3-HOURLY, 280 KM EQUAL-AREA GRID)

### 2.2.1. ARCHIVE TAPE LAYOUT

Each D1 archive tape has 4 header files, followed by a variable number of data files depending on how many days are in the month. Each month of data is archived on two tapes chronologically as follows:

- Tape 1: Days 1 through 16
- Tape 2: Days 17 through the end of the month

Each file represents one time sample at 3 hr intervals (from UTC 00 to UTC 21 each day); actual samples are within  $\pm 1.5$  hours of the nominal time. Thus, there are  $16 \times 8 = 128$  files on the first tape for each month and from 96 to 120 files on the second tape for each month.

**Table 2.2.1. D1 Archive Tape Layout**

FILE	CONTENTS	FORMAT	RECORD LENGTH (BYTES)
1	README file	ASCII	80
2	Table of Contents	ASCII	80
3	Read Software	ASCII	80
4	Ancillary Data Table	ASCII	80
5-end	D1 Cloud Data	Binary	20200

*Note: The GPC produces archive tapes using IBM standard label format which means that there are label records written before and after each file on the tape. On IBM systems, these labels provide information to the operating system about the name and format of the file and will appear transparent to the user. On non-IBM systems these label records will appear as extra short files surrounding each file listed above and should be skipped by the user. The presence or absence of these files depends on which archive supplies tape copies to the user, as they may either provide an exact copy (labels present) or a modified copy (labels absent).*

### 2.2.2. HEADER FILE CONTENTS

**File 1** is the **README** file that contains ASCII text providing descriptive information about the tape format and contents, similar to what is written in this section. The first line of text (80 bytes) gives the ISCCP tape designator code that identifies the contents (Table 2.5.12).

**File 2** is the **Table of Contents** that lists the date and spatial coverage of each data file on the tape in ASCII columns defined in Table 2.2.2. See Table 2.5.1 for Satellite ID code definitions and Table 2.5.2 for Satellite position definitions.

**Table 2.2.2. Table of Contents Layout.**

COLUMN	DESCRIPTION
1	File number
2	Year (83 - 99)
3	Month (1 - 12)
4	Day (1 - 31)
5	Time UTC (00, 03, 06...21)
6	Fraction (%) of good data
7	Fraction (%) of empty map grid cells
8	Satellite ID for Western Pacific/Australia position
9	Satellite ID for Europe/Africa position
10	Satellite ID for Eastern Pacific position
11	Satellite ID for North/South American position
12	Satellite ID for Indian Ocean/Asia position
13	Satellite ID for Afternoon polar orbit
14	Satellite ID for Morning polar orbit

**File 3** contains a sample **FORTTRAN program** and subroutines for reading, decoding and using D1 data (see Section 2.2.4).

Program SAMPLE:	Example of how to use these subroutines
Subroutine D1OPEN:	Open a D1 file and initialize
Subroutine D1READ:	Unpack D1 data for one latitude band into integer count values
Subroutine D1REC:	Used by D1READ to unpack a logical record
Subroutine D1PHYS:	Convert integer counts in latitude band to physical values
Subroutine MIDPRS:	Calculate mid-layer pressures for map grid cell
Subroutine RDANC:	Read ancillary data file
Subroutine PRINTI:	Print count values for one map grid cell
Subroutine PRINTR:	Print physical values for one map grid cell
Subroutine CENTER:	Calculate center longitude/latitude of map grid cell
Subroutine TOTIR:	Calculate total IR radiance
Subroutine TOTVIS:	Calculate total VIS radiance
Subroutine CLDHGT:	Calculate cloud top height in meters
Subroutine EQ2SQ:	Convert equal-area map to equal-angle map
BLOCK DATA:	Conversion tables and equal-area grid information

The programs should work as written on most UNIX systems. For DOS, MacIntosh or VAX systems, the OPEN statement in subroutine D1OPEN may need to be modified.



**File 4** contains the **Ancillary Data Table** that lists characteristics of each map grid cell (see Section 3.1.1) in ASCII columns defined in Table 2.2.3.

**Table 2.2.3. Ancillary Data Table Layout.**

COLUMN	DESCRIPTION
1	ISCCP map grid cell number (1 - 6596)
2	Equal-area latitude index (south-to-north = 1 - 72)
3	Equal-area longitude index (west-to-east, variable up to 144)
4	Western-most equal-angle longitude index (1 - 144)
5	Eastern-most equal-angle longitude index (1 - 144)
6	Map grid cell center latitude in degrees
7	Map grid cell center longitude in degrees
8	Map grid cell area (km <sup>2</sup> )
9	Land cover fraction (%)
10	Mean topographic altitude (m)
11	Vegetation type (see Table 2.5.3)
12	Preferred Satellite Position Code (see Table 2.5.1)
13	Second Choice
14	Third Choice
15	Fourth Choice

### 2.2.3. DATA FILE CONTENTS

Each D1 data file (Figure 2.2) reports 202 variables for each of the 6596 map grid cells in the ISCCP Equal-Area map grid (see Section 3.1.1). Each variable is reported in a single byte representing a coded value from 0-255 (see Sections 2.4 and 3.1.2), so there are 202 bytes in each map grid cell. Each physical record is 20200 bytes in length, consisting of a 202 byte record prefix, followed by up to 99 map grid cells of 202 bytes each. All map grid cells and variables are present, even when data are missing. Missing data are indicated by code values of 255. Contents of the prefix are given in Table 2.2.4 and of each map grid cell in Table 2.2.5.

Each D1 data file represents the merging of analysis results from all available satellites within a 3-hour time period into the global map grid; however, in any one map grid cell, all values reported are from a single satellite. Each map grid cell location has a pre-defined hierarchy of satellite preference, given in the Ancillary Data Table (Header File 4).

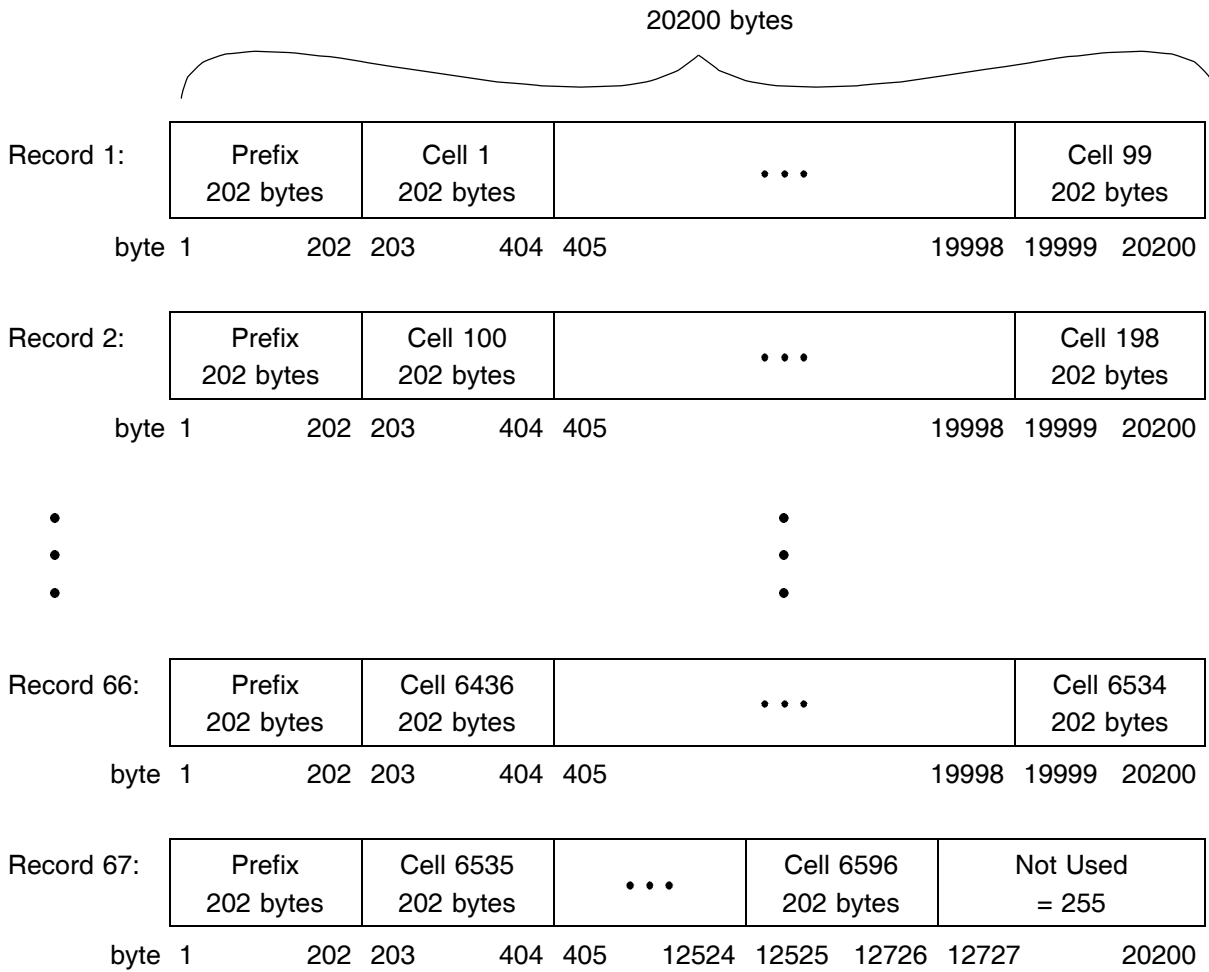


**Figure 2.2.** D1 Data File Layout.

**Table 2.2.4. D1 Data Record Prefix Layout.**

BYTE No.	DESCRIPTION
1	Record number in file (1 - 67)
2	File number on archive tape (5 - 132)
3	Year (83 - 99)
4	Month (1 - 12)
5	Day (1 - 31)
6	Time UTC (00, 03, 06....21)
7	Beginning equal-area latitude index in record
8	Beginning equal-area longitude index in record
9	Ending equal-area latitude index in record
10	Ending equal-area longitude index in record
11 - 202	Filled with 255

**Table 2.2.5. D1 Data Map Grid Cell Layout.** (see Table 2.5.4 for definitions of abbreviations and units, Table 2.5.5 for definitions of radiance threshold categories and Table 2.5.7 for cloud type definitions). *Notes: Variables labeled with "d" are defined only for local daytime and are undefined at night (undefined = 255). "VIS-adjusted" indicates that the pixel data include adjustments dependent on VIS data, whereas "unadjusted" means only IR data are used (see Section 3.1.7).*

BYTE No.	DESCRIPTION
MAP GRID CELL IDENTIFICATION	
1	Latitude index (equal-area and equal-angle)
2	Longitude index (equal-area)
3	Western-most longitude index (equal-angle)
4	Eastern-most longitude index (equal-angle)
5	Satellite ID code (see Table 2.5.1)
6	Day/night/land/water/coast code (see Table 2.5.6)
7	Ice/snow cover
8	MUE = cosine of satellite zenith angle * 100 (0-100)
9d	MU0 = cosine of solar zenith angle * 100 (0-100)
10d	PHI = relative azimuth angle (0-180 degrees)
PIXEL COUNTERS	
11	Total number of pixels
12	Number of cloudy pixels
13	Number of IR-cloudy pixels
14d	Number of IR-only-cloudy pixels
15	Number of NIR-cloudy pixels
16	Number of NIR-only-cloudy pixels
17	Number of IR-marginally-cloudy pixels
18d	Number of VIS/IR-marginally-cloudy pixels
19	Number of NIR-only-marginally-cloudy pixels

Continued.

**Table 2.2.5.** (continued).

BYTE No.	DESCRIPTION
<b>CLOUD DETECTION STATISTICS</b>	
20	Number of pixels with IR long-term statistics
21	Ratio number of IR-clear pixels < clear IR to number > clear IR
22d	Ratio number of VIS/IR-clear pixels > clear VIS to number < clear VIS
<b>CLOUD TOP PRESSURE (PC) DISTRIBUTION (UNADJUSTED)</b>	
23	Number of IR-cloudy pixels 10 ≤ PC ≤ 180 mb
24	Number of IR-cloudy pixels 180 < PC ≤ 310 mb
25	Number of IR-cloudy pixels 310 < PC ≤ 440 mb
26	Number of IR-cloudy pixels 440 < PC ≤ 560 mb
27	Number of IR-cloudy pixels 560 < PC ≤ 680 mb
28	Number of IR-cloudy pixels 680 < PC ≤ 800 mb
29	Number of IR-cloudy pixels 800 < PC ≤ 1000 mb
<b>CLOUD TOP PRESSURE-OPTICAL THICKNESS (TAU) DISTRIBUTION (VIS-ADJUSTED)</b>	
30d	Number of cloudy pixels 10 ≤ PC ≤ 180 mb, 0.02 ≤ TAU ≤ 1.27
31d	Number of cloudy pixels 10 ≤ PC ≤ 180 mb, 1.27 < TAU ≤ 3.55
32d	Number of cloudy pixels 10 ≤ PC ≤ 180 mb, 3.55 < TAU ≤ 9.38
33d	Number of cloudy pixels 10 ≤ PC ≤ 180 mb, 9.38 < TAU ≤ 22.63
34d	Number of cloudy pixels 10 ≤ PC ≤ 180 mb, 22.63 < TAU ≤ 60.36
35d	Number of cloudy pixels 10 ≤ PC ≤ 180 mb, 60.36 < TAU ≤ 378.65
36d	Number of cloudy pixels 180 < PC ≤ 310 mb, 0.02 ≤ TAU ≤ 1.27
37d	Number of cloudy pixels 180 < PC ≤ 310 mb, 1.27 < TAU ≤ 3.55
38d	Number of cloudy pixels 180 < PC ≤ 310 mb, 3.55 < TAU ≤ 9.38
39d	Number of cloudy pixels 180 < PC ≤ 310 mb, 9.38 < TAU ≤ 22.63
40d	Number of cloudy pixels 180 < PC ≤ 310 mb, 22.63 < TAU ≤ 60.36
41d	Number of cloudy pixels 180 < PC ≤ 310 mb, 60.36 < TAU ≤ 378.65
42d	Number of cloudy pixels 310 < PC ≤ 440 mb, 0.02 ≤ TAU ≤ 1.27
43d	Number of cloudy pixels 310 < PC ≤ 440 mb, 1.27 < TAU ≤ 3.55
44d	Number of cloudy pixels 310 < PC ≤ 440 mb, 3.55 < TAU ≤ 9.38
45d	Number of cloudy pixels 310 < PC ≤ 440 mb, 9.38 < TAU ≤ 22.63
46d	Number of cloudy pixels 310 < PC ≤ 440 mb, 22.63 < TAU ≤ 60.36
47d	Number of cloudy pixels 310 < PC ≤ 440 mb, 60.36 < TAU ≤ 378.65
48d	Number of cloudy pixels 440 < PC ≤ 560 mb, 0.02 ≤ TAU ≤ 1.27
49d	Number of cloudy pixels 440 < PC ≤ 560 mb, 1.27 < TAU ≤ 3.55
50d	Number of cloudy pixels 440 < PC ≤ 560 mb, 3.55 < TAU ≤ 9.38
51d	Number of cloudy pixels 440 < PC ≤ 560 mb, 9.38 < TAU ≤ 22.63
52d	Number of cloudy pixels 440 < PC ≤ 560 mb, 22.63 < TAU ≤ 60.36
53d	Number of cloudy pixels 440 < PC ≤ 560 mb, 60.36 < TAU ≤ 378.65

Continued.

**Table 2.2.5.** (continued).

BYTE No.	DESCRIPTION
54d	Number of cloudy pixels 560 < PC ≤ 680 mb, 0.02 ≤ TAU ≤ 1.27
55d	Number of cloudy pixels 560 < PC ≤ 680 mb, 1.27 < TAU ≤ 3.55
56d	Number of cloudy pixels 560 < PC ≤ 680 mb, 3.55 < TAU ≤ 9.38
57d	Number of cloudy pixels 560 < PC ≤ 680 mb, 9.38 < TAU ≤ 22.63
58d	Number of cloudy pixels 560 < PC ≤ 680 mb, 22.63 < TAU ≤ 60.36
59d	Number of cloudy pixels 560 < PC ≤ 680 mb, 60.36 < TAU ≤ 378.65
60d	Number of cloudy pixels 680 < PC ≤ 800 mb, 0.02 ≤ TAU ≤ 1.27
61d	Number of cloudy pixels 680 < PC ≤ 800 mb, 1.27 < TAU ≤ 3.55
62d	Number of cloudy pixels 680 < PC ≤ 800 mb, 3.55 < TAU ≤ 9.38
63d	Number of cloudy pixels 680 < PC ≤ 800 mb, 9.38 < TAU ≤ 22.63
64d	Number of cloudy pixels 680 < PC ≤ 800 mb, 22.63 < TAU ≤ 60.36
65d	Number of cloudy pixels 680 < PC ≤ 800 mb, 60.36 < TAU ≤ 378.65
66d	Number of cloudy pixels 800 < PC ≤ 1000 mb, 0.02 ≤ TAU ≤ 1.27
67d	Number of cloudy pixels 800 < PC ≤ 1000 mb, 1.27 < TAU ≤ 3.55
68d	Number of cloudy pixels 800 < PC ≤ 1000 mb, 3.55 < TAU ≤ 9.38
69d	Number of cloudy pixels 800 < PC ≤ 1000 mb, 9.38 < TAU ≤ 22.63
70d	Number of cloudy pixels 800 < PC ≤ 1000 mb, 22.63 < TAU ≤ 60.36
71d	Number of cloudy pixels 800 < PC ≤ 1000 mb, 60.36 < TAU ≤ 378.65
72d	Number of cloudy pixels for cloud type 4 = Cumulus, ice
73d	Number of cloudy pixels for cloud type 5 = Stratocumulus, ice
74d	Number of cloudy pixels for cloud type 6 = Stratus, ice
75d	Number of cloudy pixels for cloud type 10 = Altocumulus, ice
76d	Number of cloudy pixels for cloud type 11 = Altostratus, ice
77d	Number of cloudy pixels for cloud type 12 = Nimbostratus, ice
<b>CLOUD TOP PRESSURES (PC)</b>	
78	Mean PC for cloudy pixels (VIS-adjusted day, unadjusted night)
79	Mean PC for IR-cloudy pixels (unadjusted)
80d	Mean PC for IR-only-cloudy pixels (VIS-adjusted)
81	Mean PC for NIR-only-cloudy pixels (unadjusted)
82	Mean PC for IR-marginally-cloudy pixels (unadjusted)
83d	Mean PC for VIS/IR-marginally-cloudy pixels (VIS-adjusted)
84	Sigma-PC for IR-cloudy pixels (unadjusted)

Continued.

**Table 2.2.5.** (continued).

BYTE No.	DESCRIPTION
<b>CLOUD TOP TEMPERATURES (TC)</b>	
85	Mean TC for cloudy pixels (VIS-adjusted day, unadjusted night)
86	Mean TC for IR-cloudy pixels (unadjusted)
87d	Mean TC for IR-only-cloudy pixels (VIS-adjusted)
88	Mean TC for NIR-only-cloudy pixels (unadjusted)
89	Mean TC for IR-marginally-cloudy pixels (unadjusted)
90d	Mean TC for VIS/IR-marginally-cloudy pixels (VIS-adjusted)
91	Sigma-TC for IR-cloudy pixels (unadjusted)
<b>CLOUD OPTICAL THICKNESSES (TAU)</b>	
92d	Mean TAU for cloudy pixels
93d	Mean TAU for IR-cloudy pixels
94d	Mean TAU for IR-only-cloudy pixels
95d	Mean TAU for NIR-only-cloudy pixels
96d	Mean TAU for IR-marginally-cloudy pixels
97d	Mean TAU for VIS/IR-marginally-cloudy pixels
98d	Sigma-TAU for IR-cloudy pixels
<b>CLOUD WATER PATHS (WP)</b>	
99d	Mean WP for cloudy pixels
100d	Mean WP for IR-cloudy pixels
101d	Mean WP for IR-only-cloudy pixels
102d	Mean WP for NIR-only-cloudy pixels
103d	Mean WP for IR-marginally-cloudy pixels
104d	Mean WP for VIS/IR-marginally-cloudy pixels
105d	Sigma-WP for IR-cloudy pixels
<b>CLOUD TOP TEMPERATURE (TC) DISTRIBUTION (UNADJUSTED)</b>	
106	Mean TC for IR-cloudy pixels $10 \leq PC \leq 180$ mb
107	Mean TC for IR-cloudy pixels $180 < PC \leq 310$ mb
108	Mean TC for IR-cloudy pixels $310 < PC \leq 440$ mb
109	Mean TC for IR-cloudy pixels $440 < PC \leq 560$ mb
110	Mean TC for IR-cloudy pixels $560 < PC \leq 680$ mb
111	Mean TC for IR-cloudy pixels $680 < PC \leq 800$ mb
112	Mean TC for IR-cloudy pixels $800 < PC \leq 1000$ mb
<b>PROPERTIES OF LOW-LEVEL CLOUD TYPES (VIS-ADJUSTED)</b>	
113d	Mean TC for cloud type 1 = Cumulus, liquid
114d	Mean TAU for cloud type 1
115d	Mean WP for cloud type 1
116d	Mean TC for cloud type 2 = Stratocumulus, liquid
117d	Mean TAU for cloud type 2
118d	Mean WP for cloud type 2

Continued.

**Table 2.2.5.** (continued).

BYTE No.	DESCRIPTION
119d	Mean TC for cloud type 3 = Stratus, liquid
120d	Mean TAU for cloud type 3
121d	Mean WP for cloud type 3
122d	Mean TC for cloud type 4 = Cumulus, ice
123d	Mean TAU for cloud type 4
124d	Mean WP for cloud type 4
125d	Mean TC for cloud type 5 = Stratocumulus, ice
126d	Mean TAU for cloud type 5
127d	Mean WP for cloud type 5
128d	Mean TC for cloud type 6 = Stratus, ice
129d	Mean TAU for cloud type 6
130d	Mean WP for cloud type 6
<b>PROPERTIES OF MIDDLE-LEVEL CLOUD TYPES (VIS-ADJUSTED)</b>	
131d	Mean TC for cloud type 7 = Altocumulus, liquid
132d	Mean TAU for cloud type 7
133d	Mean WP for cloud type 7
134d	Mean TC for cloud type 8 = Altostratus, liquid
135d	Mean TAU for cloud type 8
136d	Mean WP for cloud type 8
137d	Mean TC for cloud type 9 = Nimbostratus, liquid
138d	Mean TAU for cloud type 9
139d	Mean WP for cloud type 9
140d	Mean TC for cloud type 10 = Altocumulus, ice
141d	Mean TAU for cloud type 10
142d	Mean WP for cloud type 10
143d	Mean TC for cloud type 11 = Altostratus, ice
144d	Mean TAU for cloud type 11
145d	Mean WP for cloud type 11
146d	Mean TC for cloud type 12 = Nimbostratus, ice
147d	Mean TAU for cloud type 12
148d	Mean WP for cloud type 12

Continued.

**Table 2.2.5.** (continued).

BYTE No.	DESCRIPTION
PROPERTIES OF HIGH-LEVEL CLOUD TYPES (VIS-ADJUSTED)	
149d	Mean TC for cloud type 13 = Cirrus
150d	Mean TAU for cloud type 13
151d	Mean WP for cloud type 13
152d	Mean TC for cloud type 14 = Cirrostratus
153d	Mean TAU for cloud type 14
154d	Mean WP for cloud type 14
155d	Mean TC for cloud type 15 = Deep convective
156d	Mean TAU for cloud type 15
157d	Mean WP for cloud type 15
SURFACE SKIN TEMPERATURES (TS)	
158	Mean TS from clear sky composite
159	Mean TS for clear pixels
160	Mean TS for IR-clear pixels
161d	Mean TS for VIS/IR-clear pixels
162	Sigma-TS for IR-clear pixels
SURFACE VISIBLE REFLECTANCES (RS)	
163d	Mean RS from clear sky composite
164d	Mean RS for clear pixels
165d	Mean RS for IR-clear pixels
166d	Mean RS for VIS/IR-clear pixels
167d	Sigma-RS for IR-clear pixels
NEAR-IR REFLECTANCE	
168d	Mean NIR reflectance from clear sky composite
IR RADIANCES	
169	Mean IR radiance for IR-cloudy pixels
170	Sigma-IR radiance for IR-cloudy pixels
171d	Mean IR radiance for VIS/IR-cloudy pixels
172	Mean IR radiance for IR-clear pixels
173	Sigma-IR radiance for IR-clear pixels
174d	Mean IR radiance for VIS/IR-clear pixels
175	Mean IR radiance from clear sky composite

Continued.



**Table 2.2.5.** (continued).

BYTE No.	DESCRIPTION
VIS RADIANCES	
176d	Mean VIS radiance for VIS/IR-cloudy pixels
177d	Sigma-VIS radiance for VIS/IR-cloudy pixels
178d	Mean VIS radiance for IR-cloudy pixels
179d	Mean VIS radiance for VIS/IR-clear pixels
180d	Sigma-VIS radiance for VIS/IR-clear pixels
181d	Mean VIS radiance for IR-clear pixels
182d	Mean VIS radiance from clear sky composite
TOVS ATMOSPHERIC INFORMATION	
183	Atmospheric data origin code (see Table 2.5.8)
184	Surface pressure (PS) (based on topography)
185	Near-surface air temperature (TSA)
186	Temperature at 900 mb (T)
187	Temperature at 740 mb (T)
188	Temperature at 620 mb (T)
189	Temperature at 500 mb (T)
190	Temperature at 375 mb (T)
191	Temperature at 245 mb (T)
192	Temperature at 115 mb (T)
193	Tropopause pressure (PT)
194	Tropopause temperature (TT)
195	Stratosphere temperature at 50 mb (T)
196	Stratosphere temperature at 15 mb (T)
197	Precipitable water for 1000-800 mb (PW)
198	Precipitable water for 800-680 mb (PW)
199	Precipitable water for 680-560 mb (PW)
200	Precipitable water for 560-440 mb (PW)
201	Precipitable water for 440-310 mb (PW)
202	Ozone column abundance (O3)

*Note: Additional variables are calculated in the DIREAD program provided: cloud amounts (%), cloud top height in meters, total IR radiance, total VIS radiance, and layer mid-point pressures. Cloud amounts are not explicitly reported in DI data; rather they are calculated by dividing the number of cloudy pixels in each category by the total number of pixels in each map grid cell.*

### 2.3. DX DATA (3-HOURLY, 30 KM SAMPLED IMAGE PIXELS)

#### 2.3.1. ARCHIVE TAPE LAYOUT

Each DX archive tape has 1 header file, followed by a variable number of data files. Data files vary in length and are written to tape until the tape is full. Data are arranged chronologically on the tape. Typically, there are from 50 to 100 files on each tape.

**Table 2.3.1. DX Archive Tape Layout.**

FILE	CONTENTS	FORMAT	RECORD LENGTH (BYTES)
1	Table of Contents	ASCII	80
2-end	DX Cloud Data	Binary	30720

*Note: The GPC produces archive tapes using IBM standard label format which means that there are label records written before and after each file on the tape. On IBM systems, these labels provide information to the operating system about the name and format of the file and will appear transparent to the user. On non-IBM systems these label records will appear as extra short files surrounding each file listed above and should be skipped by the user. The presence or absence of these files depends on which archive supplies tape copies to the user, as they may either provide an exact copy (labels present) or a modified copy (labels absent).*

#### 2.3.2. HEADER FILE CONTENTS

**File 1** is the **Table of Contents** file that lists the date and time of each file on the tape in ASCII columns defined in Table 2.3.2.

**Table 2.3.2. Table of Contents Layout.**

COLUMN	DESCRIPTION
1	Satellite ID name (Table 2.5.1 and Table 2.5.9)
2	Date/Time (YYMMDDHH = Year, Month, Day, Hour UTC)
3	Record Format (F = fixed length records)
4	Record Length
5	Number of Records in file
6	Internal use only
7	Production date
8	Production time

#### 2.3.3. DATA FILE CONTENTS

Each DX data file (Figure 2.3) reports up to 45 variables for each pixel in the field of view of a particular satellite or in a particular satellite sector (see Table 2.5.9) for a particular 3-hour time slot (image). Latitude and Longitude for each pixel are given, as well as X,Y coordinates for a fixed map projection (see Section 3.2.2). Missing images and pixels with no data are not reported. The number of

variables reported for a particular pixel depends on whether it is a daytime or nighttime pixel and whether there are additional wavelength measurements available. Daytime variables are not present for nighttime pixels and additional wavelength measurements and corresponding analysis results are only reported when available from that particular satellite.

Data are packed into fixed length records of 30720 bytes each. The first physical record in the file is the image header record. The remaining records contain the pixel-level data. Each data record consists of a prefix area containing location information followed by a data area containing the packed pixel data, followed by padding to the end of the record (pad value = 255). A data record contains a variable number of whole pixels. All pixel data are reported as single byte values from 0 to 255, with 255 reserved to represent missing data. Contents of the header record are given in Table 2.3.3 and of the data record in Table 2.3.4.

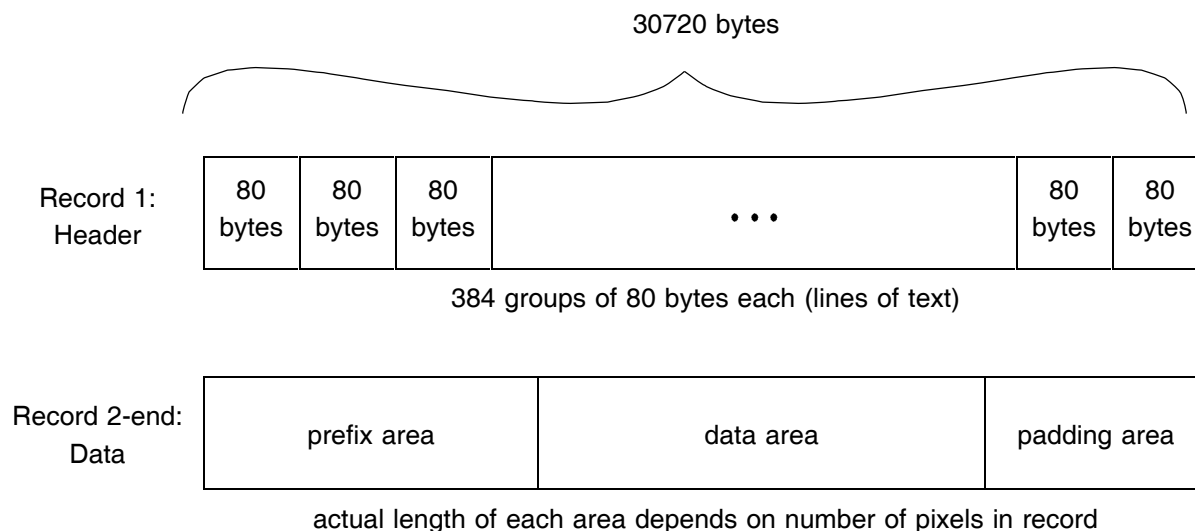


**Figure 2.3.** DX Data File Layout.

**Table 2.3.3. DX Data Header Record Layout.** See Table 2.5.1 for satellite ID codes and Table 2.5.9 for satellite type codes.

LINE (80 BYTES EACH)	DESCRIPTION (ASCII)
1	Year, Month, Day, UTC (1-8), Satellite ID code, Satellite Type Code (SATTYP), Number of channels present (NCHANS), Night Image flag
2	Production date
3	Production time
4	Input data identifier (internal use only)
5-100	Blank
101-135	Title, units, format for selected DX variables (for conversion to HDF format)
136-384	Blank

**Table 2.3.4. DX Data Record Layout.** Second column gives the FORTRAN variable name used in the DXREAD program.

No. BYTES	NAME	DESCRIPTION
PREFIX AREA		
4	IWEST	Western-most longitude (0-3600 degrees*10)
4	IEAST	Eastern-most longitude (0-3600 degrees*10)
4	INORTH	Northern-most latitude (0-1800 degrees*10)
4	ISOUTH	Southern-most latitude (0-1800 degrees*10)
4	NPIX	Number of pixels reported in data area
4	IOUT	Number of bytes in packed data BUFFER
2*NPIX	LONBUF(NPIX)	Longitudes for NPIX pixels (0-3600 degrees*10)
2*NPIX	LATBUF(NPIX)	Latitudes for NPIX pixels (0-1800 degrees*10)
2*NPIX	XBUF(NPIX)	X-positions for NPIX pixels (1-1440)
2*NPIX	YBUF(NPIX)	Y-positions for NPIX pixels (1-550)
DATA AREA		
1*IOUT	BUFFER(IOUT)	Packed pixel data for NPIX pixels

*Note:* When a pixel's data will not fit entirely in the remaining bytes of a record, that remainder is unused (filled with byte values = 255).

BUFFER contains the data for each of NPIX pixels. Pixel data are divided into six sections (Figure 2.4); not all sections are present for all pixels. Daytime sections (S2, S4) are present only for daytime pixels and the extra wavelength sections (Add1, Add3) are present only for satellites that actually report such information (Figure 2.4). The DXREAD program (see Section 2.3.4) unpacks BUFFER one pixel at a time, putting the unpacked variables into a COMMON block.

**TYPE OF PIXEL**

**SECTIONS PRESENT IN DATA**

Geostationary - Night	S1	Add1	S3			
Geostationary - Day	S1	Add1	S2	S3	S4	
Polar Orbiter - Night	S1	Add1	S3	Add3		
Polar Orbiter - Day	S1	Add1	S2	S3	Add3	S4

**Figure 2.4.** DX data packed pixel layout.

**Table 2.3.5. DX Data Section Layouts.** See Table 2.5.4 for definitions of abbreviations and units and Table 2.5.5 for definitions of radiance threshold categories. The NAME column gives the FORTRAN variable names as defined in the DXREAD program. *Note: Variables marked with '\*' are for internal use only.*

<b>Section S1:</b> 5 bytes = 40 bits, always present			
BIT No.	No. BITS	NAME	DESCRIPTION
1	1	NODAY*	BX night flag (0-1), 1 = Sections S2,S4 not present
2	1	BXSHOR*	BX shore flag (0-1)
3	1	LNDWTR	Land/water flag (0-1), 1 = water pixel
4	1	HITOP	Topography flag (0-1), 1 = high topography pixel
5-6	2	SNOICE	Snow/ice code (0-3) (See Table 2.5.10)
7-8	2	TIMSPA*	Time/space test result (0-3)
9-13	5	ICSLOG*	IR clear sky composite logic code (0-24)
14-16	3	BXITHR*	First IR threshold result (0-5)
17-24	8	MUE	Cosine of satellite zenith angle * 100 (0-100)
25-32	8	IRAD	IR radiance (0-254 counts)
33-40	8	BXICSR*	First IR clear sky radiance (0-254 counts)

<b>Section Add1:</b> 0-3 bytes = 0-24 bits, actual number of bytes present = NCHANS - 2 (from image header)			
BIT No.	No. BITS	NAME	DESCRIPTION
1-8	8	ARAD(1)	First extra wavelength radiance (0-254 counts) (present only when NCHANS > 2)
9-16	8	ARAD(2)	Second extra wavelength radiance (0-254 counts) (present only when NCHANS > 3)
17-24	8	ARAD(3)	Third extra wavelength radiance (0-254 counts) (present only when NCHANS > 4)

<b>Section S2:</b> 5 bytes = 40 bits, present only when NODAY = 0 (from section S1)			
BIT No.	No. BITS	NAME	DESCRIPTION
1	1	GLINT	Glint flag (0-1), 1 = glint condition exists
2-5	4	VCSLOG*	VIS clear sky composite logic code (0-14)
6-8	3	BXVTHR*	First VIS threshold result (0-5)
9-16	8	MU0	Cosine of solar zenith angle * 100 (0-100)
17-24	8	PHI	Relative azimuth angle (0-180 degrees)
25-32	8	VRAD	VIS radiance (0-254 counts)
33-40	8	BXVCSR*	First VIS clear sky radiance (0-254 counts)

**Table 2.3.5.** (continued).

<b>Section S3:</b> 7 bytes = 56 bits, always present.			
BIT No.	No. BITS	NAME	DESCRIPTION
1	1	DAYNIT	Day/Night flag (0-1), 1 = night pixel (no VIS)
2-4	3	ITHR	Final IR threshold result (0-5), 4,5 = cloudy
5-7	3	VTHR	Final VIS threshold result (0-5), 4,5 = cloudy
8	1	SHORE	Shore flag (0-1), 1 = near-coastal pixel
9-12	4	IRET*	IR retrieval code (0-12)
13-16	4	ICSRET*	IR clear sky composite retrieval code (0-12)
17-24	8	ICSRAD	IR clear sky composite radiance (0-254 counts)
25-32	8	ITMP	IR-retrieved cloud top or surface temperature (0-254 counts)
33-40	8	IPRS	IR-retrieved cloud top or surface pressure (0-254 counts)
41-48	8	ICSTMP	IR-retrieved clear sky composite temperature (0-254 counts)
49-56	8	ICSPRS	IR-retrieved clear sky composite pressure (0-254 counts)

<b>Section Add3:</b> 3 bytes = 24 bits, present only when SATTP > 0 (from image header).			
BIT No.	No. BITS	NAME	DESCRIPTION
1-8	8	NREF	NIR reflectivity (0-254 counts)
9-16	8	NTHR	NIR threshold result (1-13), > 8 = cloudy
17-24	8	NCSREF	NIR clear sky composite reflectance (0-254 counts)

<b>Section S4:</b> 9 bytes = 72 bits, present only when NODAY = 0 (from Section S1).			
BIT No.	No. BITS	NAME	DESCRIPTION
1-4	4	VRET*	VIS retrieval code (0-14)
5-8	4	VCSRET*	VIS clear sky composite retrieval code (0-14)
9-16	8	VCSRAD	VIS clear sky composite radiance (0-254 counts)
17-24	8	VALBTA	VIS-retrieved liquid cloud tau or surface reflectance (0-254 counts)
25-32	8	VCSALB	VIS-retrieved clear sky composite reflectance (0-254 counts)
33-40	8	VTMP	VIS-adjusted cloud top temperature (0-254 counts)
41-48	8	VPRS	VIS-adjusted cloud top pressure (0-254 counts)
49-56	8	VTAUIC	VIS-retrieved ice cloud tau (0-254 counts)
57-64	8	VTMPIC	VIS-adjusted ice cloud top temperature (0-254 counts)
64-72	8	VPRSIC	VIS-adjusted ice cloud top pressure (0-254 counts)

### 2.3.4. READ SOFTWARE

The DXREAD FORTRAN software may be downloaded from the ISCCP WWW Home Page at URL <http://isccp.giss.nasa.gov> or from NASA Langley Research Center DAAC. The program gives an example of how to use the subroutines. Subroutine DXTABS is called first to initialize tables required for unpacking bits. Subroutine DXOPEN is called once per data file to open and initialize variables. Then Subroutine DXREAD is called repeatedly until end of file to unpack one pixel at a time into a COMMON block as integer count values.

The actual cloudy/clear decision for each pixel is calculated in the DXREAD program by testing the various threshold result codes (see Table 2.5.5) as follows:

```
If ( ITHR > 3 OR VTHR > 3 OR NTHR > 8 )
then CLOUD=1 /* pixel is cloudy */
else CLOUD=0 /* pixel is clear */
```

The actual water cloud - ice cloud decision may be calculated by the user as follows:

```
If ( VTMPIC = 255 OR ( VTMP > 74 AND VTMPIC > 74 ) )
then WATER CLOUD
else ICE CLOUD
```

To convert count values to physical units the user must apply the look-up tables provided in BLOCK DATA:

Temperatures or IR radiances (K)	=	TMPTAB(count)
Pressures (millibars)	=	PRETAB(count)
Reflectances or VIS radiances	=	RFLTAB(count)
Optical thicknesses	=	TAUTAB(count)

## 2.4. CONVERSION TABLES FOR PHYSICAL VALUES

Physical values for most of the variables in all cloud products are reported as one-byte code values representing COUNTS from 0 to 254; the value 255 is reserved to represent missing data. Counts are converted to physical units (Table 2.5.4) in the READ programs using look-up tables. Note that VIS radiances are reported in the same units as reflectances, but that a reflectance is not a radiance. Users may wish to use the count values directly for image display purposes.

Since most of the parameters are obtained from measurements of satellite radiances, the precision of such measurements, though roughly constant over the response range of the radiometer, is not constant over the range of some of the parameters derived from the radiances. For example, a radiometer measurement of IR radiances with constant precision does not provide temperature values with constant precision: colder temperatures are not measured with as much precision as warmer temperatures. Hence, the look-up tables used to convert count values to physical values are not always linear because they represent the proper proportionality between the derived parameter and the original radiance measurement. The two instances of non-linear relations are for temperatures and cloud optical thicknesses: the linear variation of count values parallels the linear variation of the amount of energy measured by the radiometer. Because averaging of such non-linear relationships can change the relationship, two versions of cloud top temperature and optical thickness are provided in D1 and D2 datasets. The two **radiative** parameters, top temperature and optical thickness, are averaged so as to preserve the average radiative effect of clouds, whereas the two **physical** parameters, top pressure and water path, are averaged linearly.

Input data errors and analysis model errors can result in derived values that are non-physical, especially near zero, or are much smaller/larger than anticipated. To limit the count values to a one byte representation required establishing limits for all quantities. If these limits are violated, then either underflow or overflow occurs. In the look-up tables, special count values have been reserved to indicate underflow/overflow: count = 0 represents underflow and count = 254 represents overflow. Count 255 is reserved to mean NO DATA, exclusively. For physical quantities, count = 0 is converted to -100.0, count = 254 is converted to -200.0, and count = 255 is converted to -1000.0.



## 2.5. CODE DEFINITION TABLES

**Table 2.5.1. Satellite Identification (ID) Codes and ID Names.** See Table 2.5.2 for position codes.

IDCODE	IDNAME	POSITION	SATELLITE	SATELLITE PROCESSING CENTER	OPERATIONAL DATES
11	NOA7	6	NOAA-7	NOAA	Jul83 - Jan85
12	NOA9	6	NOAA-9	NOAA	Feb85 - Oct88
13	NOAB	6	NOAA-11	NOAA	Nov88 - Sep94
14	NOAE	6	NOAA-14	NOAA	Feb95 - present
21	GOE6	3	GOES-6	CSU	Jul83 - Jan89
31	GOE5	4	GOES-5	UWS	Jul83 - Jul84
32	GOE7	3	GOES-7	AES	Apr87 - Apr92
		4			May92 - present
33	GOE8	4	GOES-8	CSU	Mar95 - present
41	MET2	2	METEOSAT-2	ESA	Jul83 - Jul88
42	MET3	2	METEOSAT-3	ESA	Aug88 - Jun89
		2			Feb90 - Apr90
		4			May92 - Apr95
43	MET4	2	METEOSAT-4	ESA	Jul89 - Jan90
		2			May90 - Jan94
44	MET5	2	METEOSAT-5	ESA	Feb94 - present
51	GMS1	1	GMS-1	JMA	Feb84 - May84
52	GMS2	1	GMS-2	JMA	Jul83 - Jan84
		1			Jul84 - Sep84
53	GMS3	1	GMS-3	JMA	Oct84 - Nov89
54	GMS4	1	GMS-4	JMA	Dec89 - May95
55	GMS5	1	GMS-5	JMA	Jun95 - present
61	NOA8	7	NOAA-8	NOAA	Oct83 - Jun84
62	NOAA	7	NOAA-10	NOAA	Dec86 - Aug91
63	NOAC	7	NOAA-12	NOAA	Sep91 - present
71	INS1	5	INSAT-1	IMD	Apr88 - Mar89

**Table 2.5.2. Satellite Position Codes.**

CODE	POSITION	SSP LONGITUDE
1	GMS (West Pacific/Japan/Australia)	140.0°
2	METEOSAT (Atlantic/Europe/Africa)	0.0°
3	GOES-WEST (East Pacific)	225.0° - 262.0°
4	GOES-EAST (North/South America)	248.0° - 310.0°
5	INSAT (Asia/India/Indian Ocean)	74.5°
6	NOAA-Afternoon (global)	Not Applicable
7	NOAA-Morning (global)	Not Applicable

*Note: Geostationary satellites (codes 1-5) are nominally positioned on the equator at particular sub-satellite point (SSP) longitudes and cover an area roughly  $\pm 60^\circ$  from the SSP. Sun-synchronous polar orbiting satellites (codes 6-7) cover different areas of the earth at different times of day in swaths, attaining global coverage over a period of 12 hours.*

**Table 2.5.3. Vegetation Type Codes** (based on Matthews 1983).

CODE	VEGETATION TYPE
0	Water
1	Rain forest
2	Deciduous forest
3	Evergreen forest
4	Grassland
5	Tundra
6	Shrubland
7	Desert
8	Ice

**Table 2.5.4. Variable Abbreviations and Physical Units.**

ABBREVIATION	DESCRIPTION
UTC	Universal Time Convention (HH = hour)
MEASURED RADIANCES	
IR	infrared ( $\approx 11 \mu\text{m}$ wavelength) brightness temperature (165-345 K) visible ( $\approx 0.6 \mu\text{m}$ wavelength) scaled radiance (0-1.108) near-infrared ( $\approx 3.7 \mu\text{m}$ wavelength) brightness temperature (165-345 K)
VIS	
NIR	
VIEWING GEOMETRY	
MUE	Cosine of satellite zenith angle (0-1)
MU0	Cosine of solar zenith angle (0-1)
PHI	Relative azimuth angle (degrees) (0-180 degrees)
RETRIEVED CLOUD PROPERTIES	
CA	Cloud amount (0-100%) Cloud top pressure (5-1000 millibars) Cloud top temperature (165-345 K) Cloud visible optical thickness (0.02-378.65) Cloud water path ( $\text{g}/\text{m}^2$ )
PC	
TC	
TAU	
WP	
RETRIEVED SURFACE PROPERTIES	
TS	Surface skin temperature (165-345 K)
RS	Surface visible reflectance (0-1.108)
ATMOSPHERIC PROPERTIES	
PS	Surface pressure (5-1000 millibars)
PT	Tropopause pressure (5-1000 millibars)
T	Layer mean temperatures (165-345 K)
PW	Layer total water abundance (0-8 centimeters)
O3	Total column ozone abundance (0-515 Dobson)

**Table 2.5.5. Cloud Detection Threshold Codes and Threshold Categories.**

WAVELENGTH	CODE	DESCRIPTION (Threshold intervals given in Table 3.2.4)
IR	1	greater than IR Clear Sky by more than threshold interval
IR	2	greater than IR Clear Sky by less than threshold interval
IR	3	less than IR Clear Sky by less than threshold interval
IR	4	less than IR Clear Sky by more than threshold interval
IR	5	less than IR Clear Sky by more than 2 × threshold interval
VIS	0	no visible data
VIS	1	less than VIS Clear Sky by more than threshold interval
VIS	2	less than VIS Clear Sky by less than threshold interval
VIS	3	greater than VIS Clear Sky by less than threshold interval
VIS	4	greater than VIS Clear Sky by more than threshold interval
VIS	5	greater than VIS Clear Sky by more than 2 × threshold interval
NIR	1	less than NIR Clear Sky by more than threshold (daytime)
NIR	2	less than lower limit (daytime)
NIR	3	less than lower limit (nighttime)
NIR	4	greater than upper limit (nighttime)
NIR	6	greater than 3 × threshold (nighttime)
NIR	7	greater than NIR Clear Sky by less than threshold (daytime) or greater than zero by less than threshold (nighttime)
NIR	8	less than NIR Clear Sky by less than threshold (daytime) or greater than zero by less than threshold (nighttime)
NIR	9	greater than NIR Clear Sky by more than threshold (daytime) or greater than zero by more than threshold (nighttime)
NIR	10	less than zero by more than threshold (nighttime)
NIR	11	greater than NIR Clear Sky by more than 2 × threshold (daytime) or greater than zero by more than 2 × threshold (nighttime)
NIR	12	less than zero by more than 2 × threshold (nighttime)
NIR	13	greater than NIR Clear Sky by more than 3 × threshold (daytime)
CATEGORY		DESCRIPTION
cloudy		cloudy by IR or VIS or NIR thresholds
VIS/IR-cloudy		cloudy by IR or VIS thresholds
IR-cloudy		cloudy by IR threshold
IR-only-cloudy		IR cloudy but VIS clear
NIR-cloudy		cloudy by NIR threshold
NIR-only-cloudy		NIR cloudy but IR clear and VIS clear
VIS-only-cloudy		VIS cloudy but IR clear
IR-marginally-cloudy		marginally cloudy by IR threshold
VIS/IR-marginally-cloudy		marginally cloudy by IR or VIS threshold
NIR-marginally-cloudy		marginally cloudy by NIR threshold
NIR-only-marginally-cloudy		NIR marginally cloudy but IR clear and clear
clear		clear by IR and VIS and NIR thresholds
IR-clear		clear by IR threshold
VIS/IR-clear		clear by IR and VIS thresholds

**Table 2.5.6. Land/Water/Coast Codes** (based on Masaki 1972). *Note: This code is also used as a day/night code in D1 where day  $\leq 100$ , night  $> 100$ .*

	WATER (Land fraction $\leq 35\%$ )	LAND (Land fraction $\geq 65\%$ )	COAST
Stage D2	1	2	3
Stage D1 -- Day	1	2	3
Stage D1 -- Night	101	102	103

**Table 2.5.7. Cloud Types** (see Figure 2.5).

NAME	PC RANGE (mb)	TAU RANGE	TYPE CODE
LOW			
Cumulus	$> 680$	$\leq 3.55$	1 (liquid), 4 (ice)
Stratocumulus	$> 680$	3.55 - 22.63	2 (liquid), 5 (ice)
Stratus	$> 680$	$> 22.63$	3 (liquid), 6 (ice)
MIDDLE			
Alto cumulus	440 - 680	$\leq 3.55$	7 (liquid), 10 (ice)
Altostratus	440 - 680	3.55 - 22.63	8 (liquid), 11 (ice)
Nimbostratus	440 - 680	$> 22.64$	9 (liquid), 12 (ice)
HIGH			
Cirrus	$\leq 440$	$\leq 3.5$	13 (ice)
Cirrostratus	$\leq 440$	3.5 - 22.63	14 (ice)
Deep Convective	$\leq 440$	$> 22.63$	15 (ice)

## ISCCP CLOUD CLASSIFICATION

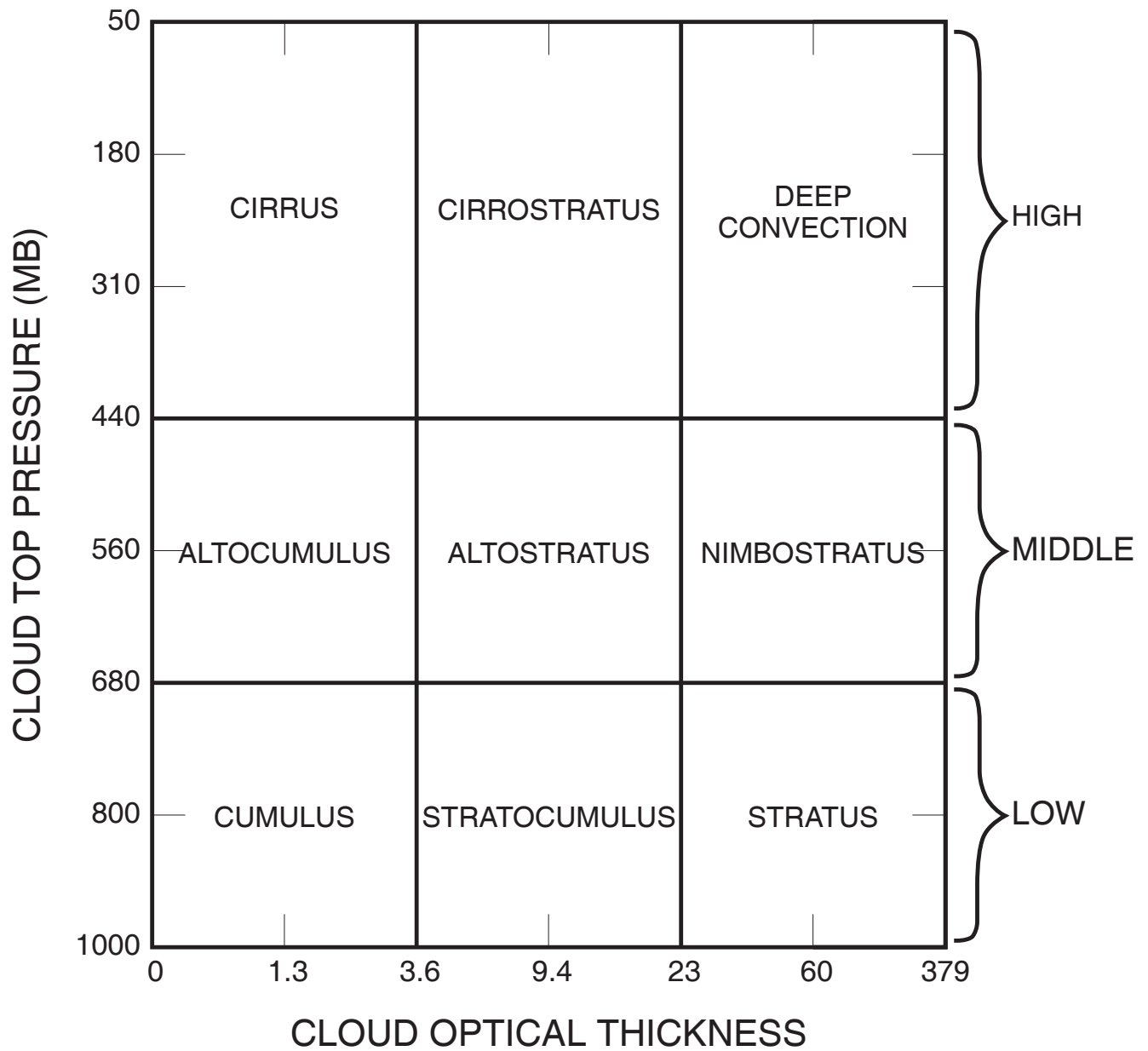


**Figure 2.5.** ISCCP Radiometric cloud classification.

**Table 2.5.8. TOVS Atmospheric Data Origin Code.**

CODE	DESCRIPTION
0	No data
1	Original TOVS observation
2	Data replicated from nearby TOVS observation
3	TOVS MONTHLY used (see Section 6.1)
4	CLIM MONTHLY used (see Section 6.1)
5	Original TOVS water vapor outside range and changed

**Table 2.5.9. DX Satellite Type Codes and Geographic Sectors.** Subsets are produced for the GEWEX regional experiments.

SATTYP	SATELLITE TYPE – REGION	SECTOR
-3	Geostationary – Geographic subset	0
-2	Polar Orbiter – Midlatitude subset	A-F
-1	Polar Orbiter – Polar subset	S, N
0	Geostationary – Full View centered on SSP	0
1	Polar Orbiter – South Polar Cap (Lat < -50°)	S
2	Polar Orbiter – North Polar Cap (Lat > 50°)	N
3	Polar Orbiter – Midlatitude Ascending Lon = 180°-300°	A
4	Polar Orbiter – Midlatitude Descending Lon = 180°-300°	D
5	Polar Orbiter – Midlatitude Ascending Lon = 300°-60°	B
6	Polar Orbiter – Midlatitude Ascending Lon = 60°-180°	C
7	Polar Orbiter – Midlatitude Descending Lon = 300°-60°	E
8	Polar Orbiter – Midlatitude Descending Lon = 60°-180°	F

**Table 2.5.10. Ice/Snow Codes.**

CODE	WATER	LAND
0	No sea ice	No snow or ice
1	Partial ice cover	Land ice
2	Full ice cover	Full snow cover
3	Ice margin	Snow or ice margin

**Table 2.5.11. Equal-Area Map Grid.** Latitude index goes from south to north. Longitude intervals are in degrees.

Lat. Index	Long. Interval	No. Cells	Begin Cell No.	End Cell No.	Lat. Index	Long. Interval	No. Cells	Begin Cell No.	End Cell No.
1	120.00	3	1	3	37	2.50	144	3299	3442
2	40.00	9	4	12	38	2.50	144	3443	3586
3	22.50	16	13	28	39	2.52	143	3587	3729
4	16.36	22	29	50	40	2.54	142	3730	3871
5	12.86	28	51	78	41	2.55	141	3872	4012
6	10.59	34	79	112	42	2.57	140	4013	4152
7	9.00	40	113	152	43	2.61	138	4153	4290
8	7.83	46	153	198	44	2.65	136	4291	4426
9	6.92	52	199	250	45	2.69	134	4427	4560
10	6.21	58	251	308	46	2.73	132	4561	4692
11	5.63	64	309	372	47	2.79	129	4693	4821
12	5.22	69	373	441	48	2.86	126	4822	4947
13	4.80	75	442	516	49	2.93	123	4948	5070
14	4.50	80	517	596	50	3.00	120	5071	5190
15	4.24	85	597	681	51	3.10	116	5191	5306
16	4.00	90	682	771	52	3.21	112	5307	5418
17	3.79	95	772	866	53	3.33	108	5419	5526
18	3.60	100	867	966	54	3.46	104	5527	5630
19	3.46	104	967	1070	55	3.60	100	5631	5730
20	3.33	108	1071	1178	56	3.79	95	5731	5825
21	3.21	112	1179	1290	57	4.00	90	5826	5915
22	3.10	116	1291	1406	58	4.24	85	5916	6000
23	3.00	120	1407	1526	59	4.50	80	6001	6080
24	2.93	123	1527	1649	60	4.80	75	6081	6155
25	2.86	126	1650	1775	61	5.22	69	6156	6224
26	2.79	129	1776	1904	62	5.63	64	6225	6288
27	2.73	132	1905	2036	63	6.21	58	6289	6346
28	2.69	134	2037	2170	64	6.92	52	6347	6398
29	2.65	136	2171	2306	65	7.83	46	6399	6444
30	2.61	138	2307	2444	66	9.00	40	6445	6484
31	2.57	140	2445	2584	67	10.59	34	6485	6518
32	2.55	141	2585	2725	68	12.86	28	6519	6546
33	2.54	142	2726	2867	69	16.36	22	6547	6568
34	2.52	143	2868	3010	70	22.50	16	6569	6584
35	2.50	144	3011	3154	71	40.00	9	6585	6593
36	2.50	144	3155	3298	72	120.00	3	6594	6596



**Table 2.5.12. ISCCP Tape Designator: GPC.TT.NNNN.V.YYDDD.YYDDD.ISCCP**

GPC	Global Processing Center, data producer
TT	Data type: D2, D1, DX, TV, IS
NNNN	Tape sequence number, starting with 0001
V	Tape version number, starting with 0
YYDDD	Year and Julian Day (1-366) of first data file
YYDDD	Year and Julian Day (1-366) of last data file
ISCCP	Project producing the data

### **3. DATA PRODUCT DESCRIPTION**

#### **3.1. GRIDDED PRODUCTS ANALYSIS (STAGE D1 AND D2)**

The Stage D1 product is produced by summarizing the pixel-level results (Stage DX data, see Section 3.2) every 3 hours on an equal-area map grid with 280 km resolution and merging the results from separate satellites with the atmospheric (TV) and ice/snow (IS) datasets to produce global coverage at each time. The Stage D2 data product is produced by averaging the Stage D1 data over each month, first at each of the eight 3 hr time slots and then over all time slots.

##### **3.1.1. MAP GRID DEFINITIONS**

Two related map grids are used for the ISCCP D1 and D2 datasets, an EQUAL-AREA grid and an EQUAL-ANGLE (square) grid. These grids are identical at the equator. Collection of statistics from the pixel-level satellite analysis (DX data), which produces global information at about 30 km resolution, is performed using an EQUAL-AREA map to maintain a nearly constant statistical weight for results at all locations (Rossow and Garder 1984). For economy of data storage, the results are also recorded in the same EQUAL-AREA grid. However, since data manipulation on computers and in image displays is more convenient using rectangular arrays, the D1READ and D2READ programs provided with the data contain optional subroutines that will re-map the data into an EQUAL-ANGLE map grid of 2.5° resolution. The data are transformed to the EQUAL-ANGLE grid by replication, which preserves all of the original statistics (Rossow and Garder 1984), since the grid cells of the EQUAL-ANGLE grid at higher latitudes represent higher resolution (in the longitudinal direction) than in the original dataset. If a user wishes to re-map the data to some other projection, the EQUAL-AREA form of the data is most convenient to use as a starting point, since the area-weights are all equal.

Both map grids are indexed in order from the south pole to the north pole, latitudes ranging from -90° to 90°. In each latitude zone, all longitudes are indexed in order from the Greenwich meridian, eastward (longitudes are given in the range 0 - 360°), before going to the next latitude zone.

##### Equal-Area Grid for Data Storage

The EQUAL-AREA map (Figure 3.1) is defined by the area of a 2.5° latitude × 2.5° longitude cell at the equator; the intersection of the Greenwich meridian and the equator is a cell corner. There are 6596 cells in this map grid. All map cells are determined by a constant 2.5° increment in latitude and a variable longitude increment. The longitude increment is selected to provide an integer number of cells in a latitude zone and to give a cell area as close to that of the equatorial cell as possible. See Table 2.5.11 for definition of index values and longitude increments as a function of latitude.

##### Equal-Angle Grid for Data Display

The D1READ and D2READ programs, provided to read the data files, contain optional subroutines that replicate the data from the 6596 EQUAL-AREA cells to an EQUAL-ANGLE map grid. This map grid has equal 2.5° increments in latitude and longitude; there are 10368 cells in this grid (72 latitude zones and 144 longitude intervals). The intersection of the Greenwich meridian and equator is a cell corner; coordinates are given as latitudes from -90° to 90° and longitudes from 0° to 360° (positive eastward).

ISCCP EQUAL-AREA MAP GRID

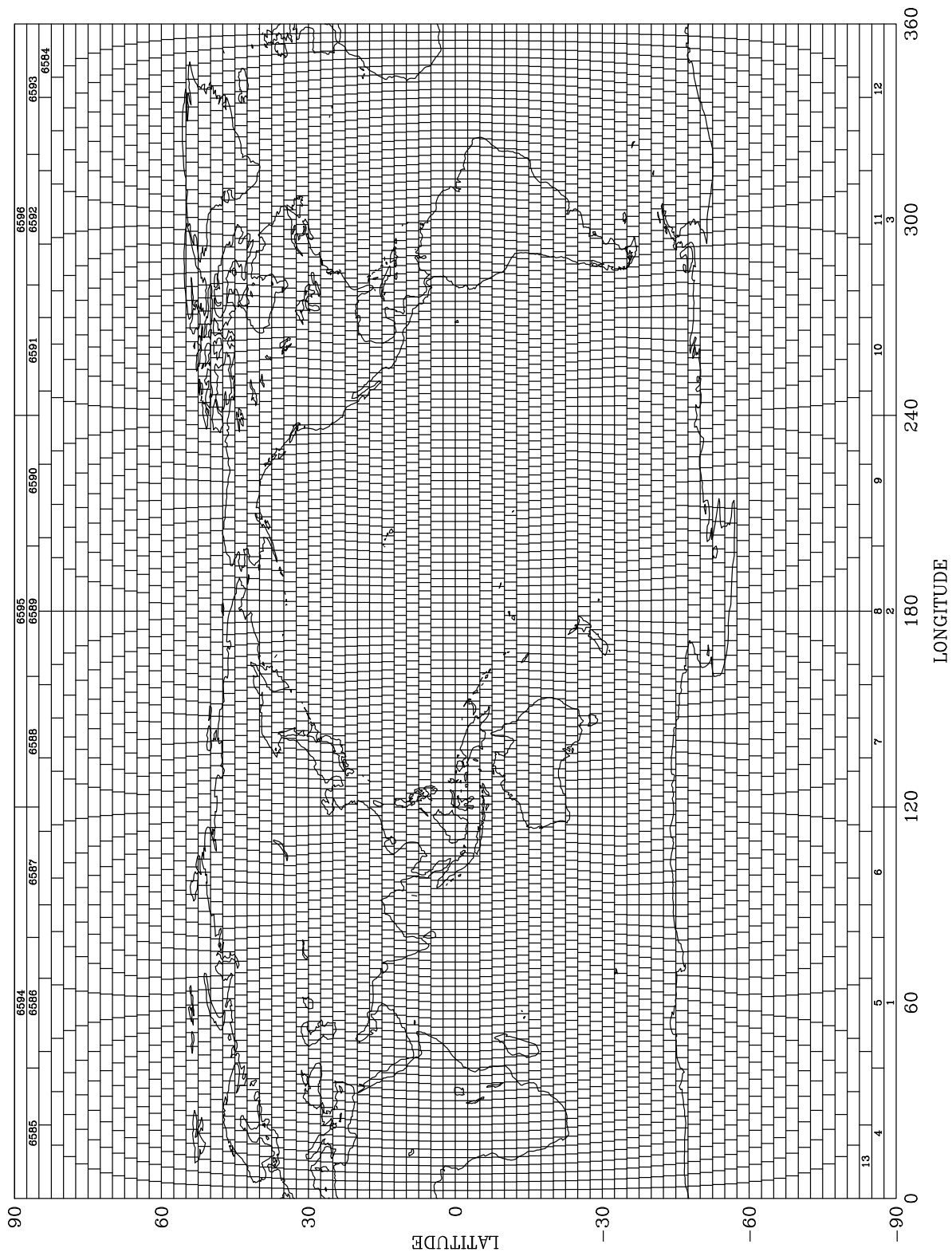


Figure 3.1. Equal-area map grid used for ISCCP data. The first and last thirteen cells are numbered for illustration.

### 3.1.2. VARIABLE DEFINITIONS

#### Missing data

The cosine of the satellite zenith angle for any pixel must be  $\geq 0.3$  (zenith angle  $\leq 72.5^\circ$ ). If there are less than 20 pixels available in a map grid cell, the pixels are discarded and the cell is labeled "missing". In this case all variables except the grid cell indices and the atmospheric (TOVS) information are given the value of 255.

#### Land/water/coast

Each EQUAL-AREA map grid cell is labeled as either land, water, or coast. If the fraction of the cell covered by land is  $\geq 65\%$ , the cell is labeled "land". If the fraction covered by land is  $\leq 35\%$ , the cell is labeled "water". Cells with land fraction  $> 35\%$  and  $< 65\%$  are labeled "coast".

#### Day/Night

If more than half of the total number of pixels in a map grid cell are "daytime" pixels (see Section 3.2.3), the cell is labeled "day", otherwise it is labeled "night". In a "day" cell, only daytime pixels (those with both IR and VIS information available) are used to calculate statistics and both IR- and VIS-dependent results are reported. In a "night" cell, all pixels are used to calculate statistics, but only the IR-dependent information is used and reported.

#### Cloud Amounts

The cloud detection procedure (Section 3.2.4) decides whether each satellite pixel is cloudy or clear and reports the results of the threshold tests for each radiance (IR, VIS, NIR) by codes that indicate the relative relationship between the observed pixel radiances and the clear radiances (Table 2.5.5). For the gridded datasets, where many satellite pixels are included in each map grid cell, cloud amount (CA) is determined by counting the number of cloudy pixels and then dividing by the total number of pixels in that cell. In the D1 dataset, the number of cloudy pixels and the total number of pixels are reported explicitly; cloud amount is calculated in the D1READ program. In the D2 dataset, D1 cloud amounts are averaged over the month and reported to the nearest 0.5%.

Several additional subsets of the total cloud amount are reported in the D1 dataset to indicate the types of clouds present and provide some information on the reliability of the cloud detection procedure (Table 2.5.5). These subsets are defined by different combinations of radiance threshold codes, indicating the degree of separation between the radiances and the clear sky values, and are illustrated in Figure 3.2. A single pixel is labeled cloudy if **any** of the following threshold results is reported: IR code = 4, 5 or VIS code = 4, 5 (or NIR code = 9, 10, 11, 12 and 13). A clear pixel occurs only when all threshold results indicate clear values. VIS = 0 indicates nighttime where no VIS threshold test can be performed. To provide cloud amount information that is consistent over the whole diurnal cycle, the number of pixels indicated as cloudy by IR, regardless of any other threshold codes (called IR-cloudy, last two columns), is reported for all times of day. Two subsets of these pixels, IR-only-cloudy and marginal IR-cloudy are also reported: the first is the number of pixels which are labeled cloudy **only** by the IR tests and the second (M-IR) is the number of pixels with IR code = 4, indicating that these clouds change the IR radiance by an amount only slightly more than the threshold amount. The corresponding VIS-only-cloudy amount is not reported because it can be determined by subtracting the IR-cloudy amount from the total cloud amount (minus the NIR-only-cloudy amount if present). The corresponding marginal VIS/IR-cloudy is defined by pixels with VIS = 4 **and** IR = 4 (M-VIS/M-IR), together with pixels labeled as M-VIS-only and M-IR-only.

VIS THRESHOLD CODE	5	VIS-only	VIS-only	VIS-only	VIS/M-IR	VIS/IR
	4	M-VIS-only	M-VIS-only	M-VIS-only	M-VIS/M-IR	M-VIS/IR
	3	VIS>	VIS> IR>	VIS> IR<	M-IR-only	IR-only
	2	VIS<	VIS< IR>	VIS< IR<	M-IR-only	IR-only
	1	VIS<< IR>>	IR>	IR<	M-IR-only	IR-only
		1	2	3	4	5
		IR THRESHOLD CODE				

**Figure 3.2.** Subset measures of Cloud Amount.

In the polar regions (latitudes polewards of 50°) over sea ice and snow-covered locations, the NIR threshold test is performed, day and night, for polar orbiter data. These results are added to the total cloud amount, but are excluded from the subsets defined above (for consistency with the C-series products). The total number of pixels labeled cloudy by this test (NIR-cloudy) are reported in the D1 dataset, together with the two subsets, NIR-only-cloudy and marginal NIR-cloudy.

An additional quality check on the clear sky radiances is to examine the distribution of the observed radiances labeled clear by the threshold test around the clear sky values. In the D1 dataset, this information is given as the ratio of the number of pixels with IR and VIS radiances just above and below their respective clear sky values (IR>, IR<, VIS>, VIS< in Figure 3.2).

In the D2 dataset, the monthly averages of the total cloud amount and the marginal IR-cloudy amount are calculated for each time UTC and then over all times to produce the monthly mean values. Two adjustments are made to total CA (see Section 3.1.7). In addition to reporting the monthly mean cloud amount, a frequency distribution of individual cloud amounts from the D1 dataset is given.

### Temperatures and Pressures

Layer-average atmospheric temperatures (T) in Kelvins are reported at the center of seven tropospheric layers with nominal center pressures (P): 900, 740, 620, 500, 375, 245, 105 mb. The layers have boundary pressures: 1000 or surface pressure (PS), whichever is smaller, 800, 680, 560, 440, 310, 180, and 30 or tropopause pressure (PT), whichever is larger. Seven troposphere layers are always present in the data, but the actual extent of the bottom and top layers in the troposphere is variable, depending on the values of PS and PT. The former depends primarily on surface topography. As examples, if PS = 850 mb and PT = 100 mb, then the first layer will extend from 850 to 800 mb with a center pressure of 825 mb and the last layer will extend from 180 to 100 mb with a center pressure of 140 mb. If PS = 750 mb and PT = 200 mb, then the first and last layers have no reported values (count values set = 255), the second layer will extend from 750 to 680 mb with a center pressure of 715 mb, and the sixth layer will extend from 310 to 200 mb with a center pressure of 255 mb. As illustrated, the temperatures are reported at the center pressures of these variable layers which are calculated in D1READ and D2READ. There are also two stratospheric temperatures reported at 50 and 15 mb, representing the

centers of two layers with fixed extent from 70 to 30 mb and 30 to 0 mb, independent of the location of the tropopause.

Cloud top temperatures (TC) are reported in Kelvins; the pressure of the atmosphere at the same temperature is reported as the cloud top pressure (PC) in millibars. The D1READ program also calculates the corresponding cloud top heights from the cloud top temperature using the atmospheric temperature profile; the D2READ program uses the differences of cloud top and surface temperatures to estimate a cloud top height using a fixed temperature lapse rate of  $6.5 \text{ K km}^{-1}$ .

Surface temperatures (TS) in Kelvins retrieved from satellite IR radiances represent the brightness temperatures of the solid surface "skin" (usually the first millimeter, but the situation is more complicated in vegetation). Two values of TS are reported, one based on the IR clear sky radiances from the 5-day composites and one based on any available clear pixel IR radiances (if cloud cover is 100%, this value will be undefined = 255). In addition a "surface" temperature based on the TV dataset is reported that represents the near-surface air temperature.

#### Cloud Optical Thicknesses and Water Paths

Cloud optical thicknesses (TAU) are visible ( $0.6 \mu\text{m}$  wavelength) values retrieved using two different cloud microphysical models:

- (i) a liquid water droplet model with a water sphere size distribution described by a gamma distribution with effective mean radius =  $10 \mu\text{m}$  and effective variance = 0.15, and
- (ii) an ice crystal model with a random fractal crystal shape and a -2 power law size distribution from 20 to  $50 \mu\text{m}$ , giving an effective radius of  $30 \mu\text{m}$  and an effective variance of 0.10.

Optical thickness values from individual pixels are averaged with non-linear weights that preserve the average cloud albedo. Water path values are stored in the D1 and D2 datasets as optical thickness values, but they represent linear averages of individual pixel values of optical thickness proportional to cloud water content. The D1READ and D2READ programs convert these values to  $\text{g/m}^2$  by multiplying WP by 6.292 for liquid water clouds and WP by 10.500 for ice clouds.

#### Ice/Snow cover

Sea ice and snow cover are reported as the fraction of the region, without regard for land or water classification, that is covered by either snow or ice. An absence of data is reported as zero coverage.

### **3.1.3. CLOUD TYPE DEFINITIONS**

Since the actual distributions of the cloud properties are not symmetric in shape, the mean and standard deviation do not represent all of the characteristics of the clouds. Hence the D1 dataset also includes explicit distributions of cloud properties for each map grid cell. For diurnal studies based solely on the IR analysis, the number of IR-cloudy pixels with cloud top pressures located in each of the seven tropospheric layers is reported along with the average cloud top temperature of the pixels in each layer. In daytime when visible radiances are available, the number of VIS/IR cloudy pixels is given for each of 42 categories defined by seven cloud top pressure intervals and six optical thickness intervals.

**Table 3.1.1. PC Categories Used to Define Cloud Types.**

PRESSURE LAYERS	PRESSURE	APPROXIMATE HEIGHT ABOVE MEAN SEA LEVEL (m)
	1000 (or surface)	100
1	900	1000
	800	2000
2	740	2600
	680	3200
3	620	4000
	560	4700
4	500	5600
	440	6500
5	375	7600
	310	8900
6	245	10500
	180	12500
7	105	15900
	30 (or tropopause)	19600

**Table 3.1.2. TAU Categories Used to Define Cloud Types.**

TAU INTERVAL	TAU	APPROXIMATE ALBEDO
	0.02	0.005
1	0.50	0.075
	1.27	0.150
2	2.30	0.225
	3.55	0.300
3	6.00	0.400
	9.38	0.500
4	14.50	0.600
	22.63	0.700
5	34.74	0.780
	60.36	0.860
6	109.8	0.915
	378.65	0.970

Original ISCCP plans called for reporting the properties of five cloud types: low, middle, high, cirrus, and deep convective clouds. The latter two types were qualitatively defined to be optically thin and thick high-level clouds, respectively. In the C-series datasets, only the PC and PC-TAU pixel number distributions were reported in the C1 dataset and the average properties of a smaller number of cloud types (low, middle and high from the IR analysis and seven types from the daytime VIS/IR analysis) were estimated in the C2 dataset. Research with these data has shown the value of reporting the average properties of these cloud types more precisely in the D-series datasets. The cloud types for the D1 and

D2 datasets are defined by their values of TC, PC and TAU and differ slightly from the definitions used in the C-series. From the IR analysis, three cloud types (same as for C-series data) are defined by the range of PC: low ( $PC > 680$  mb), middle ( $680 \leq PC < 440$  mb), and high ( $PC \leq 440$  mb). In daytime, nine categories are defined by three PC and three TAU intervals; in C2 data low and middle cloud levels were divided into only two TAU intervals and the TAU value dividing cirrus and cirrostratus increased as PC decreased. The major difference for D1 and D2 datasets is that clouds at lower levels may be either ice or liquid water clouds within the same PC-TAU category, while high level clouds are always ice clouds: if  $TC < 260$  K, a low or middle cloud is classified as an ice cloud, otherwise it is a liquid water cloud. Fifteen cloud types are defined in Table 2.5.7.

In the D1 dataset, the actual average properties (TC, TAU and WP) of each cloud type are reported in addition to their amounts. The amounts of each type are not reported explicitly, but are calculated from the more detailed PC-TAU distribution of pixels by the D1READ program. Consequently, the monthly mean cloud type properties in the D2 dataset are calculated more precisely than they were in the C2 dataset.

### 3.1.4. SPATIAL AVERAGING

The distribution of cloud and surface parameter values for the pixels in each map grid cell represents their variations on small spatial scales (from about 5 to 280 km, cf., Sèze and Rossow 1991a,b). Spatially averaged results are reported every three hours for the whole globe in the Stage D1 dataset in the form of a mean value and a standard deviation. The total number of pixels used to calculate both of these statistics is also reported.

Since the primary objective of ISCCP is to determine the statistical properties of the clouds (and surface) that influence the radiation balance of the Earth, a description of the average properties and their variability must assign proper weight to the cloud and surface values according to their contribution to the total radiation. For example, warmer objects contribute more to the total IR flux than colder objects. Additionally, since the basic measurements used to infer these values are radiance measurements themselves, the relative precision of the measurements is linear in energy rather than in the retrieved parameter. To study cloud microphysical and dynamical processes, we need average quantities that give linear weight to the vertical location of the cloud and the amount of water in it. Hence, the averages of some cloud properties are performed in two ways. The first averaging method uses representations of the values that are linear in their equivalent radiative energy amounts: the cloud and surface temperatures are represented in increments that are linear in radiance and the cloud optical thicknesses have linear increments in reflectance. The surface reflectance is already linear in this sense. The second averaging method is represented by averaging cloud top pressures, which is equivalent to the linear average of cloud top temperature, and a linear average of cloud optical thicknesses reported as an average water path. The water path values are coded as optical thicknesses and converted in the READ programs using the expression

$$WP = \frac{4\rho r_e}{3Q_{ext}} \times \tau \quad \text{g/m}^2 \quad (1)$$

where  $r_e$  is the effective particle radius in microns,  $Q_{ext}$  is the normalized Mie extinction efficiency at  $0.6 \mu\text{m}$  wavelength, and  $\rho$  is the mass density of the cloud particle in  $\text{g/cm}^3$ . For liquid water clouds,



the cloud particle size distribution gives  $r_e = 10 \mu\text{m}$ ,  $Q_{\text{ext}} = 2.119$  and  $\rho = 1.0 \text{ g/cm}^2$ :

$$\text{WPW} = 6.292 \text{ PATH} \quad \text{g/m}^2. \quad (2)$$

For ice clouds,  $r_e = 30 \mu\text{m}$ ,  $Q_{\text{ext}} = 2.0$  and  $\rho = 0.525 \text{ g/cm}^2$ :

$$\text{WPI} = 10.500 \text{ PATH} \quad \text{g/m}^2. \quad (3)$$

The density of an ice particle is determined by the bulk density of ice times the ratio of the actual crystal volume to that of a sphere with the same scattering cross-section.

### 3.1.5. MERGING RESULTS FROM SEVERAL SATELLITES

The D1 data is constructed by combining the analysis results from several satellites, up to five geostationary satellites and two polar orbiting satellites, to obtain complete global coverage every 3 hrs. Since the polar orbiters provide complete global observations twice daily and adjacent geostationary satellites view some overlapping portions of the globe, there are many coincident observations available. Rather than average two or more measurements, usually obtained at somewhat different times within the 3 hr periods and under different viewing geometries, only observations from a specific satellite are used in each map grid cell in each 3 hr period. That is, data from different satellites are merged on a grid cell by grid cell basis, not pixel by pixel.

#### Definition of Satellite Hierarchy

To maintain as much continuity and uniformity as possible, a hierarchy of satellites is specified for each map grid cell, indicating the order of preference when several observations are available. This hierarchy is defined by two general rules: geostationary data are preferred over polar orbiter data equatorward of  $55^\circ$  and preference is given to the best viewing geometry (smallest satellite zenith angle). The transition between geostationary and polar regimes at high latitudes is selected as a compromise between the rapidly increasing satellite zenith angles of the geostationary observations and obtaining sufficient orbit overlap to provide complete diurnal coverage with polar orbiter observations.

Since the preferred satellite data may not always be available, each map grid cell has a specified hierarchy of preference for any other satellites that may observe that location.

#### Global Coverage

Figure 3.3 shows the global coverage provided by the primary satellites (first preference level of the hierarchy) and indicates the next level of the hierarchy of other satellites at each location. At low latitudes, the two polar orbiters do not actually observe the same location at the same time. The figure assumes no INSAT data are available as only one year of data have been obtained to date. The "morning" polar orbiter is used to supplement the "afternoon" polar orbiter coverage. If no data are available from any satellite at a particular location and time, only the map indices and the TV data are reported. No form of interpolation or "bogusing" is used.

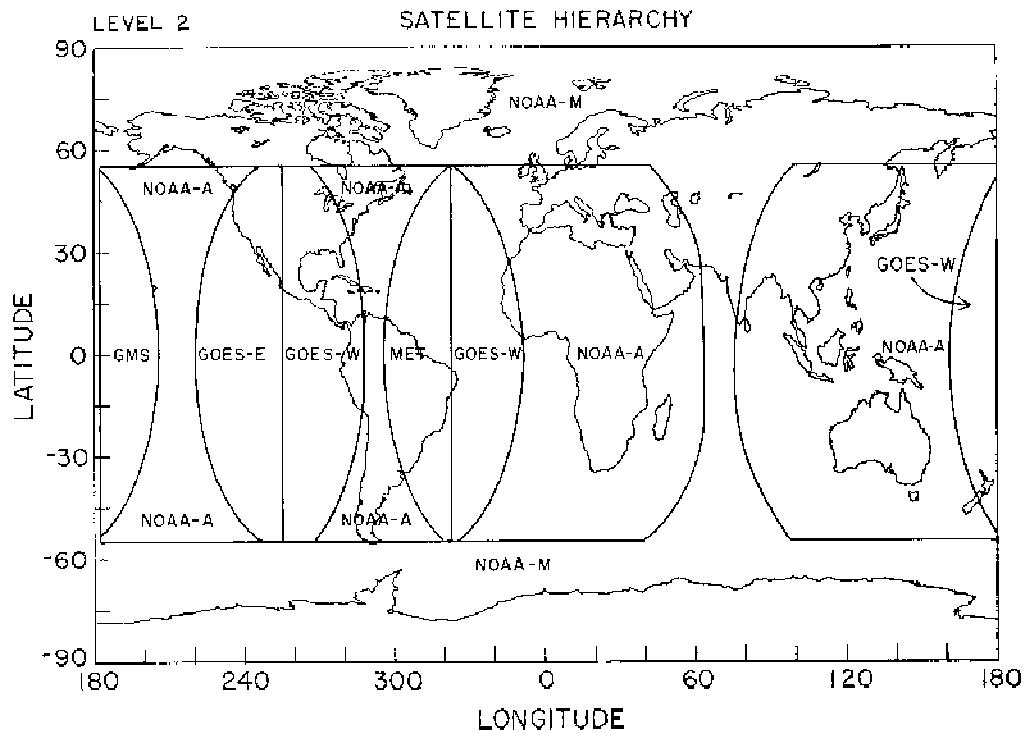
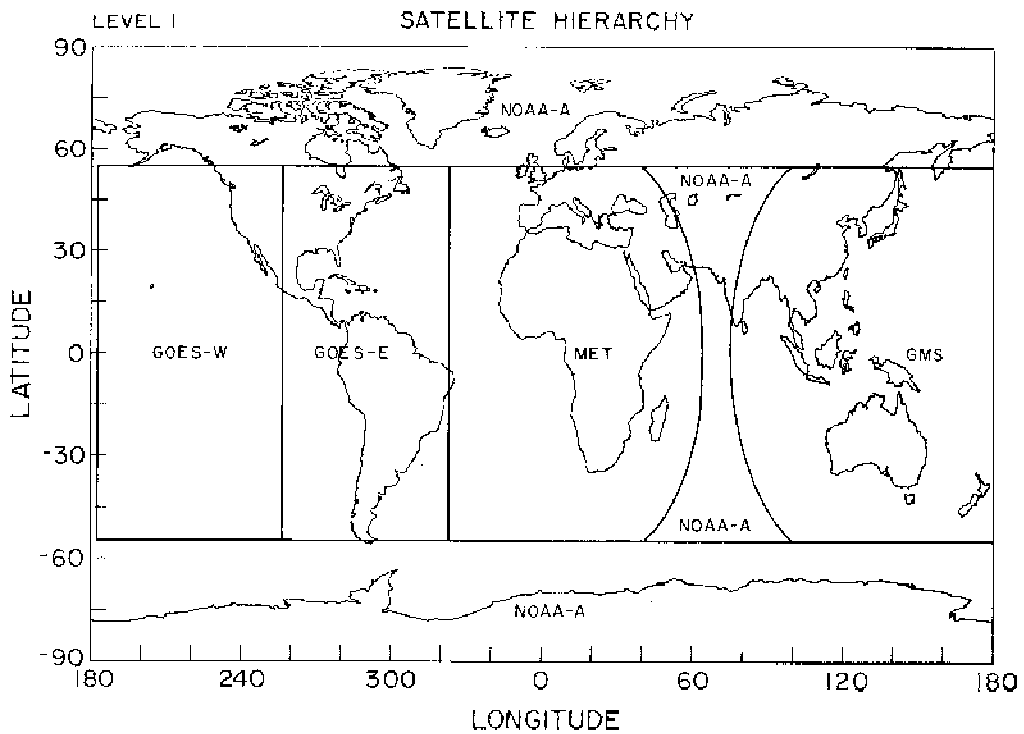


**Figure 3.3.** Regional coverage provided by satellites used for ISCCP: Level 1 of hierarchy indicates the preferred satellite for each location while Level 2 indicates the second choice used if the preferred satellite is not available. There are 4 levels available as indicated in the Ancillary Data Table. The actual satellite used in each map grid cell is reported in the D1 dataset. NOAA-A is "afternoon" and NOAA-M is "morning" orbiter.

## Overlapping Results

The overlap of observations from different satellites provides an opportunity to check the cloud detection algorithm and radiative retrieval model, since the analysis of each dataset is performed independently. Studies of the earlier versions of these data have shown that the cloud amount increases, cloud top pressure decreases, and optical thickness decreases systematically as satellite zenith angle increases (Rossow and Garder 1993b, Zhang *et al.* 1995). In the C1 data, the difference between the cloud amounts and satellite zenith angles was reported whenever two observations were available. Since these differences are relatively small (generally < 10%) and since the DX dataset is now archived, this overlap information is not reported in the D1 dataset. However, the overlapping observations are used in the production stream to check for small residual differences in satellite radiance calibration (see Section 3.1.7).

### **3.1.6. TIME AVERAGING**

A basic objective of the analysis is to summarize the cloud analysis results on a monthly time scale. To preserve information about diurnal variability, the results are first averaged over the calendar month, separately for each time of day, 00, 03, 06, 09, 12, 15, 18 and 21 UTC. These eight datasets are the hour-monthly means. The number of days of observations contributing to the average value is also recorded in each map grid cell. Then, the hour-monthly mean values are averaged to obtain the monthly mean values. Hour-monthly mean values that consist of less than three daily observations are excluded from the monthly mean. Some adjustments are made to the hour-monthly mean datasets before averaging over time-of-day and a small diurnal-sampling adjustment is made to the monthly mean (see Section 3.1.7).

In the D2 datasets the time averages of the spatial standard deviation values from the D1 dataset and the standard deviations over time of the spatial mean values are reported. The number of days contributing to these statistics are also reported.

### **3.1.7. ADJUSTMENTS**

#### Daytime

At pixel level, the analysis is performed using only IR radiances at all times of day and using VIS and IR radiances in daytime. In the Stage D1 data, two different averages for cloud amount and cloud top temperature/pressure are reported for daytime conditions. One version of cloud amount uses the IR-based analysis as must be done for nighttime conditions; the other version combines cloud detections from both the VIS and IR radiances. Because IR radiances are insensitive to low-level clouds, especially broken ones, the VIS radiance analysis detects more low-level cloudiness than the IR analysis. Thus, the combined VIS/IR analysis is superior to the IR-only analysis. Likewise, one version of the cloud top temperature/pressure is obtained directly from the IR radiances as is done for nighttime conditions and the other version adjusts the values consistent with the value of cloud optical thickness retrieved from the VIS radiances. This adjustment is significant only for optically thin clouds, which transmit IR radiation from below the cloud and, consequently, appear to have a higher temperature than they actually do. Thus, the VIS/IR radiative retrieval is superior to the IR-only version. Stage D2 data contain the VIS/IR versions of cloud amount, cloud top temperature and cloud top pressure for daytime locations.

## Nighttime

The mean differences between the VIS/IR and IR-only results during daytime conditions are used to adjust the nighttime results in the hour-monthly mean datasets. Daytime differences between VIS/IR and IR-only values of total cloud amount, mean cloud top pressure and cloud top temperature are linearly interpolated over the nighttime periods between the dusk and dawn values. This interpolated difference is then added to the IR-only value during nighttime. In addition, values of the cloud optical thickness (both TAU and WP) are interpolated over the nighttime period between the dusk and dawn values. The magnitude of the CA, PC and TC corrections is generally  $< 10\%$ ,  $< 100$  mb, and  $< 5$  K, respectively. Larger adjustments occur in near coastal regions, over land and ocean at low latitudes, primarily associated with tropical rainforests and marine stratus regimes. The cloud top pressure and temperature corrections are positive where low clouds predominate, primarily in marine stratus regimes over oceans, and negative where high, thin clouds predominate, primarily over land, especially in desert areas. The adjustments are made only to total cloud properties; cloud type information is not changed.

## Calibration Adjustment

Although procedures are applied to normalize the radiances measured by various satellites to the reference polar orbiter (afternoon) measurements (Rossow *et al.* 1987, 1996, Desormeaux *et al.* 1993), the precision of the normalization procedures leaves small residual differences which can be amplified by the retrieval of physical quantities. Collection of monthly comparison statistics during the processing of the C-series datasets provided more statistical weight with which to estimate these residuals. In regions where more than one satellite provides results, the merger process selects the preferred satellite according to a specified hierarchy that favors data continuity and observations made closer to the nadir view. Frequency histograms of the differences in the overlapping measurements between all pairs of satellites are collected and the modal difference value estimated from the average of the mode value and the three nearest values above and below the mode value. These estimated differences for each satellite when compared to the reference polar orbiter are applied to adjust for small residual radiance calibration differences. The quantities in the hour-monthly mean that are corrected are: cloud top and surface temperature, cloud optical thickness and water path, and surface reflectance.

For the production of the D-series datasets, if the monthly correction factors exceed 1.0 K for temperatures and 0.02 for reflectances, then the Stage B3 radiance calibrations are adjusted and the data re-processed to eliminate such large differences (Rossow *et al.* 1995). Any residual difference is still corrected in the Stage D2 datasets, but the magnitudes are below these thresholds: the adjustments for each month are reported in the Header file 5 on D2 tapes.

The spectral response of the METEOSAT "visible" channel covers a larger range of wavelengths than that of the other radiometers used in the ISCCP analysis; normalization of METEOSAT radiances is done using spectrally uniform targets (clouds and clear ocean areas) (Desormeaux *et al.* 1993). However, the spectral response difference means that surface reflectances determined for vegetated land areas are larger for METEOSAT than for the other satellites. This difference in surface reflectances is reduced in the hour-monthly mean datasets by using regression relations that are obtained from the overlapping METEOSAT and NOAA measurements as a function of vegetation type every month. Adjustment factors are reported in Header file 5 on D2 data tapes.

## Diurnal Sampling Adjustment

Small corrections to the overall monthly mean are made to account for incomplete sampling of the diurnal variations of cloud and surface properties. For locations with less than 4 hour-monthly observations in the polar regions or less than 8 hour-monthly observations at low and middle latitudes, adjustments are determined using the zonally averaged variations of the quantities in local time for the same surface type. The diurnal average is calculated for the number of samples actually available and compared with the average of eight samples to determine the effect of sub-sampling on the diurnal average. The difference is added to the mean values of total cloud amount, cloud top temperature and pressure, cloud optical thickness and water path, and the surface temperature. These adjustments affect only the monthly mean values and are not applied to the individual hour-monthly means.

## 3.2. PIXEL LEVEL ANALYSIS (STAGE DX)

### 3.2.1. OVERVIEW

The ISCCP cloud analysis, shown schematically in Figure 3.4, is applied separately to the Stage B3 radiance data (Schiffer and Rossow 1985; Rossow et al. 1987) from each satellite, together with the TV and IS datasets (see Sections 6.1 and 6.2). The absolute radiometric calibrations of all Stage B3 radiances have been normalized to that of the NOAA-9 AVHRR (Brest and Rossow 1992, Brest et al. 1996; Desormeaux et al. 1993; Rossow et al. 1992, 1996). The analysis is composed of two major

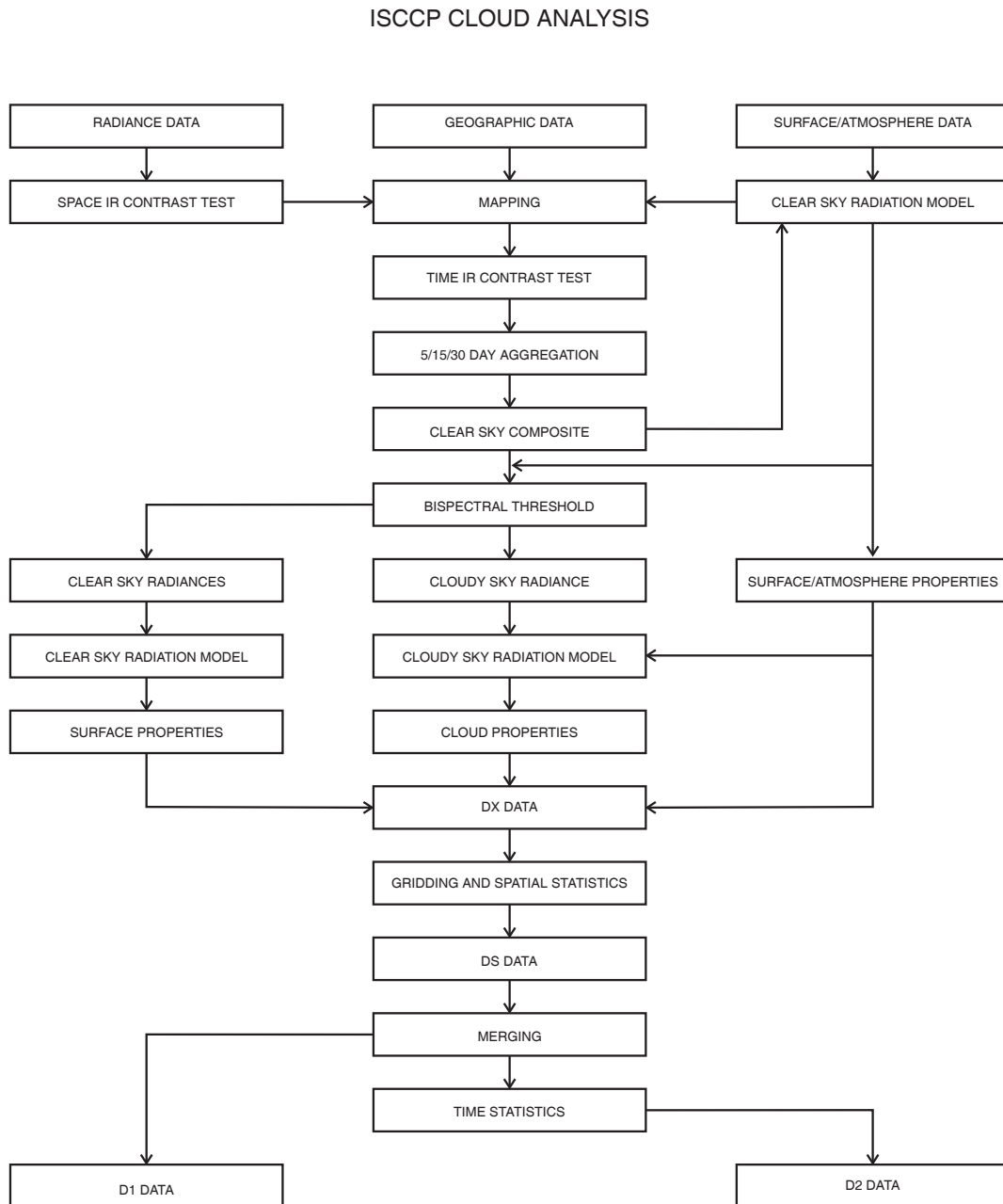


**Figure 3.4.** Schematic of ISCCP cloud analysis.

procedures: the cloud detection procedure divides the B3 radiances into cloudy and clear groups and the radiative analysis procedure retrieves physical properties of clouds and the surface, respectively.

The cloud detection procedure (Section 3.2.4) analyzes the radiance data in four steps: the first two steps represent the original cloud detection procedure used to produce the C-series of cloud products (Rossow and Garder 1993a) with minor revisions and the second two steps are refinements added to produce the D-series cloud products. The first step uses a series of tests of the space-time variations of the IR and VIS radiances to obtain the first estimate of the radiance values that represent clear conditions at each place and time. The second determines which radiance measurements deviate from the first clear sky values by an amount greater than the uncertainty in the estimated clear radiances (first threshold test). The third step conducts an additional series of tests, based on the results of the first two steps, to remove some infrequent errors in the clear sky radiances that occur under certain circumstances. For polar orbiter data, the third step also obtains an estimate of the daytime clear solar reflectances for the near-infrared channel. Together these results are the refined clear-sky radiances. The fourth step is the final threshold test using the refined clear sky radiances and, in the case of polar orbiter data, an additional threshold test for near-infrared radiances over ice and snow-covered surfaces. Cloudy conditions are **defined** by those radiances that are sufficiently different from the clear values in any spectral channel.

The radiation analysis procedure (Section 3.2.5) first retrieves the properties of the surface from the clear sky composite radiances and the atmospheric data for each pixel (ranging from 4 to 7 km in size). These surface properties are then used, along with the same atmospheric properties, to analyze individual pixel radiances. For each individual pixel, **either** surface properties or cloud properties are retrieved from the pixel radiances depending on whether the threshold tests indicate clear or cloudy conditions. When only IR data are available, all clouds are assumed to be completely opaque to IR radiation. When both VIS and IR data are available (daytime only), the IR retrieval is adjusted to account for the effects of variable cloud optical thickness on the radiances. Both the unadjusted (IR only) and VIS-adjusted results are reported in daytime. For the C-series cloud products, the VIS/IR analysis used a single microphysical model representing a liquid water cloud to analyze all clouds. In the D-series cloud products, the analysis uses two models: the original liquid water cloud model and an ice crystal microphysical model. In daytime conditions in the polar regions over snow or sea ice, NIR reflectances are used to aid in the retrieval of cloud optical thicknesses.

### 3.2.2. MAP PROJECTIONS

The input radiance dataset (Stage B3) is in "image" form, a projection of the Earth onto the image plane at the satellite detector; however, motions of the satellites cause variations of the relation between image position and geographic location. To compare the radiances at the same location over the whole month, as required in the cloud detection procedure, all satellite images for each satellite and month are re-mapped into fixed map projections so that each array position represents a fixed latitude/longitude. For the geostationary satellites, the map projections approximate the original image with the sub-satellite latitude/longitude fixed for the whole month (Figure 3.5); these positions may vary from month to month. The GOES and GMS data use the General Perspective, spherical equations (U.S. Geological Survey Bulletin 1532); METEOSAT and INSAT data are projected into fixed views by the satellite operators that appear similar to the General Perspective projections. For the polar orbiter data, two different map projections are used: a simple latitude/longitude grid at low latitudes (between  $-50^\circ$  and  $50^\circ$ ) and a Lambert Azimuthal Equal-Area projection (U.S. Geological Survey Bulletin 1532) for the two polar regions (Figure 3.6).

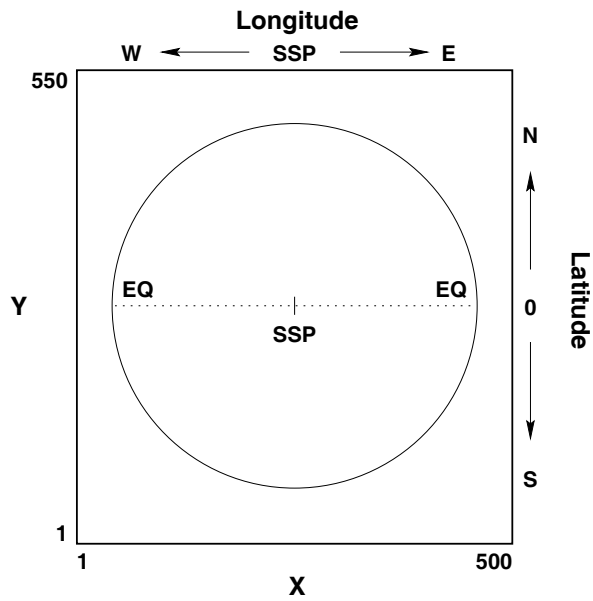


**Figure 3.5.** Geostationary projection with nominal sub-satellite point (SSP) on the equator at a specified longitude. The X,Y coordinates indicate position within DX data array.

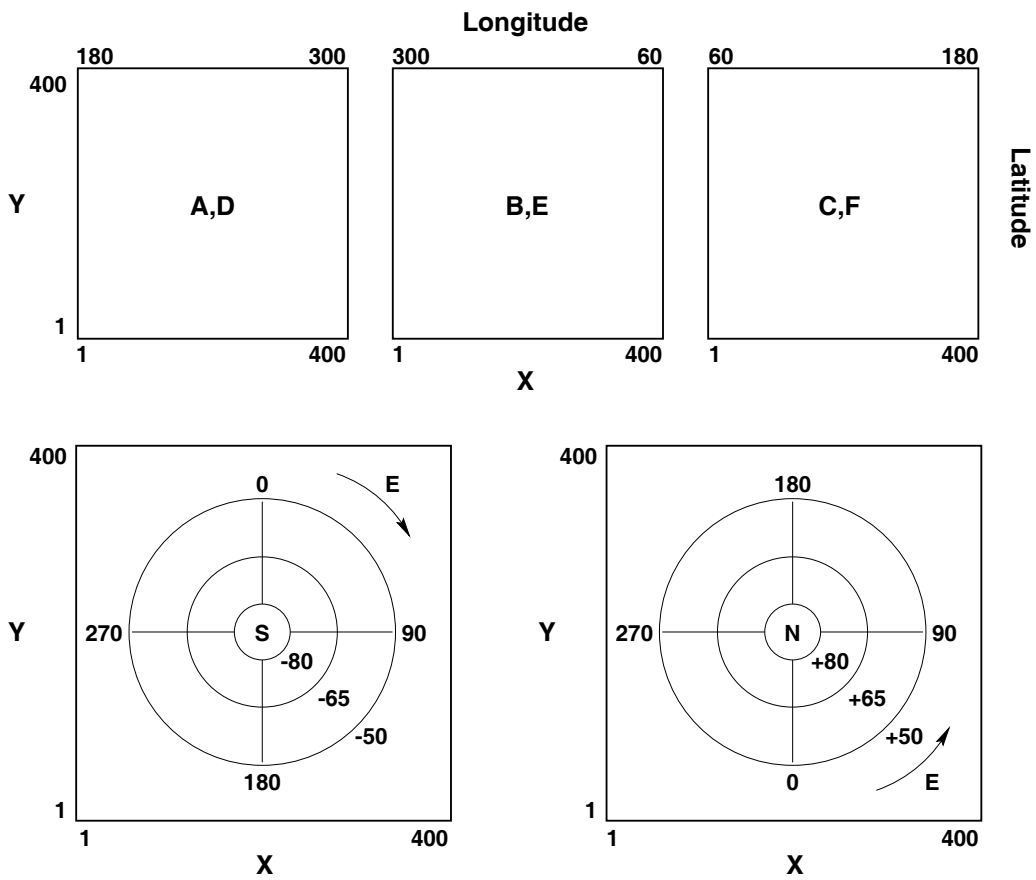


**Figure 3.6.** Geographic regions for polar orbiter DX data. Lower latitudes (A-F) in latitude-longitude grids and two polar cap projections (S,N). The X,Y coordinates indicate position within DX data array.



The original radiance data represent measurements over fields-of-view (FOV) ranging from 4 to 7 km in size at nadir (pixels); however, the Stage B3 data are sampled to a spacing of about 25-30 km. Although navigation accuracy may be higher for some satellites, overall accuracy is confirmed to be about  $\pm 25$  km. The analysis to determine clear radiances uses the sampled data mapped to 25 km resolution; hence, we consider the smaller individual image pixels to represent a *sample* of the distribution of surface and cloud conditions over this larger spatial scale. Although the variability of surfaces and clouds is generally smaller at such small scales than at scales  $\geq 100$  km (Sèze and Rossow 1991), all pixel-level quantities are treated as having a certain amount of intrinsic variation about an average value representing the spatial domain of approximately 25 km in size. In any case, the cloud detection tests and radiative analysis are applied to the original image pixels, so we will continue to refer to the smallest unit of data as a pixel, whether it is the original image pixel or the small 25 km domains from the mapped images.

### 3.2.3. VARIABLE DEFINITIONS

#### Land/Water

At pixel level the basic surface type is either land or water; pixels labeled as coast in the Stage B3 dataset are discarded.

#### Day/Night

Pixels with  $MU0 < 0.2$  (solar zenith angle  $> 78.5$  degrees) are labeled "night". If  $MU0 \geq 0.2$  and VIS information is available, the pixel is labeled "day". If any VIS radiance information is missing and  $MU0 < 0.3$ , the pixel status is changed to "night", otherwise it is discarded.

To avoid spurious diurnal variations of cloudiness caused by changes in methodology associated with the presence or absence of VIS data, the results of two separate analyses are reported during the daytime: one dependent on both VIS and IR information (including NIR results) and one dependent only on IR information. Clear sky IR and VIS radiances are determined independently and all threshold decisions are recorded separately. (Clear sky NIR radiances are also determined independently.)

#### Viewing Geometry

Satellite viewing geometry is defined by the cosine of the satellite zenith angle at the surface point ( $MUE = 0 - 1$ ); the solar illumination geometry is defined by the cosine of the solar zenith angle at the surface point ( $MU0 = 0 - 1$ ) and the relative azimuth angle between the solar and satellite vectors to the surface point ( $PHI = 0^\circ - 180^\circ$ ). *Note: In radiative transfer applications, the relative azimuth angle that is reported is defined as  $180^\circ$  minus the usual geometric relative azimuth angle, which is the difference of two position azimuth angles.*

#### Radiances

Infrared (wavelength  $> 3 \mu\text{m}$ ) radiances are reported as brightness temperatures in Kelvins (165 K - 345 K). Shortwave (wavelength  $< 3 \mu\text{m}$ ) radiances are expressed as scaled radiances, fractions from zero to 1.108. Scaled radiances are calculated by dividing the measured radiance by the value that would be

reflected from a surface with albedo = 1 at the mean sun-Earth distance weighted by the instrument response function.

### Cloudy/Clear Decision (Threshold Results)

For each pixel in the DX dataset, the results of all threshold tests are recorded by reporting the relative relationship between the pixel radiances and the corresponding clear sky radiances. The numerical codes for each radiance indicate how far the particular pixel radiance is from the clear sky value in intervals of the threshold magnitude (see Table 2.5.5 and Figure 3.2).

A pixel is considered cloudy if **any** of the following threshold results is reported: IR code = 4, 5; VIS code = 4, 5 or NIR code = 9, 10, 11, 12 and 13. A clear pixel occurs only when all threshold results indicate clear.

### Cloud Retrievals

Cloud top temperature/pressure values are obtained using three different radiative models: blackbody, liquid water droplet cloud ( $r_e = 10 \mu\text{m}$ ) and ice polycrystal cloud ( $r_e = 30 \mu\text{m}$ ). The first retrieval model assumes that all clouds are blackbodies, ie., the cloud emission temperature, corrected for atmospheric water vapor effects, is its physical temperature. This assumption is equivalent to assuming that all clouds are opaque ( $\text{TAU} > 10$ ) and non-scattering and the results are independent of cloud optical thickness. These values (ITMP and IPRS) are reported for all clouds at all times of day. The other two models determine cloud top temperatures and pressures by correcting for variations in cloud emission and scattering that are functions of the optical thickness and particle size/shape. The results obtained assuming a liquid water cloud model are reported for all cloudy pixels as  $\text{TAU} = \text{VALBTA}$ ,  $\text{TC} = \text{VTMP}$  and  $\text{PC} = \text{VPRS}$ . The results obtained assuming a ice crystal cloud model are reported as  $\text{TAU} = \text{VTAUIC}$ ,  $\text{TC} = \text{VTMPIC}$  and  $\text{PC} = \text{VPRSIC}$  when  $\text{VTMPIC} < 273 \text{ K}$ .

### Clear Retrievals

Surface "skin" temperatures (TS) in Kelvins are obtained from clear IR radiances by assuming that the surface emission temperature, corrected for atmospheric water vapor effects, is its physical temperature. This assumption is equivalent to assuming a surface emissivity of unity at  $\approx 11 \mu\text{m}$  wavelength. Values of TS retrieved from the clear sky composite radiances are present for all pixels (ICSTMP). If the pixel is clear, then ITMP represents the surface temperature retrieved from the measured radiance. The corresponding surface pressures are ICSPRS for the clear sky composite analysis and IPRS for a clear pixel.

Visible ( $\approx 0.6 \mu\text{m}$  wavelength) reflectances (RS), reported as fractions from 0 to 1.108, are obtained from clear VIS radiances of daytime pixels by correcting for variable sun-Earth distance and for Rayleigh scattering and ozone absorption in the atmosphere. The surface is assumed to be an isotropic scatterer in the retrieval, which introduces only a small error for darker surfaces; the actual viewing/illumination geometry is given for each pixel. Values of RS retrieved from the clear sky composite radiances are present for all daytime pixels ( $\text{RS} = \text{VCSALB}$ ). If the pixel is clear, then VALBTA represents the surface visible reflectance retrieved from the measured radiance.

### 3.2.4. CLOUD DETECTION

The first version of the cloud detection procedure is described by Rossow and Garder (1993a, 1993b, see also Rossow *et al.* 1991). Validation is described in Rossow and Garder (1993b) and Rossow *et al.* (1993). The new cloud detection procedure is composed of the original steps, with four minor modifications, plus two new steps.

#### 3.2.4.1. FIRST CLEAR SKY RADIANCES

Clear radiance values are needed for every location at each time (each day for each 3 hour period, separately). Since clouds obscure the view of the surface at some times and do so more or less frequently in different climate regimes, the object of the analysis is to infer the unseen values from the observed values. The accuracy of this procedure is dependent on the frequency of cloudiness at each location (see Rossow *et al.* 1989 and Rossow and Garder 1993a for reviews of the history of methods to detect clouds).

In the first cloud detection step, four basic premises are used to identify clear pixels from an examination of the spatial and temporal variations of radiances: (1) clear pixels are assumed to exhibit less spatial and/or temporal variability than cloudy pixels, (2) clear pixels are assumed to be warmer (larger IR radiance) and/or darker (lower VIS radiance) than cloudy pixels, (3) the first two characteristics vary with surface type (climate regime), and (4) no single test is reliable under all conditions for all cloud types. If the time comparisons are arranged in daily sequences for each UTC separately to avoid confusion with the generally larger diurnal variations of the surface and of the solar illumination, then the time variability tests are much more reliable indicators of cloudiness than the space variability tests. The clear sky radiances are estimated at all locations and times from the result of two tests and the accumulation of three kinds of statistics over two spatial domains and three time periods. The test parameters vary with location to give preference to one type of test over another depending on local characteristics. All these tests are conservative in that any "hint" of contamination is used to discard values, including some actually clear values, to ensure the accuracy of the resulting clear sky radiance values.

The clear sky analysis procedure provides an **estimate** of the clear radiances for every 25 km scene (now called pixel) every three hours; however, the effective space/time resolution attained is about 75 km (IR) or 25 km (VIS and NIR) and 5-days (IR) or 30-days (VIS and NIR). If cloudiness is very frequent, the effective time resolution for IR clear radiances may be reduced to 15 or 30 days. Diurnal variations are resolved, however, by conducting the whole analysis separately at eight diurnal phases.

#### Surface Types and Correlative Data

Four correlative data sets are used to specify different surface types as a function of latitude/longitude: (1) land/water/coast classification (based on a revision of Masaki 1972), (2) topographic height (U.S. Navy dataset from NCAR), (3) land vegetation type (based on Matthews 1983), and (4) sea ice/snow cover (Section 6.2). Individual pixels identified as coast are roughly equal mixtures of land and water at a scale of 25 km and are discarded. The IR clear sky logic uses four different surface types, in order of increasing variability, and the VIS clear sky logic uses eleven surface types (Table 3.2.1).

**Table 3.2.1. Surface Types Used in Clear Sky Analysis.**

TYPE	DEFINITION
IR 1	"low variability" water - all open water except Type 2
IR 2	"high variability" water - water within 75 km of a coastline, water within 50 km of sea ice, or sea ice-covered water
IR 3	"low variability" land - all open land (including land within 50 km of a coastline) or snow-covered land except Type 4
IR 4	"high variability" land - high topography pixels (height > 1750 m), all pixels within 300 km regions that are rough topography (standard deviation of heights > 1000 m) or that are high topography (mean height > 2500 m), or permanently ice-covered locations (Iceland, Greenland and Antarctica).
VIS 1	all open water including near-coastal
VIS 2	sea ice-covered water
VIS 3-5	tree-covered land: tropical rainforest, deciduous forest, woodland
VIS 6-8	"short" vegetated land: shrubland, grassland, tundra
VIS 9	desert
VIS 10	ice-covered land
VIS 11	snow-covered land or within 100 km of snow regardless of permanent vegetation classification

Radiance Angle Corrections

To compare radiances observed at different times, corrections must be made to reduce radiance variations caused by changes in satellite viewing geometry or solar illumination geometry. The main procedure is to make all time comparisons independently for each 3-hr interval of the day (i.e., constant diurnal phase), so that variations of solar geometry and diurnal variations in surface temperature are minimized within one month (variations of actual image time of up to 1.5 hours about the nominal time can occur). The satellite viewing geometry is actually nearly constant for each location in geostationary satellite images. The polar orbiter observations, though nominally sun-synchronous, actually have varying viewing and solar illumination geometries, but the range of angles at each location is limited. Thus, the remaining geometry variations of the radiances are small and can be removed accurately enough by simple transformations.

For the IR, the radiances (as brightness temperatures) are corrected to a nadir view using

$$T(1) = T(\mu) + C_0(\mu) + C_1(\mu) [ T(\mu) - 250 ]$$

$$C_0(\mu) = - (1.93 + 2.520\mu) (1/\mu - \mu) / 4.8$$

$$C_1(\mu) = (0.267 + 0.053\mu) (1/\mu - \mu) / 4.8$$

where  $\mu$  is the cosine of the satellite zenith angle and the numerical coefficients were derived by a best fit to radiative transfer model calculations using a global distribution of seasonal mean TOVS temperatures and humidities. The factor  $(1/\mu - \mu)$  is the function used to interpolate between two brightness temperature values; the extra factors involving  $\mu$  arise because the correction procedure must approximate the dependence on  $T$  (first atmospheric level) and the surface temperature by using the observed brightness temperature,  $T(\mu)$ . The radiative model is the same one used later in the analysis of the satellite IR radiances (Section 3.2.5). This formula fits all the data to within about 1-2 K. Since the polar orbiter data are limited to  $\mu > 0.45$ , the errors in using the same formula for all latitudes and seasons are actually  $\leq 1$  K.

For the VIS, the radiances are corrected to nadir sun using

$$R(\mu_0) = \mu_0 R(1)$$

where  $\mu_0$  is the cosine of the solar zenith angle and is the value for the actual image **pixel** time and location. This correction neglects the weak anisotropy of land surface reflectances and the  $\mu$ -dependence of Rayleigh scattering and ozone absorption, which partially offset each other. Tests of the errors introduced by neglecting these effects show that they are  $\leq 0.01$ - $0.02$  (absolute) for the range of geometries encountered by the polar orbiter at any one location. Only the very dark water surfaces are affected noticeably by this approach; however, we compare the resulting clear VIS radiances to a water reflectance model to eliminate cloud contamination, so that this effect is also removed. The corrected values are true reflectances only for the sun at the mean sun-Earth distance.

### Tests for Clear Conditions

The first pass through the B3 data tests the spatial variability of the IR radiances within small regions (about 100 km over land and 300 km over water). This test is performed in the original satellite image coordinates for convenience. All pixels determined to be colder (by 3.5 K over water and 6.5 K over land) than the locally warmest pixel are labeled CLOUDY; all others (including the warmest) are labeled UNDECIDED.

The radiance images are then corrected for viewing geometry effects and mapped onto fixed map grids with a resolution approximating the nadir resolution of the original images (25 km). The second pass through the B3 data then tests the time variability of the IR radiances over three days at the same time each day (each UTC is tested separately over the whole month). All pixels determined to be colder (by 3.5 K over water and 8.0 K over land) than the values at the same location on the previous or following day are labeled CLOUDY; all pixels found to have a similar temperature (to within 1.1 K over water and 2.5 K over land) as they have on the previous or following day are labeled CLEAR. The remaining pixels with intermediate variability are labeled UNDECIDED. On some occasions, the test result for one direction in time will conflict with the result in the other direction; if the conflict is strong (i.e., CLOUDY and CLEAR are determined), these cases are labeled MIXED. The UNDECIDED result is not considered a strong conflict.

The final classification of the IR radiance for each pixel is determined by the following logic (Figure 3.7):

TIME TEST RESULT	SPACE TEST RESULT	
	CLOUDY	UNDECIDED
CLOUDY	CLOUDY	CLOUDY
UNDECIDED	CLOUDY	UNDECIDED
MIXED	MIXED	MIXED
CLEAR	MIXED	CLEAR

**Figure 3.7.** Space-Time classification logic.

### Clear Sky Statistics - IR

From the classified data, several statistics are collected over 5-day periods at each UTC, separately, to be used in the IR clear sky composite tests:

- (i) the number of CLEAR observations, NCLEAR, in a spatial domain, centered on each pixel and including its nearest neighbors (a region about 75 km in size),
- (ii) the average IR brightness temperature, TAVG, for all CLEAR observations in this domain, and
- (iii) the two largest values of IR brightness temperature, TMAX1 and TMAX2, for all observations in this domain.

If  $TMAX1 - TMAX2 > 12$  K for any individual 5-day interval, then  $TMAX = TMAX2$ ; otherwise  $TMAX = TMAX1$ . The 5-day values of NCLEAR, TAVG and TMAX are the short-term values (NCLEAR-ST, TAVG-ST and TMAX-ST) and are used to calculate long-term values (NCLEAR-LT, TAVG-LT, and TMAX-LT). For surface Type 1 (open water), short-term is taken to be 15 days and long-term is 30 days; for surface Types 2, 3, and 4, short-term is 5 days and long-term is 15 days. If the total number of observations available in a 5-day interval is less than 15, the comparison of TMAX1 and TMAX2 is not performed; if the total number of observations is less than 3 in a 5-day interval, then no clear sky analysis is performed at all for that location.

Because of slow seasonal trends of surface temperature, TMAX for one month may be biased towards the earlier or later part of the month. To correct for this effect, the modes of the differences between the two 15-day values of TMAX in each  $2.5^\circ$  latitude zone for each surface type are used to calculate a linear trend correction to TMAX for each 5-day period in the month. This correction is performed only if the number of pixels in each latitude zone for a given surface type is  $> 300$  and if the fraction of the total number of pixels that have different values of the two TMAX values is  $\geq 65\%$ .

### Clear Sky Statistics - VIS

For each daytime pixel, the value of RMIN is calculated from all the VIS radiances for each 5-day period (RMIN-ST) and for a 30-day period (RMIN-LT); RMIN is calculated for 5-day and 15-day periods poleward of 50° latitude. If any nighttime data are found in the record within the 30-day (or 15-day) period for a particular pixel, no RMIN value is reported and the classification of that pixel is changed to "nighttime" for all days within the month.

### Clear Sky Compositing - IR

Intercomparison of all the pixel statistics determines the estimate of the clear radiance for each pixel every five days, separately at each diurnal phase. These radiance values are called the clear sky composite; the comparison logic is illustrated in Figure 3.8.

The IR clear sky compositing logic assumes that the relatively small variations of surface temperatures (at constant diurnal phase) and their (almost global) tendency to be larger than cloud temperatures produce a characteristic shape of the warmer part of the IR radiance distribution that varies with surface

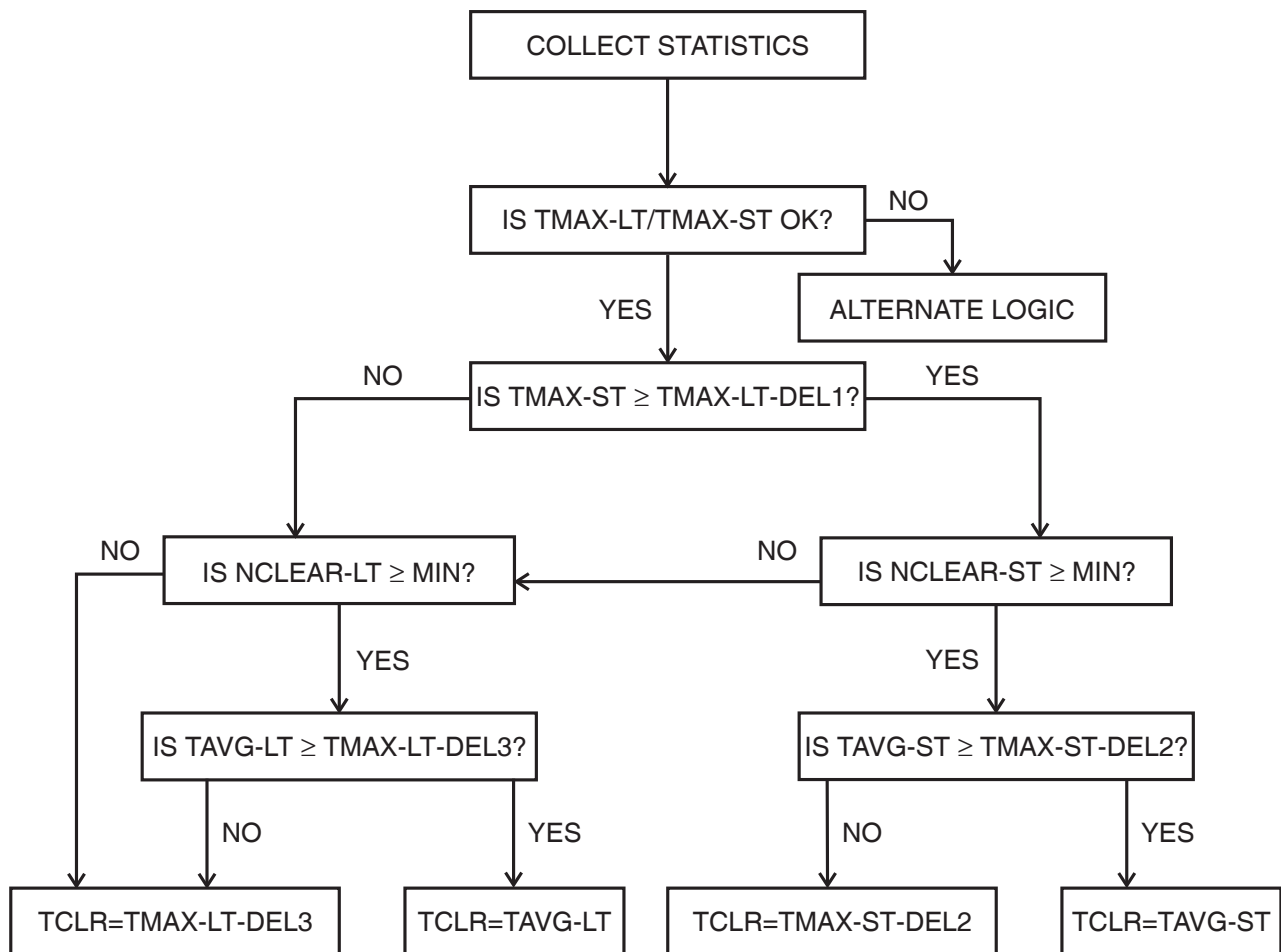


Figure 3.8. Infrared clear sky radiance compositing logic.

type (Seze and Rossow 1991a, Rossow and Garder 1993a). The composite logic tests the shape of the IR radiance distribution using the differences between TMAX-LT and TMAX-ST and between TMAX and TAVG (either short- or long-term). If the differences exceed their specified magnitudes, this is interpreted to indicate cloud contamination of one or more of these quantities. Cloud contamination is assumed to decrease over larger time intervals. An additional use of this shape assumption is to reduce TMAX values, whenever they are used for the clear radiance, to approximate the TAVG values, using the assumed maximum difference between TMAX and TAVG.

Five situations may occur.

- (i) The pixel is partially cloudy but the cloudy-clear contrast is very low or the cloudiness is complete and constant with cloudy radiances that exhibit little space *and* time variability.
- (ii) The pixel is mostly cloudy and the cloudy-clear contrast is relatively small, but still larger than the variability of the surface, or cloud persistence and extent are large but not total.
- (iii) The pixel is mostly cloudy but the cloudy radiances exhibit relatively large variability in space and/or time.
- (iv) The pixel is partly cloudy (spatially) or almost totally cloudy occasionally and the cloudy-clear contrast is relatively large.
- (v) The pixel is relatively clear.

The first and last case resemble each other in that the magnitude of the cloudy radiance variability in case 1 is similar to that in case 5 or the cloud cover is complete for 30 days with little variation in cloudy radiances. If this resemblance is strong enough, there is no way to detect such clouds using satellite data alone (see discussion in Rossow and Garder 1993a).

In case 2, either the radiance variations caused by cloudiness are relatively small or almost no observation represents completely clear conditions. This is indicated by the fact that  $TMAX-LT > TMAX-ST + DEL1$  and  $TAVG-LT + DEL3$ , in which case the estimate of clear radiance is  $TCLR = TMAX-LT - DEL3$  (see Table 3.2.2 for values of DEL1, DEL2, DEL3 and DEL4). The value of TMAX-LT used has been corrected for any zonal mean trend over the month. The larger variability of land surface temperatures makes this test much less effective over land than it is over water.

In case 3, in contrast to case 2, the cloudy radiance variability is large enough that the space/time tests detect the clouds. That the location is mostly cloudy is indicated by a very low NCLEAR value. If this condition persists for most of the 30-day period ( $NCLEAR-LT < 10\%$ ), then the estimate of  $TCLR = TMAX-LT - DEL3$ , where TMAX-LT is for 30-days, even for surface Types 2, 3, and 4. If the condition only occurs on the short-term ( $NCLEAR-LT \geq 10\%$ ), then the estimate of  $TCLR = TAVG-LT$ . In both case 2 or 3 (when the long-term information is used for TCLR), the consistency of the result is maintained by ensuring that the value of TCLR obtained is  $\geq TMAX-ST - DEL2$ . This test is more effective over land than over ocean.

In case 4, while there are enough CLEAR values available on the short-term, there is still enough cloud contamination that  $TMAX-ST > TAVG-ST + DEL2$ , in which case  $TCLR = TMAX-ST - DEL2$ .

In case 5, the CLEAR values provide an accurate measure of the clear radiances; the best estimate for the whole 5-day period is  $TCLR = TAVG-ST$ .



**Table 3.2.2. Radiance Difference Values Used in IR Clear Sky Composite Tests.**

SURFACE TYPE (Table 3.2.1)	DEL1	DEL2	DEL3	DEL4
1	2.0	2.0	2.5	4.0
2	4.0	3.0	4.0	6.0
3	6.0	5.0	8.0	8.0
4	9.0	7.0	11.0	10.0

Since the compositing tests rely on the relationships with TMAX values, some protection is required to prevent false results because of a few spurious data values that occasionally represent very large temperatures. The protection procedure compares the value of TMAX-LT for each pixel against the regional distribution of these values: if the particular TMAX-LT – DEL4 > the regional modal value **and** its corresponding TAVG-LT, then this value is replaced using the regional distribution. If a value of TMAX-LT is determined to be too large by this procedure, any value of TMAX-ST that is too close to TMAX-LT is also avoided. In practice this procedure is not very successful, so it is augmented by the 5-day TMAX test described above; and consequently, it is very rarely invoked.

A spatial filter was applied in the old analysis procedure (Rossow and Garder 1993a), but it has been eliminated from the new procedure.

Clear Sky Compositing - VIS

The VIS clear sky compositing logic (Figure 3.9) assumes that the small variations of surface reflectance (at approximately constant viewing and illumination geometry) and their almost global tendency to be smaller than cloud reflectances produce a characteristic shape of the darker part of the VIS radiance distribution (Sèze and Rossow 1991a, Rossow and Garder 1993a). Time variations for surface reflectances for most surface types are generally much smaller than the spatial variations. The relatively simpler time/space behavior of surface reflectances allows use of a simple statistic: the minimum VIS radiance over a sufficiently long time period to insure that clear conditions occur. However, this approach does bias the actual clear radiance value (Matthews and Rossow 1987, Rossow *et al.* 1989), so the same shape assumption is used to increase the minimum value by an amount representing the typical separation of the minimum and the mean value.

The eleven surface types (Table 3.2.1) are grouped into five categories: (1) variable water, (2) rapidly time-varying land, (3) temporally constant, spatially heterogeneous land, (4) constant water, and (v) spatially/ temporally constant land.

- (1, 2) Variable water and rapidly varying land are determined by the presence of sea ice cover and snow cover, respectively (permanently ice covered land is treated as snow covered land). These two surfaces also have reflectances that are more nearly the same as those of clouds, so that the VIS radiance contrast is low. The clear radiance  $RCLR = RMIN-ST + DEL1$ .
- (3) Some locations exhibit relatively large spatial variations of surface reflectance but small time variations (Sèze and Rossow 1991a): these types are high topography regions (because of stronger solar zenith angle dependence and shadowing effects), deserts, tundra, and grasslands.  $RCLR = RMIN-LT + DEL2$ .

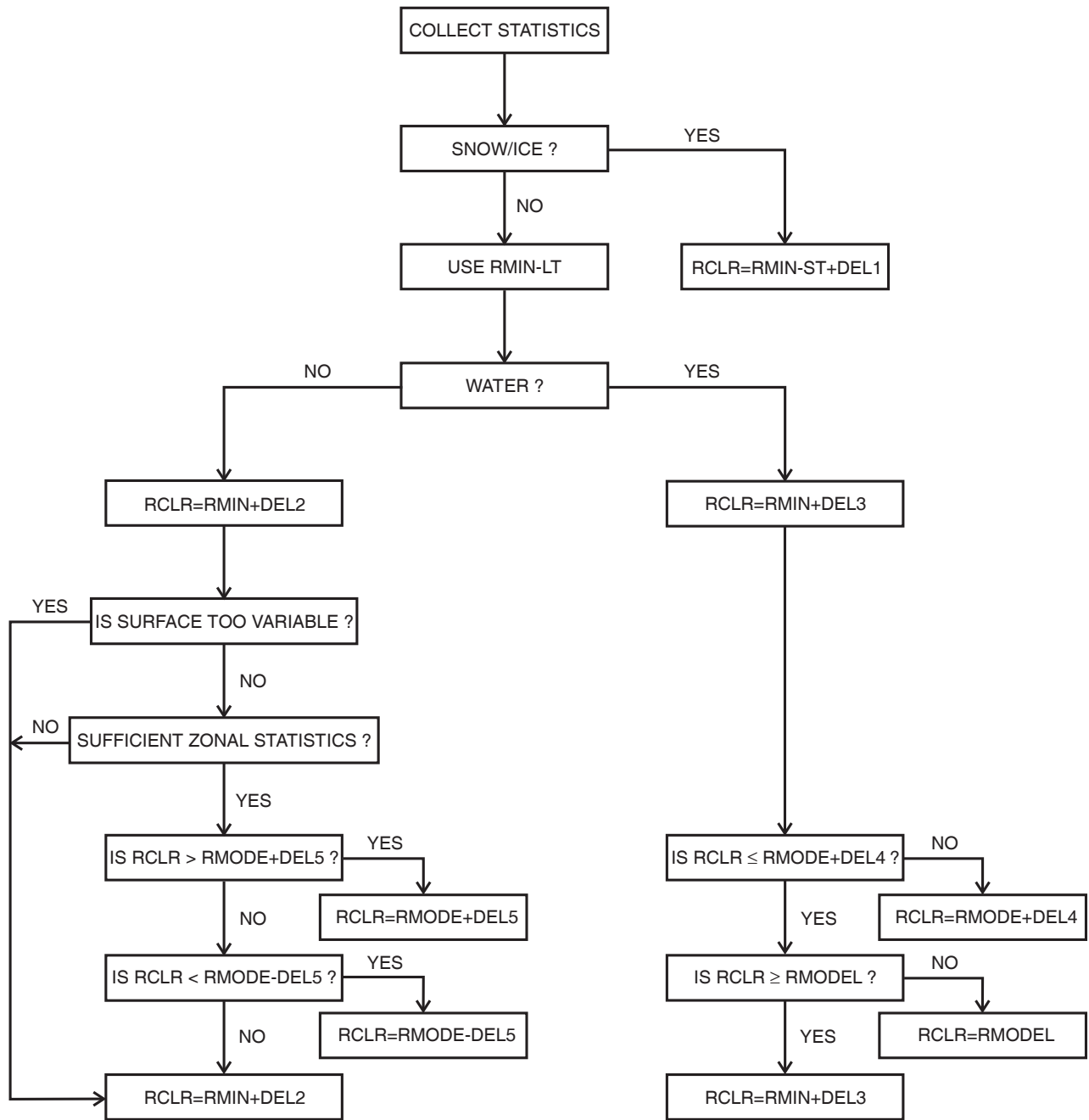


**Figure 3.9.** Visible clear sky radiance compositing logic.

- (4) Open water generally exhibits constant reflectance in time and space at constant viewing/illumination geometry; however, since the viewing/illumination geometry for satellites varies (especially for the polar orbiter), the observed reflectance varies more because of the strong anisotropy of the surface. In particular, the reflectance of sun glint is highly variable because of the variation of surface roughness with surface winds.  $RCLR = RMIN-LT + DEL3$ . This value is not allowed to deviate from an empirical model of water VIS reflectance (derived from the model of Minnis and Harrison 1984). The model includes an additional augmentation for glint conditions. For a conservative estimate of the reflectance,  $RMODEL + DEL4 \geq RCLR \geq RMODEL$ .
- (5) The surface types that are spatially as well as temporally homogeneous are vegetated land surfaces: shrubland, woodland, forest and tropical rainforest.  $RCLR = RMIN-LT + DEL2$ ; however, the individual values are compared to the distribution of values for the same surface type in  $10^\circ$  latitude zones and are required to meet the condition:  $RMODE + DEL5 \geq RCLR \geq RMODE - DEL5$ .  $RMODE$  is the peak value of the distribution. If  $RCLR$  for a particular pixel is outside the range, it is re-set to the nearest value in the range.

The DEL values in scaled radiances are:  $DEL1 = 0.050$ ,  $DEL2 = 0.035$ ,  $DEL3 = 0.015$ ,  $DEL4 = 0.030$  and  $DEL5 = 0.060$ .

#### First Clear sky radiances

The clear sky composites are constructed for every pixel for every 5-day period. Note, however, that the IR clear sky composite procedure uses some nearest-neighbor information; thus, the effective spatial resolution of the IR composite is about 75 km. The composite radiances have had the viewing geometry dependence removed before compositing, so in the threshold step the nearest-in-time clear sky composite is selected and the **inverse** angle corrections applied, using the specific viewing geometry for each pixel in that image. Thus, although the values in the clear sky composites are held constant over 5-day periods, the clear radiances used to detect clouds can undergo some day-to-day variation as viewing geometry varies.

Glint geometry over water is determined by the magnitude of the solid angle between the specularly reflected solar illumination vector direction (the outgoing direction not the incoming direction) and the actual satellite view vector direction. The reflected solar vector direction is defined by the solar zenith angle,  $\theta_0$ , where  $\mu_0 = \cos(\theta_0)$ , and a position azimuth angle; the satellite view vector is defined by the satellite zenith angle,  $\theta$ , where  $\mu = \cos(\theta)$ , and another position azimuth. In radiative transfer applications, the relative azimuth angle,  $\phi$ , is defined as  $180^\circ$  minus the difference of the usual position azimuth angles. Thus, the solid angle,  $\alpha$ , between these two vector directions is given by

$$\cos(\alpha) = \cos(\phi) [ \cos(\theta_0) \cos(\theta) + \sin(\theta_0) \sin(\theta) ]$$

Glint conditions are defined by  $\alpha < 30^\circ$ . An empirical model of water reflectance replaces the clear sky composite values in glint conditions. The model is based on a four month (one from each season) survey of clear sky radiances from the C-series cloud analysis for geostationary and polar orbiting satellites.

### 3.2.4.2. FIRST CLOUD DETECTION THRESHOLDS

The status of each individual pixel, CLOUDY or CLEAR, is decided by threshold tests for each spectral radiance, independently and without regard to the labels previously assigned in the clear sky composite analysis. In order to improve the detection of cirrus and low-level clouds, single channel detections are allowed. Thus, using the clear sky radiances derived for each location and time, any pixel with **any** radiance value that is sufficiently different from the corresponding clear sky radiance is declared to be CLOUDY. The magnitude of the difference required (called the threshold) is set by the estimate of the uncertainty in the clear radiance values. All remaining pixels are called CLEAR.

The success of the overall cloud detection is indicated by whether the clear sky composite analysis and threshold labels generally agree or not (Rossow and Garder 1993a): more than 90% of pixels labeled as cloudy or clear in the clear sky composite analysis are similarly labeled by the threshold decision. The pixels in the undecided category are usually divided into cloudy and clear in rough proportion to the number of pixels already labeled as cloudy or clear.

The magnitudes of the thresholds vary with the IR surface types defined on page 61, but sea ice is treated as Type 3 for VIS. Note that the VIS threshold test is performed, **not on reflectances, but on radiances**, which are represented as fractions of the instrument response obtained when measuring the full solar flux. IR radiances are represented as brightness temperatures in Kelvins. The threshold values used are:

**Table 3.2.3. First Cloud Detection Threshold Values.**

RADIANCE	SURFACE TYPES (Table 3.2.1)			
	1	2	3	4
IR (K)	2.5	4.0	6.0	8.0
VIS	0.03	0.03	0.06	0.06

In the old version of the cloud detection algorithm, there were a few specific exceptions to these threshold values, but these have been eliminated in the new version. The most important difference that this introduces is to reduce the effective VIS threshold over snow and ice surfaces from 0.12 to 0.06.

### 3.2.4.3. FINAL CLEAR SKY RADIANCES

In the old cloud detection procedure, the above threshold tests of the IR and VIS radiances (only IR at night) were the last step. In the new cloud detection procedure, there are two additional steps. In the third step, some small refinements are made to the clear radiances based, in part, on the results of the first threshold tests. In addition in polar orbiter data (from AVHRR), radiances measured at 3.7  $\mu\text{m}$  are processed, using the results of the first threshold step, to obtain clear sky composites: in daytime the thermal emission contribution is removed to obtain composite solar reflectivities and at night the composite difference of 3.7  $\mu\text{m}$  and IR brightness temperatures is obtained.

## IR Clear Sky Refinements

The results of the first two steps for a whole month are examined several times at each time of day UTC, separately. The first pass through the data identifies the two largest brightness temperatures (called TMAX1 and TMAX2) for each pixel and classifies each pixel into one of five types (note that these five types differ from the four types used in the first clear sky analysis - see Table 3.2.1):

Type 1 = near-coast land and water, high topography if not covered by ice

Type 2 = open water, water that is in the margin zone near sea ice or covered by sea ice for only part of the month

Type 3 = water fully covered by sea ice all month

Type 4 = open land, land that is in the margin zone near snow or covered by snow for only part of the month

Type 5 = land covered by snow all month, land ice

In the second pass, a HOT flag is set for each pixel where  $TMAX1 - TMAX2 > 10$  K, except for Type 1. In a third pass, the neighboring pixels in a 5x5 domain around each flagged pixel are checked to see whether any unflagged pixel in the same class has a TMAX value larger than the flagged value. If so, the flag for the center pixel is turned off.

The fourth pass through the dataset re-creates (with angle corrections made) the complete 5-day IR clear sky radiance maps for each UTC, separately, that resulted from the first part of the cloud analysis. In addition, flags are set for each pixel indicating which short-term or long-term statistic (TAVG-ST, TMAX-ST, TAVG-LT, TMAX-LT) was used for the original clear sky radiance (see Section 3.2.4.1). Results from the old cloud analysis indicated that the values of DEL2 and DEL3 separating short-term and long-term TMAX and TAVG for land pixels, respectively, were too large. Hence, the IR clear sky radiances for snow-free land pixels are increased by 1.0 K when TMAX-ST was used and by 1.5 K when TMAX-LT was used; the clear sky radiances are increased by 2.0 K for snow-covered land when TMAX-LT was used.

Next, three procedures are applied to each 5-day map to correct for spuriously large IR brightness temperature values (TCLR), to correct for the effects on TCLR near coast lines of errors in image navigation, and to correct for some cases of residual cloud contamination. The first procedure reads each map, together with the values of TMAX1 and TMAX2 collected over the whole month for each corresponding location. All pixels that are not Type 1 and do not have the HOT flag set are tested: if  $TCLR > TMAX1 + 1.0$  K, then the HOT flag is set. A 5x5 domain around each pixel with a HOT flag set and TCLR greater than the average of TMAX1 and TMAX2 is searched for all values of TCLR in the same type without a HOT flag set. If at least two such neighbors are found, then the flagged value of TCLR is replaced by the average TCLR of all these neighbors and the flag turned off. If insufficient neighbors are found, nothing is done.

The second procedure searches each clear sky map for unflagged land or open water pixels that are within 75 km or 50 km of a coastline, respectively. A 7x7 domain about each target pixel is examined

for unflagged pixels that are the same type, land or water, as the target. If any sea ice is found within the domain, this procedure is skipped. The average TCLR values are calculated for the pixels of the same type, TSAME, and for the pixels of the opposite type, TOPP, as long as at least two unflagged values are available. If there are insufficient values available, the procedure is skipped. If the absolute value of TSAME – TOPP is  $> 6.0$  K, there is a strong contrast of clear sky brightness temperature at the coast. If, in addition, the target pixel TCLR differs from TOPP by no more than  $\pm 2.5$  K, this is assumed to mean that the "opposite" type has contaminated the clear sky map because of navigation errors in locating the coastline, so a flag is set for the target pixel. Once all pixels have been examined, flagged values of TCLR are replaced by TSAME and flags turned off.

The third procedure examines  $3\times 3$  and  $5\times 5$  domains around each pixel (except Type 1 pixels); if any neighboring pixel is Type 1, a different land/water category or a different snow/ice category than the center pixel, nothing is done. For homogeneous regions with at least three neighbors in either the  $3\times 3$  domain or the  $5\times 5$  domain, the spatial variance of the TCLR values is calculated. If a variance is available and it exceeds  $0.6$  K over open water or  $7.6$  K over land, then the smallest TCLR value is flagged as COLD. Once flags have been set, the flagged TCLR values are replaced by the average TCLR of any unflagged neighbors.

### VIS Clear Sky Refinements

The results of the first two steps for a whole month are examined several times at each time of day UTC, separately. The first pass collects for each UTC, separately, the two lowest VIS radiances for each pixel, RMIN1 and RMIN2. The second pass re-creates (with angle corrections made) the 5-day VIS clear sky radiance maps for each UTC that resulted from the first part of the cloud analysis. In the third pass, the original VIS clear sky radiance, RCLR, for each pixel is compared with RMIN1 and RMIN2 in different ways depending on the cloudy fraction of the pixels in a  $5\times 5$  domain centered on that pixel. In the case of smaller cloud amounts, disagreement among these values is interpreted to be caused by cloud shadows that cause the RMIN values to underestimate the proper VIS clear sky radiance, particularly over more reflective surfaces. In the case of larger cloud amounts, disagreements are interpreted as cloud contamination of the RMIN values. This comparison is not performed in the polar regions (latitudes poleward of  $50^\circ$ ), for ice or snow-covered pixels, or for water pixels in sunglint geometry. For sunglint open water, the clear sky radiances are replaced by a revised empirical model. If cloud fraction is  $< 0.80$  and  $RMIN2 - RMIN1 > 0.05$ , then if the corresponding value of  $RCLR < RMIN2$ , RCLR is replaced by RMIN2. If cloud fraction is  $\geq 0.80$  over ocean and RCLR is more than  $0.03$  larger than the average of RMIN1 and RMIN2, then RCLR is replaced by the average plus  $0.03$ . If cloud fraction is  $\geq 0.80$  over land and  $RCLR \geq RMIN1 + 0.03$ , RCLR is replaced by RMIN1.

### NIR Clear Sky Radiances (polar orbiter data only)

Radiance data from the AVHRR on the NOAA polar orbiters are obtained at additional wavelengths besides IR and VIS. To improve detection of low-level clouds in the polar regions, additional tests have been added to the cloud detection procedure using  $3.7 \mu\text{m}$  radiances (called NIR). At night, the radiances at this wavelength are thermal infrared emission. During daytime, the radiances at this wavelength are dominated by reflected sunlight; but some thermal emission is included. Because the signal-to-noise ratio at this wavelength can be low, a statistical check is performed for each image, separately for each UTC (polar orbiter data is also segmented into three geographic regions, north and south polar and low latitudes, so separate statistics are checked for each region). All NIR radiances are collected into a

frequency histogram for each image (all brightness temperatures < 222 K are excluded). If the histogram has less than 1000 pixels or any single brightness temperature occurs more than 15% of the time, then no further use is made of the NIR radiances for that image. To construct clear sky maps, a whole month of data is analyzed for each time-of-day UTC, separately.

For **nighttime** images a frequency histogram of the difference between NIR brightness temperature (TNIR) and IR brightness temperature (TIR) in Kelvins is collected for pixels labeled as clear by the first IR threshold tests. Radiances from pixels for which TNIR < 222 K or TIR < 230 K are excluded. Histograms are produced for four surface types: open water, all other water, open land, and all other land. The mode value in each histogram is determined. If the histogram is composed of less than 5000 pixels, if the mode value is < -11 K or > 9 K, or if there is a secondary mode value separated from the first by more than 10 K, no further NIR tests are made. Valid mode values represent the clear sky values of the NIR and IR brightness temperature difference, which is nearly zero for most surfaces at high latitudes where atmospheric effects are weak.

For **daytime** images all NIR radiances in pixels determined to be clear by the first IR and VIS threshold tests and with TNIR ≥ 222 K and TIR ≥ 230 K are converted to top-of-atmosphere reflectances (at mean sun-Earth distance):

$$RNIR = (RAD_3 - RAD_4) / (\mu_0 S_3)$$

where RAD<sub>3</sub> is the observed radiance (energy) in the instrument bandpass at 3.7 μm, RAD<sub>4</sub> is the radiance at 3.7 μm produced by a black-body with a physical temperature equal to the observed brightness temperature at 11 μm, and S<sub>3</sub> is the amount of sunlight in the instrument bandpass at 3.7 μm reflected from a surface with unit reflectivity. The two lowest values of RNIR are collected for each pixel, except those with a BAD quality flag. Clear sky values for RNIR are determined as the average of the two lowest values, if they are available for that pixel, and, if they are not available, the clear sky value is the average over other pixels in the same land/water category in a 5×5 domain centered on that pixel. The clear sky values of RNIR are then increased by 0.02 for all surface types, except open land for which they are increased by 0.03.

#### 3.2.4.4. FINAL THRESHOLDS

The final new part of the cloud detection procedure (fourth step) is to repeat the threshold tests using the final clear sky radiances with three changes: the IR thresholds for land surfaces (Types 3 and 4) are reduced by 2.0 K, the VIS threshold test is changed to a test of **reflectance** values instead of **radiance** values and a NIR threshold test is added over ice and snow-covered surfaces only. A pixel is labeled cloudy if **any** observed radiance differs from the corresponding clear sky value for that pixel by more than the threshold values given in the Table 3.2.4. The label is assigned without regard for the results of previous tests. For the IR test, the four surface types are: Type 1 = open water, Type 2 = near-coastal water, sea ice margin and sea ice, Type 3 = open land, and Type 4 = near-coastal land, high topography, snow margin, and snow and ice-covered land. For the VIS and NIR tests, the same four surface types are used, except that sea ice margin and sea ice are changed to Type 3. The only special exception is that the VIS threshold test is not performed in sunglint geometry over open water.

**Table 3.2.4. Final Cloud Detection Threshold Values.**

WAVELENGTH	SURFACE TYPES			
	1	2	3	4
IR (K)	2.5	3.5	4.0	6.0
VIS Reflectance	0.030	0.030	0.060	0.090
VIS Radiance Limit	0.025	0.025	0.040	0.040
TNIR (K)	8.0	8.0	8.0	8.0
NIR Reflectance	0.045	0.045	0.055	0.055

Since a constant **reflectance** threshold represents progressively smaller **radiance** differences as solar zenith angle increases ( $\mu_0$  decreases), the threshold can decrease to values smaller than the uncertainties in the measured radiances or the inferred clear sky radiances. To avoid this, the VIS threshold test is actually performed as a radiance test, where the *radiance* threshold is equal to the values given in Table 3.2.4 multiplied by  $\mu_0$  for that pixel at that time, as long as the value is greater than or equal to the corresponding limit given in the table.

At night TNIR is nearly equal to TIR for clear pixels, but differs significantly in both the positive and negative directions for some clouds. Thus, the threshold test on TNIR labels a pixel cloudy if the absolute value of the difference,  $|\text{TNIR} - \text{TIR}|$ , is larger in magnitude than the values given in Table 3.2.4. Before the test, an adjustment is made to the value of  $\text{TNIR} - \text{TIR}$  based on the mode value of a frequency histogram of all clear values of  $\text{TNIR} - \text{TIR}$  collected for the whole month over open water and land. This adjustment compensates for any changes in relative calibration between the two wavelength channels. The difference values are also constrained to be  $\geq -18$  K and  $\leq 25$  K; values outside this range are considered clear. During the daytime, the RNIR threshold test is similar to the VIS threshold test: the observed value of RNIR (as long as  $\text{TNIR} - \text{TIR} > -17$  K) is compared to the clear sky composite value and the pixel labeled cloudy if RNIR is greater than the clear sky value by more than the values given in Table 3.2.4 (there is no lower limit because the sensitivity of this channel and the threshold magnitudes are large enough to avoid loss of precision).

### 3.2.5. RADIATIVE TRANSFER MODEL ANALYSIS

Once pixels are classified as cloudy or clear, the radiances are compared to radiative transfer model calculations designed to simulate the measurements of the AVHRR channels (to which all the radiometers have been normalized). Note that the model simulates **spectral radiances**; that is, the model calculates the full angular variation of radiant intensity over finite spectral intervals at particular wavelengths as functions of the physical properties of the clouds, atmosphere and surface. Comparison of observed radiances to simulated radiances are used to retrieve the surface reflectances and temperatures from clear radiances and the cloud optical thickness and top temperature from cloudy radiances. Atmospheric properties that affect the satellite measured radiances are specified from correlative data.

For the C-series of the cloud products, the VIS and IR absolute calibrations were referenced to the AVHRR on NOAA-7 (Brest and Rossow 1992). For the D-series of the cloud products, the VIS and IR absolute calibrations are referenced to that of the NOAA-9 AVHRR, which has been calibrated by



aircraft instruments (Rossow *et al.* 1996). The new VIS and IR calibrations are estimated to be accurate to within  $\pm 7\%$  and  $2\%$ , respectively.

The radiative model analysis proceeds in five steps (Figure 3.10).

- (1) Retrieval of surface temperature, TS, from the clear IR radiance obtained from the IR clear sky composite for the particular image pixel. The effects of atmospheric water vapor absorption are removed, using the atmospheric data for the particular location and time. A new formulation of the water vapor continuum absorption is used for the D-series of the cloud products.
- (2) Retrieval of surface reflectance, RS, from the clear VIS radiance obtained from the VIS clear sky composite for the particular image pixel. A correction for varying sun-Earth distance is made and the effects of Rayleigh scattering and ozone absorption are calculated, using ozone abundance data for the particular location and time. No aerosol effects are included and no retrieval is performed at night.
- (3) Retrieval of TS from the observed IR radiance, if the pixel is labeled CLEAR, or retrieval of cloud top temperature, TC, if the pixel is labeled CLOUDY. All clouds are assumed to be opaque to IR radiation. The effects of atmospheric water vapor absorption are removed, using the atmospheric data for the particular location and time. A new formulation of the water vapor continuum absorption is used for the D-series of the cloud products. Cloud top pressure, PC, is inferred from the atmospheric temperature profile for the particular location and time.
- (4) Retrieval of RS from the observed VIS radiance, if the pixel is labeled CLEAR, or retrieval of cloud optical thickness, TAU, if the pixel is labeled CLOUDY. The effects of Rayleigh scattering and ozone absorption are calculated; for a cloudy pixel the Rayleigh scattering is calculated, using the cloud top pressure retrieved in Step 3. Calculation of cloud optical thickness also uses the surface reflectance from the VIS clear sky composite, obtained in Step 2 for land and sea ice surfaces or from a model for water surfaces. In the D-series of the cloud products, NIR radiances are used to improve the retrieval of TAU over highly reflective snow and ice surfaces in the polar regions. Optical thickness is retrieved for each cloudy pixel using two cloud microphysical models: the same liquid droplet model used in the C-series of the cloud products and an ice crystal model (results reported only for clouds with top temperatures  $< 273$  K). No retrievals of RS and TAU are done at night.
- (5) If the optical thickness of the cloud is small, the cloud top temperature is adjusted to account for transmission of radiation from the surface using the retrieved optical thickness. The adjusted cloud top pressure is then used to re-calculate the optical thickness. In the D-series of the cloud products, an additional adjustment is also made to account for the small effect of scattering on IR radiances. No adjustment is performed at night.

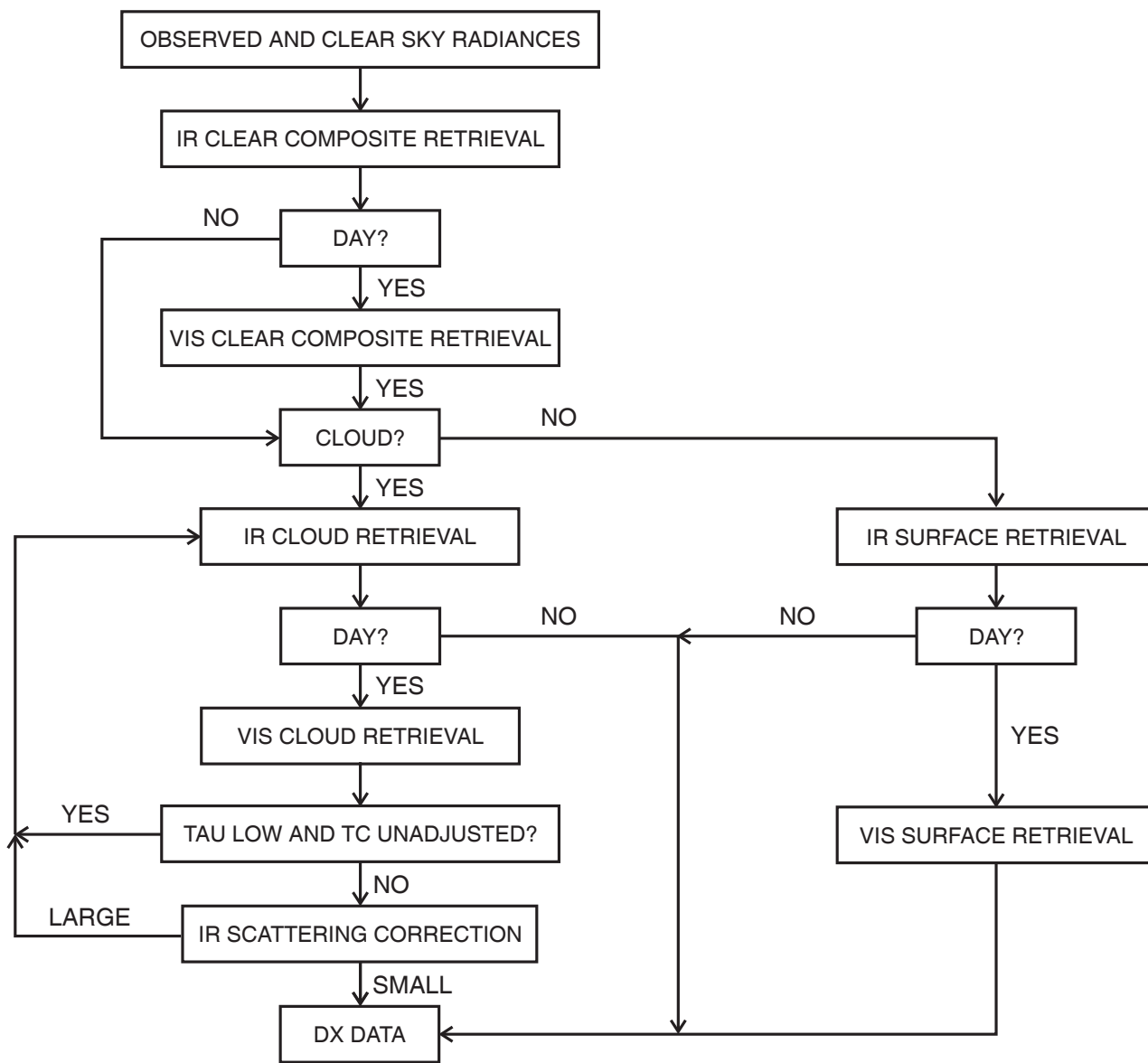


**Figure 3.10.** Radiative model analysis logic.

### 3.2.5.1. RADIANCE MODEL DESCRIPTIONS

All retrieved parameters are model-dependent quantities. The accuracy with which they represent real quantities depends on two factors:

- (i) the extent to which variations of other cloud and surface characteristics, which are held constant in the model, change the radiances, and
- (ii) the importance of effects neglected in the model.

The first of these factors will affect the accuracy of a specific observation, but will not, generally, affect the statistical results (climatology) as long as the estimated values for these parameters are "climatologically" correct. The variations in the satellite-measured radiances that are caused by changes of other cloud properties will be included as variations of optical thickness and top temperature. One important assumption in the model is the microphysical properties of the cloud particles. In the C-series of the cloud products, a specific spherical droplet distribution with an effective radius of 10  $\mu\text{m}$  was used. Subsequent research has shown that this is reasonably close to the global mean value for liquid water clouds ( $\approx 11 \mu\text{m}$ , Han *et al.* 1994). However, spherical particles do not provide a good approximation to ice crystals in high-level clouds (cf., Minnis *et al.* 1993). In the D-series of the cloud products, an ice crystal model, similar to that investigated by Minnis *et al.* (1993), is also employed. Both optical thickness values are reported if the ice model top temperature  $< 273 \text{ K}$ ; only the liquid water value is reported at higher temperatures.

The second of these factors may introduce important biases into these results. The most uncertain issue in this category is the assumption of optical homogeneity (of clouds and surfaces) at pixel spatial scales ( $\approx 5 \text{ km}$ ). One feature of the results that may be related to this issue is a small systematic variation of the retrieved cloud properties with increasing satellite viewing zenith angle (Rossow and Garder 1993b). Research activities continue to address these questions.

The following sections describe the detailed assumptions made about the cloud, atmosphere, and surface characteristics. Key highlights are:

- (1) Surface and atmospheric optical properties are assumed to be uniform over the image pixels (4-7 km, but actually interpreted to be uniform over the mapped cell scale of 25 km).
- (2) No aerosol effects are included in the radiative models; hence, the mean properties of the surface include the climatological effects of aerosols. Variations in aerosols that change the radiances enough in time, particularly dust storms, will be detected as clouds.
- (3) All surface types are assumed to be black bodies in modeling IR radiances; hence, the retrieved temperatures are brightness temperatures that are slightly lower than the actual skin temperatures of the surface. These values will differ from near-surface air temperatures by an amount that varies with time of day and season (see Rossow and Garder 1993b).
- (4) Land and sea ice surfaces are assumed to be isotropic reflectors. The water surface reflectance is represented by an anisotropic model derived from satellite observations (Minnis and Harrison, 1984; see also Rossow *et al.* 1989).
- (5) Cloud optical properties are assumed to be uniform over the image pixels; hence, cloud cover of pixels is assumed to be either zero or one.
- (6) Clouds are assumed to be single, physically thin layers (no vertical temperature gradients) that are strong absorbers of IR radiation. In the D-series of the cloud products, the effects of IR radiation scattering, which are a function of optical thickness, are also included for daytime retrievals.

- (7) Clouds are assumed to be single, thin layers that are pure (conservative) scatterers of VIS radiation. No gaseous absorption or scattering is included in the cloud layer. Scattering in the liquid droplet model is calculated as Mie scattering from a size distribution of water spheres with an effective radius of 10  $\mu\text{m}$  and effective variance of 0.15. In the D-series of the cloud products, scattering in the ice crystal model is calculated using a fractal phase function (Macke 1994, Mishchenko et al. 1996) and a -2 power law size distribution between 20 and 50  $\mu\text{m}$  that has an effective size of 30  $\mu\text{m}$  and an effective variance of 0.1.

### IR Model

The infrared radiance model is very similar to that described in Rossow *et al.* (1989), with optical constants adjusted to the spectral response of Channel 4 on the NOAA-9 AVHRR (see Rossow *et al.* 1992). The model represents the clear atmosphere as seven layers of absorbing gas (the pressure intervals are surface or 1000, 800, 680, 560, 440, 310, 180, tropopause or 30 mb) above a black-body surface; no aerosol effects are included. Each pixel is assumed to correspond to a column of gas with horizontally uniform properties; the surface and any cloud layers are also assumed to be horizontally uniform over the image pixels (4-7 km).

Clear gas layers in the model are not isothermal; rather the gas temperature varies from top to bottom of the layer so that the Planck function is linear (this is equivalent, however, to a nearly linear temperature variation with pressure for the relatively thin layers used). Radiances (brightness temperatures) are calculated as a function of satellite zenith angle. Absorption is due to water vapor; the total amount of water vapor within each pressure layer is vertically distributed with a constant mixing ratio.

Water absorption has two contributions: continuum and weak line absorption. The formulation of the continuum absorption follows that of Ma and Tipping (1991, 1992, 1994) (the previous version of the analysis used the continuum absorption formulation of Roberts et al., 1976) and includes the temperature dependence of both the self-broadening and foreign-broadening effects. The optical thickness of continuum absorption in a specific atmospheric layer with pressure interval  $dP$  is given by

$$\tau_s = (L_0 V_0 / mg) (1.607 AS) dP / (\log AS_b - \log AS_t)$$

$$\tau_f = (L_0 V_0 / mg) (1.607 AF) dP / (\log AF_b - \log AF_t)$$

where  $L_0$  is Loschmidt's number =  $2.68714 \times 10^{19}$  mole/cm<sup>3</sup>,  $V_0$  is the molar volume =  $2.24207 \times 10^4$  cm<sup>3</sup>/mole,  $m = 18$  g/mole is the molecular weight of water,  $g = 980$  cm/s<sup>2</sup> is the acceleration of gravity, and  $dP$  is the layer pressure interval in mb. The quantities  $AS_t$ ,  $AS_b$ ,  $AF_t$ , and  $AF_b$  are determined for the atmospheric temperatures at the top and bottom of each atmospheric layer by multiplying temperature-dependent coefficients, calculated from the model of Ma and Tipping, by the square of the mass mixing ratio of water vapor for AS and of the rest of the atmosphere for AF. The quantities AS and AF are given by

$$AS = AS_t P_t - AS_b P_b - (AS_b - AS_t) dP / (\log AS_b - \log AS_t)$$

$$AF = AF_t P_t - AF_b P_b - (AF_b - AF_t) dP / (\log AF_b - \log AF_t)$$

The factor of 1.607 is ratio of atmospheric and water molecular weights that converts one factor of mass mixing ratio into a number mixing ratio. This formulation provides an accurate treatment of the

temperature dependence of the water vapor absorption variation over a finite atmospheric layer with vertical variations of temperature and water mixing ratio. If the variation of the AS and AF across a layer is too small, an alternative formula is used that replaces the factors  $AS / (\log AS_b - \log AS_t)$  and  $AF / (\log AF_b - \log AF_t)$  by  $AS_t (P_t^2 - P_b^2) / 2$  and  $AF_t (P_t^2 - P_b^2) / 2$ , respectively.

The optical thickness of line absorption is obtained, using a fit to calculations with a Malkmus model for very narrow spectral intervals and weighted by the response function of AVHRR. Using the line strengths given by Rothman *et al.* (1983), we get

$$\tau = U \times \frac{0.000067 + 0.0065 U}{1 + 115 U + 1.3 U^{1.6}}$$

The coefficients multiplying U in the numerator and denominator have been changed (previously 0.0081 and 109, respectively) to correct a small error in the model fit. Line absorption is generally much weaker than the continuum absorption.

Figure 3.11 shows the variation of these two optical thicknesses with the amount of water in a 200 mb layer at 282 K, expressed in precipitable centimeters.

Clouds are assumed to be single, physically thin layers with no vertical temperature gradients. In the cloud top temperature retrieval, all clouds are treated as opaque blackbodies (emissivity = 1) and scattering is neglected. In the adjustment step, two microphysical models are used in Mie scattering calculations to relate the visible optical thickness to the IR absorption and scattering optical thicknesses. The first model assumes a gamma distribution of water spheres with effective radius = 10  $\mu\text{m}$  and effective variance = 0.15 and uses the optical constants for liquid water from Downing and Williams (1975) for infrared wavelengths. The IR absorption optical thickness used to adjust cloud top temperatures for liquid

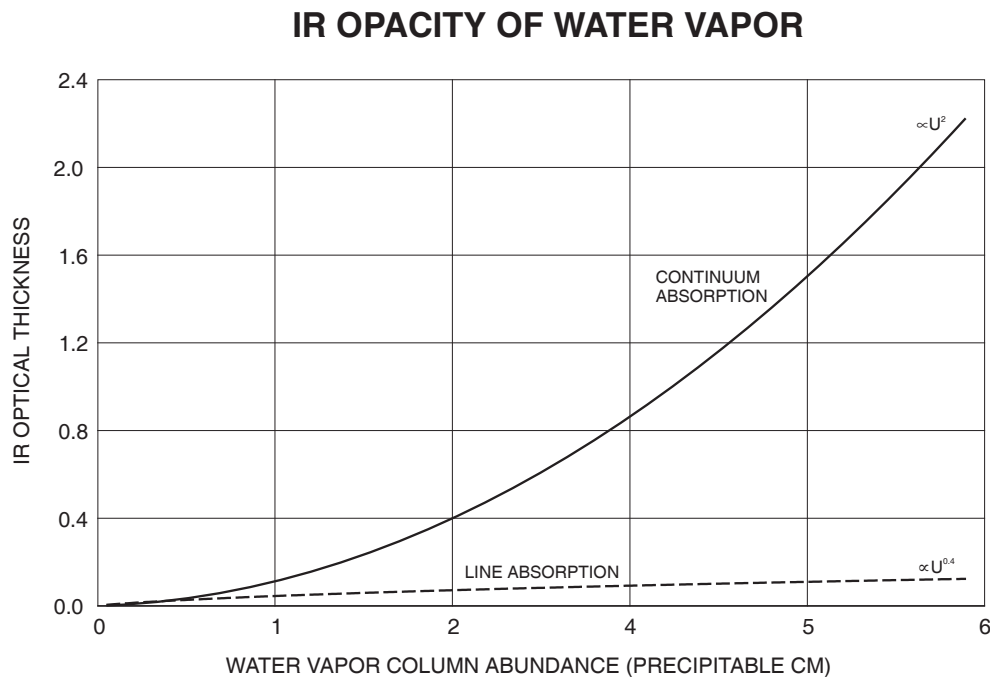


**Figure 3.11.** Variation of water vapor infrared opacity at 10.5  $\mu\text{m}$  with total water amount.

water clouds is given by 0.39 TAU, where TAU is the visible optical thickness. The second model assumes a -2 power law of ice spheres between 20 and 50  $\mu\text{m}$  (effective radius = 30  $\mu\text{m}$  and effective variance = 0.10) and uses optical constants for ice from Warren (1984). The IR absorption optical thickness for ice clouds is given by 0.47 TAU (cf. Minnis et al. 1993). The scattering calculations produce two look-up tables used in the cloud analysis, one for water spheres and one for ice spheres (IR scattering is insensitive to particle shape) that give the physical cloud top temperatures as a function of the IR brightness temperature retrieved neglecting scattering, the optical thickness, and the viewing angle.

In preparation for the radiative analysis, the IR model is used to convert the TOVS atmospheric profiles of physical temperature and humidity into profiles of top-of-atmosphere brightness temperature at three satellite zenith angles ( $\mu = 0.3, 0.6, 1.0$ ) as a function of location and time by placing an opaque (emissivity = 1) surface at each pressure level. Note that the effective wavelength of the AVHRR radiometer channel is about 0.5  $\mu\text{m}$  shorter than that of the geostationary satellite radiometers, but this difference is ignored in the analysis because the geostationary radiometer calibrations are normalized to that of the AVHRR. The cloud radiative processing uses these results as a dataset for the cloud top temperature retrieval, where all clouds are treated as blackbodies (scattering neglected). The water vapor values provided in the TOVS data set are rather noisy (quoted estimates of error are about 25-35%, Smith *et al.* 1979). To reduce this noise somewhat, all water vapor values are averaged over a 5-day period centered on the day being analyzed. Also calculated are the top-of-atmosphere brightness temperature corresponding to the TOVS physical surface temperature, the total atmospheric transmission (TRANS), and the total atmospheric emission (EMISS). These quantities are calculated at nine satellite zenith angles ( $\mu = 0.2, 0.3, 0.4, \dots, 0.9, 1.0$ ).

### VIS Model

The visible radiance model is very similar to that described in Rossow *et al.* (1989), with optical constants adjusted to the spectral response of Channel 1 on the NOAA-9 AVHRR (see Rossow *et al.* 1992); however, none of the calculations are very sensitive to the precise spectral dependence or wavelength used over the range from 0.55 to 0.7  $\mu\text{m}$  covered by the satellite radiometers (the exception is the surface reflectance for vegetated land surfaces). The model represents the clear atmosphere as three gas layers above a reflecting surface; no aerosol effects are included. Each pixel is assumed to correspond to a column of gas with horizontally uniform properties; the surface and any cloud layers are also assumed to be horizontally uniform over the image pixels (4-7 km).

The three gas layers are an absorbing layer at the top, representing ozone, and two Rayleigh scattering layers (total gas amount represented by a maximum surface pressure of 1000 mb), one above and one below any cloud layer. The small effect of variations in surface pressure is ignored. Ozone absorption is calculated, using a fit to line-by-line calculations weighted by the spectral response of the AVHRR:

$$\tau = U [ 0.085 - (0.00052 U) ]$$

where U is the column amount of ozone in cm-STP. Continuum absorption strengths in the Chappuis band are from Inn and Tanaka (1953). The transmission is given by

$$\text{Tr} = \exp \{ - U [ 0.085 - 0.00052 U ] / \mu \}$$

where  $\mu$  can be the cosine of either solar or satellite zenith angle.

To calculate the effects of Rayleigh scattering, the VIS model is used to pre-calculate a look-up table of isotropic surface reflectance as a function of VIS radiance values (normalized to the mean solar constant of the instrument) and viewing/illumination geometry. Given a VIS radiance, corrected for varying sun-Earth distance and ozone absorption, and the geometry, the table provides a corresponding value of isotropic surface reflectance.

The effects of the atmosphere on the broader "visible" channel on METEOSAT satellites are slightly overestimated by the analysis. In general this difference in spectral response is insignificant, except for the retrieved surface reflectances for vegetated land areas, which will be significantly larger in areas observed by METEOSAT satellites. The difference is land surface reflectances obtained from METEOSAT is removed in Stage D2 data.

Land and sea ice covered surfaces are assumed to be isotropic reflectors. Reflection from water is specified by a model obtained by removing the atmospheric effects from the clear radiance model of Minnis and Harrison (1984). The consistency of this model has been checked by comparing it to directly retrieved surface reflectances for a summer and winter month from both polar and geostationary satellites, using the VIS retrieval model. The retrieval agrees with the model to within 2% (random error) except near glint conditions. In glint geometry the model is found to be too bright by  $\approx 5\%$  in a majority of cases, but too dark in many other cases. The model in glint geometry is based on a four month survey of observed clear sky radiances.

Clouds are assumed to be single, physically thin layers that are pure (conservative) scatterers of VIS radiation. No gaseous absorption or scattering is included in the layer. When clouds are present, the VIS radiances are calculated from the individual scattering and absorption layers using the doubling-adding procedure (Hansen and Travis, 1974); the amount of gas above the cloud is determined by the cloud top pressure and the remaining gas is below the cloud.

Visible reflectance from clouds is calculated in complete multiple scattering calculations using two cloud particle size-shape models. The first model is for liquid water clouds (cloud top temperature  $\geq 260$  K): the optical constants of liquid water are from Hale and Querry (1973) for solar wavelengths. A gamma distribution of spheres defines an effective radius of  $10 \mu\text{m}$  and a variance of 0.15 (see Hansen and Travis 1974). The second model is for ice crystal clouds (cloud temperature  $< 260$  K): the optical constants of ice are from Warren (1984). A -2 power law of ice polycrystals between  $20$  and  $50 \mu\text{m}$  gives an effective radius =  $30 \mu\text{m}$  and an effective variance = 0.10; the fractal scattering phase function is from Macke (1994). Figure 3.12 compares the two scattering phase functions (Mishchenko et al. 1996). In preparation for the cloud analysis, the scattering calculations are used to pre-calculate two look-up tables. The main one gives cloud optical thickness values for liquid spheres as a function of the observed VIS radiance, surface reflectance, cloud top pressure and illumination and viewing geometry. The second table matches the solutions for liquid water spheres with those for the ice polycrystals to convert liquid water optical thicknesses to ice values as a function of illumination and viewing geometry (this technique was designed by P. Minnis, NASA Langley Research Center).

Figure 3.13 shows the model relationships between TAU and the cloud spherical albedo (over a black surface) and IR (narrowband) emissivity.

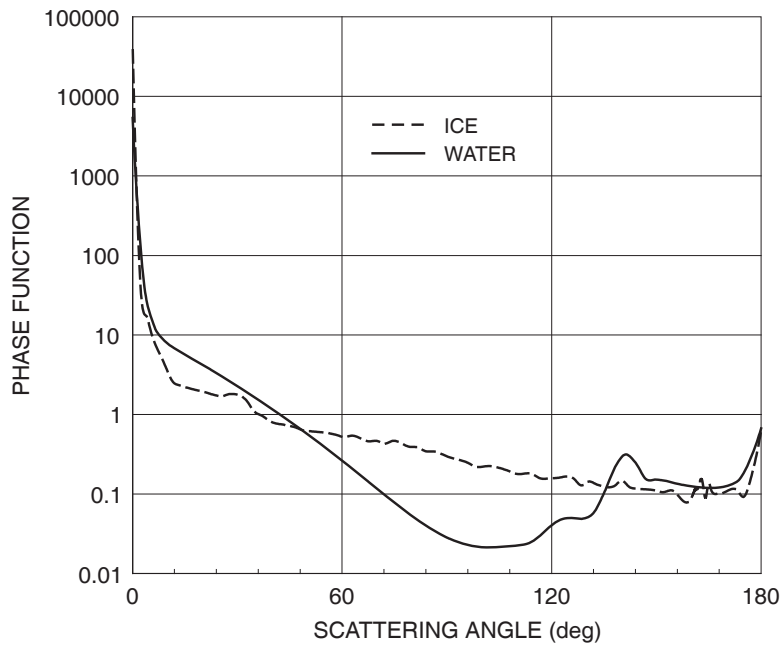


**Figure 3.12.** Scattering phase functions for 10  $\mu\text{m}$  spheres (solid curve) and 30  $\mu\text{m}$  fractal polycrystals (dashed curve) at visible wavelength (0.6  $\mu\text{m}$ ).

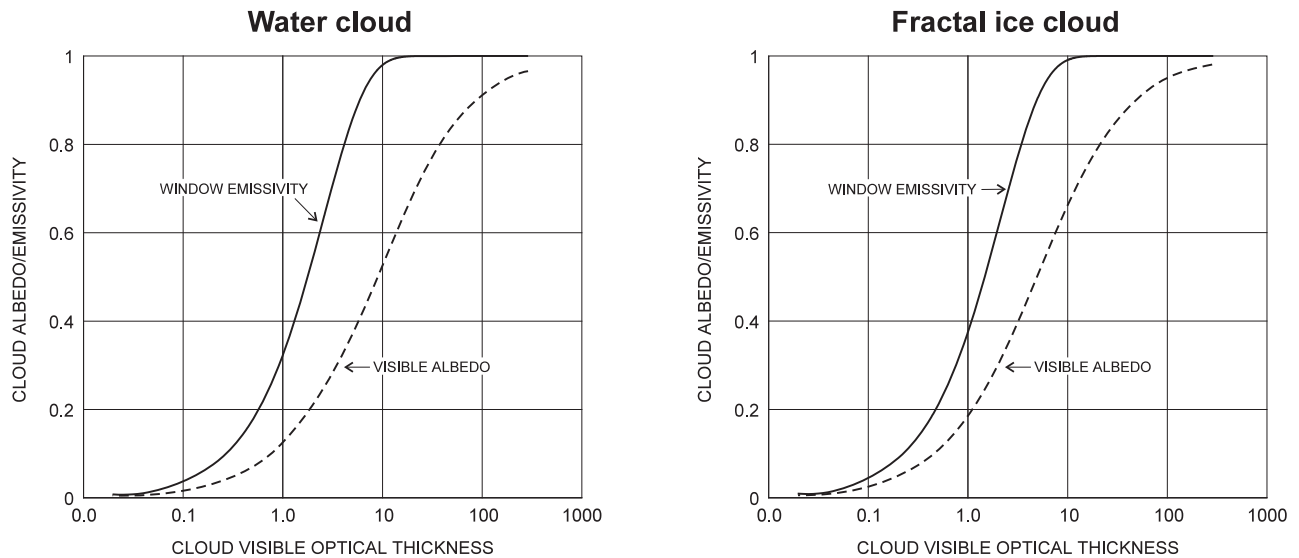


**Figure 3.13.** Relations of cloud visible (0.6  $\mu\text{m}$ ) albedo (scene albedo over black surface with no atmosphere) and infrared (10.5  $\mu\text{m}$ ) emissivity as a function of optical depth at 0.6  $\mu\text{m}$  for the liquid (left) and ice (right) water cloud models used in the ISCCP radiative analysis.



## NIR Model

In the polar regions, NIR ( $\approx 3.7 \mu\text{m}$ ) radiances are used to augment detection of clouds over snow and ice surfaces, where the VIS-based detections over such reflective surfaces are uncertain and where there appear to be numerous low-lying clouds exhibiting little temperature contrast with the surface. The threshold tests in daytime are performed on NIR solar reflectances (RNIR) after removal of the thermal emission contribution. The thermal emission at  $3.7 \mu\text{m}$  is calculated assuming a blackbody wavelength spectrum at the temperature observed at  $11 \mu\text{m}$ .

In the radiative analysis, NIR reflectances are used to aid the retrieval of cloud optical thicknesses over snow and ice surfaces. Since the reflection from snow and ice surface is more nearly isotropic than the reflection from a cloud, there are geometries at which optically thinner clouds over a snow or ice surface can appear less reflective than clear conditions. In these circumstances there are two possible cloud optical thicknesses that produce the same scene reflectance (Figure 3.14). In the C-series of the cloud retrievals, the larger optical thickness solution was always selected. Because water and ice absorb strongly at  $3.7 \mu\text{m}$ , RNIR is a strong function of particle size. Since surface ice tends to have much larger particle sizes than clouds, snow and ice surfaces are much less reflective than clouds. Thus, at  $3.7 \mu\text{m}$  the scene reflectivity increases more nearly monotonically with increasing cloud optical thickness (Figure 3.14). In the D-series of the cloud retrievals over snow and ice surfaces in the polar regions, if  $\text{RNIR} < 0.07$ , the smaller solution for visible optical thickness is used; if  $\text{RNIR} \geq 0.07$ , the larger solution is selected.

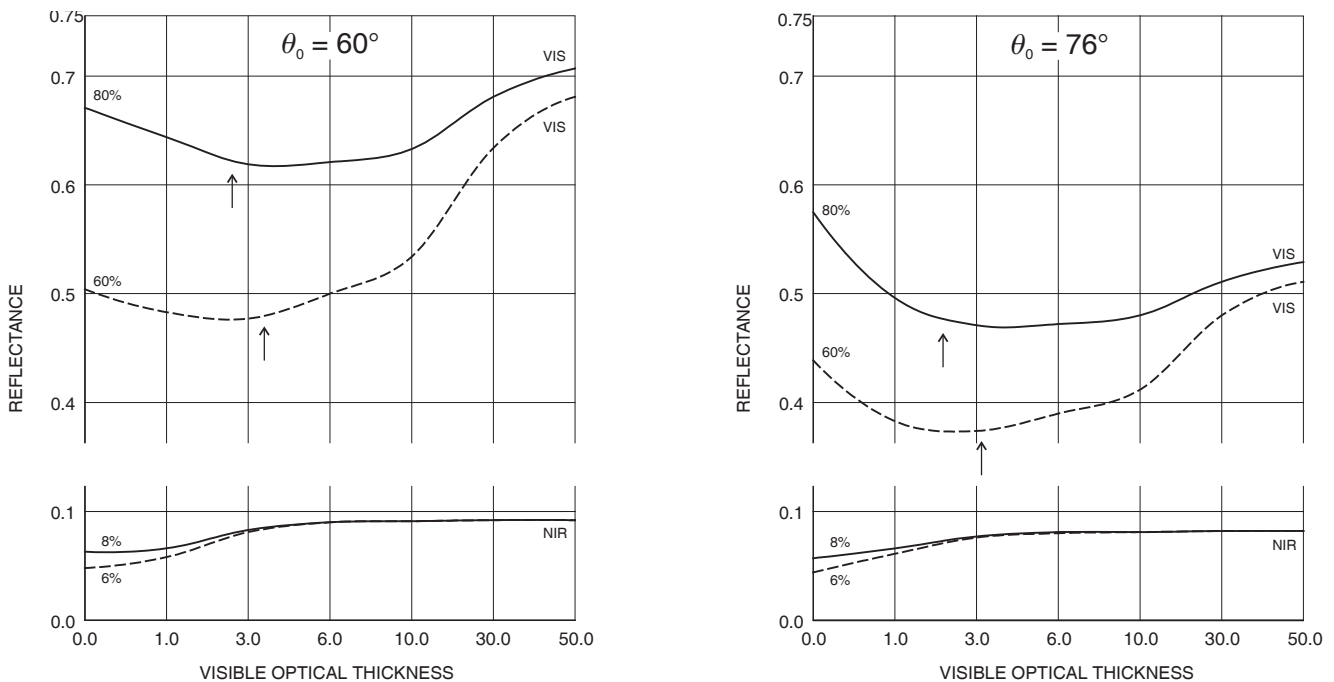


**Figure 3.14.** Variations of scene reflectances at VIS ( $0.6 \mu\text{m}$ ) and NIR ( $3.7 \mu\text{m}$ ) wavelengths as a function of cloud visible optical thickness at two solar zenith angles,  $\theta_0$ , and two visible surface albedos, 80% (solid) and 60% (dashed). The corresponding surface albedos at  $3.7 \mu\text{m}$  are approximately equal to 8% and 6%. Arrows indicate threshold NIR reflectance and corresponding visible optical thicknesses separating the upper and lower branches of the curves.

### 3.2.5.2. CLEAR RETRIEVALS

Clear radiances from the clear sky composites are available for every pixel, whether clear or cloudy. Retrievals of surface temperature (TS) from the IR radiance and surface visible reflectance (RS) from the VIS radiance (daytime only) are performed first, so that these quantities are available for use in retrievals of cloud properties from cloudy pixels. For clear pixels, another set of values of surface temperature and visible reflectance is retrieved from the observed radiances. In both cases (composite or observed) the procedure is the same.

#### Surface Skin Temperature

The surface temperature, TS, corresponding to the clear IR radiance (brightness temperature, TOBS) is given by

$$BTS = [ BTOBS - EMISS ] / TRANS$$

where BTS is the Planck radiation of a black body (weighted by the response function of the NOAA-9 AVHRR) for the surface temperature, BTOBS is the clear IR radiance, and EMISS and TRANS are the total atmospheric emission and transmission calculated with the IR radiance model from the TOVS atmospheric data and interpolated to the value of  $\mu$  for the particular observation. TS is obtained from BTS by inverting the Planck function (weighted by the AVHRR response). Since the atmosphere is relatively transparent at 11  $\mu\text{m}$  wavelength, TS corresponds to the **brightness** temperature of the surface skin; the physical temperature of surfaces with 11  $\mu\text{m}$  emissivities  $< 1$  will be larger. The corresponding pressure is the surface pressure from TOVS.

Although this formula is theoretically correct, when the water opacity becomes very large, TRANS becomes very small. Then errors in the observed radiances, in the inference of the clear IR radiance and in the properties of the atmosphere are multiplied by a very large number, (1/TRANS). This is equivalent to saying that, when TRANS is small, the measured signal contains little actual information about the surface and is dominated by the atmospheric emission. This "de-coupling" of the observations from the surface properties is also indicated by large differences between the surface emission and the top-of-atmosphere emission. Such conditions occur in the tropics when satellite zenith angles are relatively large. Thus, whenever  $TRANS < 0.25$  or the calculated surface and top-of-atmosphere emission difference exceeds a threshold, an alternate procedure is used to estimate surface temperature:

$$BTS = BTOBS + [ BTST - BTBT ]$$

where BTST is the Planck radiation corresponding to the TOVS surface temperature and BTBT is the corresponding top-of-atmosphere brightness temperature calculated for the TOVS temperature/humidity profile at the same viewing geometry. In other words, we assume, in cases of large water vapor opacity, that the difference between the observed brightness temperature and the actual surface temperature is the same as it is for the TOVS values. This is approximately equivalent to assuming that the atmospheric and surface temperatures vary together, i.e., that if the actual surface temperature is higher than the TOVS value, so is the atmospheric temperature which dominates the observed radiances. This assumption appears accurate over tropical oceans but less accurate over tropical land areas, especially deserts.

## Surface Visible Reflectance

The VIS radiances are corrected to a constant sun-Earth distance. Ozone absorption is removed by dividing by the two transmission factors (for the solar-to-surface and surface-to-satellite pathlengths). The corrected clear VIS radiances are then compared to the pre-calculated look-up table which gives isotropic surface reflectances as a function of  $\mu = \cosine$  satellite zenith angle,  $\mu_0 = \cosine$  solar zenith angle, and  $\phi =$  relative azimuth angle.

### **3.2.5.3. CLOUD RETRIEVALS**

For each cloudy pixel, cloud top temperature (TC), cloud top pressure (PC) and cloud optical thickness (TAU) are retrieved.

#### Cloud Top Temperature - Pressure (opaque limit)

The first retrieval of the cloud top temperature assumes that the cloud is opaque to IR radiation (emissivity = 1) and uses the pre-calculated profiles of IR brightness temperatures at three satellite zenith angles ( $\mu = 0.3, 0.6, 1.0$ ) corresponding to the physical atmospheric temperatures at various pressure levels for the particular location and time. These values are interpolated to the particular satellite zenith angle of the pixel, using

$$T(\mu) = C (1/\mu - \mu) [ T_L - T_U ] + R_L T_U - R_U T_L$$

where either  $0.3 \leq \mu < 0.6$  or  $0.6 \leq \mu \leq 1.0$ ,  $T_L$  and  $R_L = C * (1/\mu - \mu)$  are the brightness temperature and the coefficient at the lower value of  $\mu$ , and  $T_U$  and  $R_U = C * (1/\mu - \mu)$  are the values at the higher value of  $\mu$  in either interval. The value of  $C$  in the two intervals is calculated from

$$C^{-1} = (1/\mu - \mu)_L - (1/\mu - \mu)_U$$

The brightness temperature of the cloudy pixel is compared to the values interpolated to the satellite zenith angle of each pixel to find a match at some pressure level (which can be interpolated between the values on the profile); the corresponding physical temperature and pressure are then reported as the cloud top temperature and pressure. If the observed cloudy brightness temperature is less than any value on the TOVS profile, then the cloud top temperature is set equal to the brightness temperature (since the opacity of the water vapor above the tropopause is negligible) and the cloud top pressure is calculated using the hydrostatic equation above the tropopause level. If the observed brightness temperature is warmer than any value on the TOVS profile (the surface air temperature is the warmest value and is obtained by extrapolating the atmospheric temperature profile to the surface, but this may not correspond to the surface skin temperature inferred from the satellite-measurements), then the cloud top pressure is set equal to the surface pressure and the cloud top temperature is retrieved using the surface temperature procedure described above. If an isothermal or inversion layer exists in the atmospheric temperature profile, the uppermost point with the same temperature is used to determine cloud top pressure.

## Visible Optical Thickness

Cloud optical thicknesses are retrieved by comparing observed VIS radiances with values pre-calculated from the radiative model. These values are in a table that relates the liquid water cloud visible optical thickness, TAUW, to the VIS radiance (corrected for sun-Earth distance and ozone absorption), the viewing/illumination geometry, the surface reflectance from the clear sky composite value of the VIS radiance, and the cloud top pressure from the IR radiance analysis. Interpolation errors in this table are less than 10%, relative; interpolation errors are reduced in the D-series analysis, especially at low optical thicknesses, by changing to an interpolation that is linear in the logarithm of optical thickness. This change also eliminated the occasional occurrence of negative optical thickness values at low VIS radiances. A value of TAUW is obtained for all cloudy pixels.

At some illumination/viewing geometries over highly reflective surfaces, there are two possible values of TAUW that give the same VIS radiance. Because cloud reflectances are more anisotropic than most surface reflectances, there are situations where adding cloud (usually with relatively low optical thicknesses) to a scene can decrease the reflectance. This situation occurs much more frequently for surface reflectances  $> 0.5$ . In the C-series cloud analysis, the larger of the two values of TAUW was always selected. In the D-series analysis, whenever AVHRR data are analyzed over snow and ice-covered surfaces, the part of the  $3.7 \mu\text{m}$  radiances that is reflected sunlight (RNIR) is used to select either the smaller or larger value of TAUW: if  $\text{RNIR} \leq 0.07$ , the smaller value of TAUW is used.

In the D-series cloud analysis, ice cloud visible optical thickness values, TAUI, are also retrieved for each cloudy pixel. The values of TAUI are obtained from a pre-calculated table that matches values of TAUW and TAUI that produce the same VIS radiances for the same illumination/viewing geometry (a procedure developed by P. Minnis at NASA Langley Research Center -- cf. Minnis et al. 1993). However, for very large VIS radiances and certain illumination/viewing geometries there are situations for which there is no value of TAUI corresponding to TAUW because the asymptotic reflectivity for the larger ice crystals is lower than for the smaller liquid water spheres. In such cases, a second table that matches optical thicknesses giving the same visible **albedo** is used to estimate values of TAUI. Values of TAUI are reported for all cloudy pixels with ice cloud top temperature is  $< 273 \text{ K}$ .

## Cloud Top Temperature Adjustments

The value of the cloud optical thickness is checked for consistency with the assumption that the clouds are opaque to IR radiation. The optical thickness value calculated in the VIS model (TAU-VIS) is the value at  $0.6 \mu\text{m}$  wavelength. In the C-series of the analysis an empirical value (2.00) of the ratio TAU-VIS/TAU-IR was used to get TAU-IR. In the D-series a Mie scattering radiation code is used to calculate the optical thickness at  $10.7 \mu\text{m}$  wavelength (TAU-IR) for both TAUW ( $10 \mu\text{m}$  particle radius) and TAUI ( $30 \mu\text{m}$  particle radius). Use of spherical shapes for calculating this ratio is acceptable because the infrared scattering is insensitive to particle shape (cf. Minnis et al. 1993). The ratios obtained are  $\text{TAUW-VIS/TAUW-IR} = 2.56$  and  $\text{TAUI-VIS/TAUI-IR} = 2.13$ .

The observed IR radiance is modeled as the sum of two contributions: the emission from the cloud layer and the transmitted radiation from the surface (the results are corrected for weak scattering effects in a subsequent step). To account for water vapor absorption below the cloud, which is the majority of the

total, we use the clear sky radiance at top-of-atmosphere to represent the radiation coming from the surface and the lower atmosphere:

$$\text{BTOBS} = (1 - \text{TRANS}) \times \text{BTC} + \text{TRANS} \times \text{BTS}$$

where BTOBS is the observed radiance (Planck function for a temperature, TOBS, weighted by the spectral response function of NOAA-9), BTC is the radiance emitted by a cloud with temperature, TC, and emissivity (1 - TRANS), and BTS is the clear sky (surface) brightness temperature. The transmission of the cloud is given by

$$\text{TRANS} = \exp [ - \text{TAU-IR} / \mu ]$$

where  $\text{TAU-IR} = \text{TAUW}/2.56$  or  $\text{TAUI}/2.13$ .

If  $\text{TAU-IR}/\mu > 5.5$ , the cloud is considered opaque (since  $\text{TRANS} < 0.5\%$ ) and no adjustment of TC is required. If  $\text{TAU-IR}/\mu \leq 5.5$ , then an adjusted cloud top temperature is obtained from:

$$\text{BTC} = [ \text{BTOBS} - \text{TRANS} \times \text{BTS} ] / (1 - \text{TRANS})$$

The adjusted cloud top pressure that corresponds to TC is found from the temperature profile. If TC is smaller than any value on the profile, the cloud top pressure is calculated as a value smaller than the tropopause value using the hydrostatic formula.

This procedure encounters difficulties with very thin clouds because of errors in the VIS radiance measurements, uncertainties in the determination of the retrieved surface reflectances and temperatures, and in the retrieval of TAU-VIS and TAU-IR. In other words, even though a cloud may be "obvious" in the IR image, its VIS radiance effect may be negligible (dust storms also produce this effect), making an accurate determination of its optical thickness (which is near zero) difficult. This can lead to non-physical relations in the above equation for BTC. Also when (1 - TRANS) is too small, all of these errors are amplified.

Thus, we also solve the equation for a minimum value of TAU-IR (TAU-MIN) by assuming TC to be 5 K colder than the tropopause temperature:

$$\text{TRANS-MAX} = [ \text{BTOBS} - \text{BTC-MIN} ] / [ \text{BTS} - \text{BTC-MIN} ]$$

where TAU-MIN is obtained from  $\text{TRANS-MAX} = \exp [ - \text{TAU-MIN} / \mu ]$ . If  $\text{TRANS-MAX} \geq 1$  (ie, the observed brightness temperature is greater than or equal to the clear sky brightness temperature as might occur for a dust storm cloud), no correction of TC is performed. If  $\text{TRANS-MAX} < 0.001$  (ie, the observed brightness temperature is colder than the minimum temperature as can occur over high topography, especially in the polar regions), no correction of TC is performed as this cloud already appears to be in the lower stratosphere. If the optical thickness retrieved from VIS radiances is less than this minimum value or if the transmitted radiance calculated from the retrieved optical thickness exceeds the observed IR radiance, then the cloud top temperature is set to the tropopause temperature minus 5 K (cloud pressure equals tropopause pressure) and the optical thickness is set to its minimum value.

If the values of the cloud top temperature and pressure are adjusted and the value of TAU has not been re-set to the minimum value, then the retrieval of TAU-VIS is repeated with the new cloud top pressure. The cycle of retrievals is repeated until the values converge (usually no more than one iteration is needed but if more than ten iterations are performed the pixel is discarded). Adjustment of the values of cloud top temperature and pressure is performed only during the daytime.

### IR Scattering Adjustment

During daytime there is an additional small adjustment of cloud top temperatures and pressures for the viewing angle-dependent effects of scattering at IR wavelengths. The scattering correction is calculated from the Mie scattering radiation code for water and ice spheres, since the particle shape has little effect on the results. The scattering effect causes a small increase of brightness temperatures when a cloud is viewed from the near-nadir direction as compared with other directions. If the adjusted cloud top temperature differs from the original value by  $\leq 0.3$  K, no adjustment is made. If the retrieved cloud top temperature is more than 5 K larger than the clear sky IR radiance, no adjustment is performed.

## 4. ISCCP PROJECT INFORMATION

### 4.1. DATA PROCESSING STRATEGY

The strategy adopted for implementing the ISCCP reflects the diverse nature of the spaceborne observing system and the large volume of imaging and other data produced. The primary data processing is done by nine ISCCP centers (Figure 4.1): a Sector Processing Center (SPC) for each satellite (up to two polar orbiters and five geostationary satellites), the Satellite Calibration Center (SCC), and the Global Processing Center (GPC). Another center coordinates the delivery of other satellite and conventional weather data (correlative data) to the GPC for use in the cloud analysis and an additional center acts as the ISCCP Central Archive (ICA) for all data produced by the project. Table 4.1.1 shows the institutional commitments as of January 1996. The main processing task of the SPCs is to reduce the volume of the satellite radiance data by sampling in space and time. The SCC normalizes the calibration of the geostationary satellite radiometers to the reference polar orbiter radiometer; the GPC monitors the calibration of the polar orbiters and makes other short-term calibration adjustments. The GPC conducts the cloud analysis and the ICA archives all of the ISCCP data products. The SAPCs are not currently active.

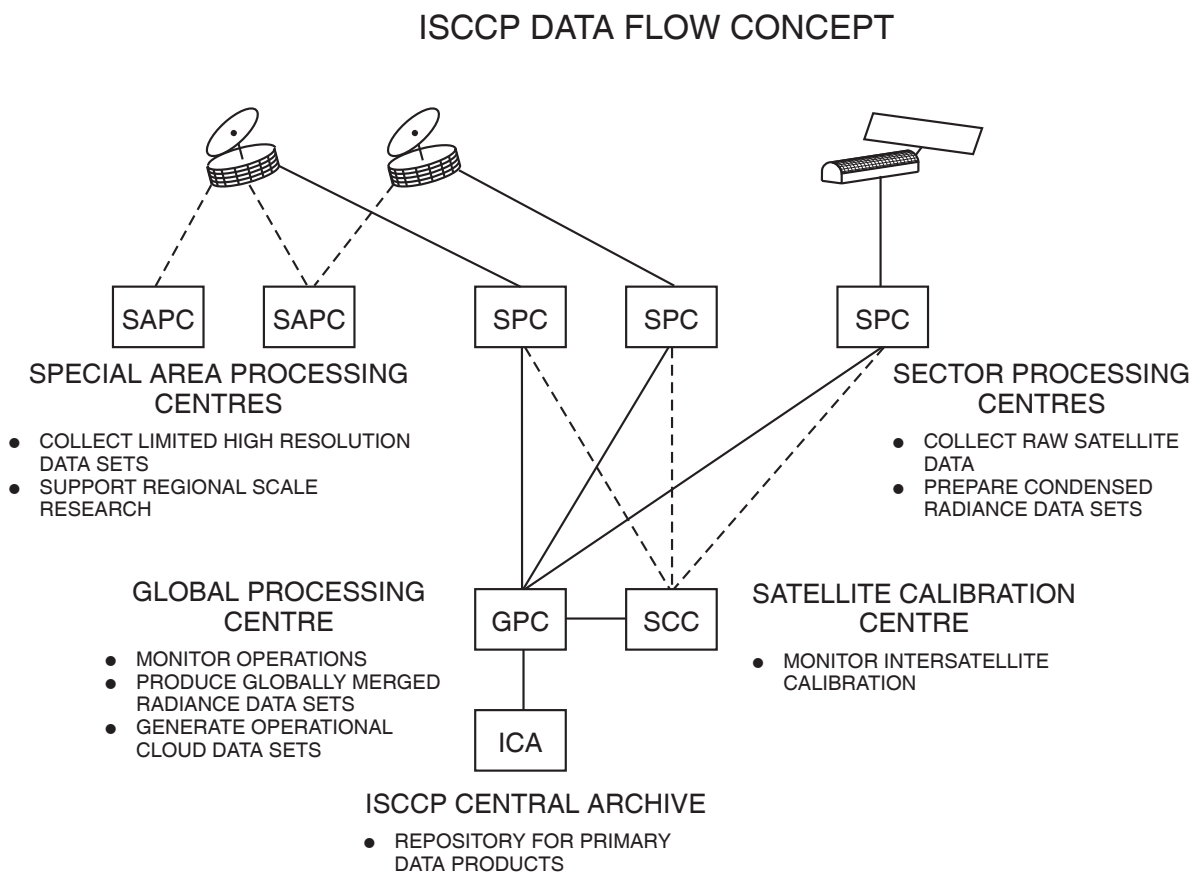


**Figure 4.1.** Schematic of ISCCP data processing.

**Table 4.1.1. ISCCP Data Management Commitments.**

RESPONSIBILITY	PRIMARY INSTITUTION	BACKUP INSTITUTION
SPC for NOAA/TIROS-N	USA/NOAA/NESDIS	+
SPC for METEOSAT	EUMETSAT*	+
SPC for GOES-EAST	Canada/AES**	USA/UWS
SPC for GOES-WEST	USA/CSU	USA/UWS
SPC for GMS	Japan/JMA	+
SPC for INSAT	India (no commitment)	+
SCC	France/CMS****	+
Correlative Data Center	USA/NOAA/NESDIS	+
GPC	USA/NASA/GISS	+
ICA	USA/NOAA/NESDIS	+
+ No commitment sought.		
* ESA served as the SPC for METEOSAT from July 1983 to November 1995.		
** USA/UWS served as the SPC for GOES-EAST from July 1983 to July 1984.		
*** FRG/U. Koln served as SCC for the Data Management Systems Test and assisted France/CMS in the development of the radiance normalization technique.		

## 4.2. VALIDATION STRATEGY

Limitations of the satellite radiance measurements and other information, together with the developing nature of cloud analysis methods, make a research program a crucial component of the ISCCP. This research program provides validation of the ISCCP cloud climatology and the basis for developing improved methods for remote sensing of clouds by comparing the ISCCP analysis products with other cloud observations. Validation of the ISCCP cloud climatology addresses not only the quantitative assessment of measurement errors, but also the refinement of the interpretation of the results in terms of atmospheric and cloud processes. This research also improves radiative transfer models of cloudy atmospheres. A major source of comparison observations comes from an on-going series of intensive field experiments conducted by various nations. The results of validation studies have already been used to improve the ISCCP analysis, leading to a replacement and extension of the C-series datasets by the D-series datasets.

The first cloud detection method for ISCCP (Rossow and Garder 1993a) was developed from a three year pilot study that compared the performance of nine different algorithms applied to the same data (Rossow *et al.* 1985). These tests showed that all methods then available detected a majority of the cloudiness on Earth because the spatial and temporal radiance changes produced by most clouds in both the visible and infrared bands are large compared to the total range of radiances observed. However, these methods disagreed most in partially cloudy situations, where there are many radiance values that are only slightly different from those representing clear conditions, in locations where the surface is



unusually cold or bright (e.g., winter land areas), which reduces the contrast with clouds, or for certain cloud types that do not cause very large changes in the observed radiances (cirrus in the visible or marine boundary layer clouds in the infrared). The pilot study also provided a practical way to define the accuracy of satellite cloud detections by determining the accuracy of the clear radiances, which are determined primarily by the properties of the Earth's surface: verification of the accuracy of the clear radiances provides a quantitative assessment of the detection accuracy of the analysis. The results of such verification studies, together with comparisons of the ISCCP cloud amount with other observations and climatologies, are reported in Wielicki and Parker (1992), Rossow and Garder (1993b), and Rossow *et al.* (1993). These results led to some re-design of the ISCCP cloud detection method which was used to produce the D-series of cloud products.

Once the radiance data are divided into clear and cloudy populations, quantitative interpretation to infer specific properties of clouds requires a radiative model of the effects of clouds, as well as the atmosphere and surface, on the satellite radiances. The three most important uncertainties in the first radiative model were the effects of the assumed cloud microphysical model (gamma distribution of liquid water spheres with effective radius of 10  $\mu\text{m}$  and variance of 0.15), the effects of the assumed macrophysical model (single, physically thin, plane-parallel cloud layer), and the effects of neglecting the smaller scale (sub-pixel scale < 5 km) variations of cloud properties. A subsequent survey of the droplet radii in liquid water clouds (Han *et al.* 1994) showed that the actual range of variations introduced a random uncertainty in ISCCP optical thickness values of 12% and biases of < 3%. However, the particular microphysical model produced larger errors for ice crystal clouds, approaching 100% in optical thickness and 1 - 2 km in cirrus cloud top locations (Minnis *et al.* 1993). Consequently, an ice crystal microphysical model has been introduced into the revised ISCCP radiative model. One study (Liao *et al.* 1995a, 1995b) shows that the tops of high-level clouds, particularly in the tropics, are diffuse such that IR emission arises from a significant distance below the physical cloud top. Hence, ISCCP cloud top pressure estimates are biased high by 50 - 100 mb, but still represent the radiatively effective top. Other aspects of cloud layer structure and the effects of small scale inhomogeneity are still under study.

### **4.3. ISCCP WORKING GROUP ON DATA MANAGEMENT**

Representatives of the ISCCP Data Management Centers listed in Table 4.1.1 originally formed the ISCCP Working Group on Data Management (WGDM) for the Joint Scientific Committee (JSC) of the World Climate Research Program. Scientific guidance was provided to the project by the International Radiation Commission of IAMAP and by the JSC Working Group on Radiation Fluxes. A re-organization of the WCRP in the early 1990's led to the WGDM being made responsible for all radiation projects within WCRP as part of the Global Energy and Water Experiment (GEWEX). Table 4.3.1 lists the WGDM membership as of July 1995.

**Table 4.3.1. Working Group on Data Management.**

NAME	AFFILIATION	ISCCP AFFILIATION
<b>CURRENT MEMBERS</b>		
G. Campbell	USA/CSU	SPC GOES-WEST
Y. Desormeaux	France/CMS	SCC
Y. Durocher	Canada/AES	SPC GOES-EAST
R. Francis	EUMETSAT	SPC METEOSAT
V. Gärtner	ESA	SPC METEOSAT
K. Kidwell	USA/NOAA/NESDIS	SPC NOAA, ICA
N. Shimizu	Japan/JMA	SPC GMS
W. Rossow	USA/NASA/GISS	GPC
<b>MEMBERS FROM JSC/CAS WORKING GROUP ON RADIATION FLUXES</b>		
E. Raschke	Germany/GKSS	N/A
<b>EX-OFFICIO MEMBERS</b>		
R. Schiffer	USA/NASA	Project Manager
S. Benedict	JPS for WCRP ICSU/WMO	N/A
<b>PREVIOUS MEMBERS</b>		
N. Beriot	France/CMS	SCC
K. Black	ICSU/RSA	SAPC METEOSAT
F. Bowkett	Canada/AES	SPC GOES-EAST
H. Drahos	USA/NOAA/NESDIS	SPC NOAA, ICA
R. Fox	USA/UWS	SPC GOES-EAST
J. Gibson	USA/NOAA/NESDIS	SPC NOAA, ICA
H. Jacobowitz	ISCCP Office NOAA	SPC GMS
S. Kadowaki	Japan/JMA	SPC GMS
T. Kaneshige	JPS for WCRP ICSU/WMO	N/A
I. Kubota	Japan/JMA	SPC GOES-EAST
A. Kurosaki	Japan/JMA	SPC METEOSAT
S. Lapczak	Canada/AES	SPC NOAA, ICA
B. Mason	ESA	SPC GOES-EAST
M. Mignono	USA/NOAA/NESDIS	SPC GMS
C. Norton	USA/UWS	SAPC
T. Nuomi	Japan/JMA	SPC METEOSAT
R. Reeves	NOAA	SPC GMS
R. Saunders	ESA	JSC/CAS Working Group
K. Shuto	Japan/JMA	SPC GOES-EAST
T. Vonder Haar	USA/CSU	SAPC
S. Woronko	Canada/AES	GOES-EAST/WEST
D. Wylie	USA/UWS	SAPC

#### 4.4. SUMMARY OF PROJECT PHASES

The ISCCP project has several stages of activity, **Phase 1:** (1982 - 1984) initial implementation of data processing systems, (1983 - 1987) complete development of cloud analysis, (1988 - 1992) complete processing of first 8 years of data, (1992 - 1995) refinements of processing system, (1995 - 1997) re-processing of first 8 years of data and completion of next 4 years of data and **Phase 2:** (1995 - 1997) development of enhanced processing for GEWEX, (1997 - 2001) complete processing of next 5 years of data together with enhanced processing.

During ISCCP Phase 2, the Stage DX, D1, and D2 datasets will continue to be produced unchanged; however, several additional data products will be developed. Ideas for other cloud property retrievals that are being explored include the following:

- (i) identification of multi-layer cloud systems involving thin cirrus as the upper layer using additional IR wavelengths
- (ii) retrieval of effective cloud particle sizes for liquid droplet and ice crystal clouds using additional near-IR and IR wavelengths
- (iii) retrieval of cloud liquid and ice water path using combined visible and microwave wavelengths
- (iv) improvement of phase discrimination and retrievals of nighttime and winter polar clouds using additional IR wavelengths.

The first series of the ISCCP cloud products, called Stage C1 and C2 data, was produced covering the time period July 1983 - June 1991. No more of these products will be produced. The final version numbers included in the dataset ID for the Stage C1, and Stage C2 datasets and their corresponding TV and IS datasets can be found in a table on the ISCCP Home Page.

## 5. REFERENCES

### 5.1. GENERAL

- Brest, C.L., and W.B. Rossow, 1992: Radiometric calibration and monitoring of NOAA AVHRR data for ISCCP. *Int. J. Remote Sens.*, **13**, 235-273.
- Brest, C.L., W.B. Rossow, and M.D. Roiter, 1996: Update on ISCCP calibration for visible and infrared radiances. *J. Atmos. Ocean. Tech.*, (submitted).
- Cavalieri, D.J., P. Gloersen, and W.J. Campbell, 1984: Determination of sea ice parameters with the NIMBUS-7 SMRR. *J. Geophys. Res.*, **89**, 5355-5369.
- Desormeaux, Y., W.B. Rossow, C.L. Brest, and C.G. Campbell, 1993: Normalization and calibration of geostationary satellite radiances for ISCCP. *J. Atmos. Ocean Tech.*, **10**, 304-325.
- Dewey, K.F., 1987: Satellite-derived maps of snow cover frequency for the northern hemisphere. *J. Clim. Appl. Meteor.*, **26**, 1210 - 1229.
- Downing, H.D., and D. Williams, 1975: Optical constants of water in the infrared. *J. Geophys. Res.*, **80**, 1656-1661.
- Hale, G.M., and M.R. Querry, 1973: Optical constants of water in the 200-nm to 200- $\mu$ m wavelength region. *Appl. Opt.*, **12**, 555-563.
- Han, Q.Y., W.B. Rossow, and A.A. Lacis, 1994: Near-Global Survey of Effective Droplet Radii in Liquid Water Clouds Using ISCCP Data. *J. Climate*, **7**, 4, 465-497.
- Hansen, J.E., and L.D. Travis, 1974: Light scattering in planetary atmospheres. *Space Sci. Rev.*, **16**, 527-610.
- Hilsenrath, E., and B.M. Schlesinger, 1981: Total ozone seasonal and interannual variations derived from the 7 year NIMBUS-4 BUUV data set. *J. Geophys. Res.*, **86**, 12087-12096.
- Inn, E.C.Y., and Y. Tanaka, 1953: Absorption coefficient of ozone in the ultraviolet and visible regions. *J. Opt. Soc. Amer.*, **43**, 870-873.
- Kidwell, K.B., 1995: *NOAA Polar Orbiter Data Users Guide (TIROS-N, NOAA-6, NOAA-7, NOAA-8, NOAA-9, NOAA-10, NOAA-11, NOAA-12, NOAA-13 and NOAA-14)*. National Oceanic and Atmospheric Administration, National Environmental Satellite, Data and Information Service, Washington, DC, 394.
- Liao, X., D. Rind, and W.B. Rossow, 1995a: Comparison between SAGE II and ISCCP high-level clouds, Part I: Global and zonal mean cloud amounts. *J. Geophys. Res.*, **100**, 1121-1135.
- Liao, X., D. Rind, and W.B. Rossow, 1995b: Comparison between SAGE II and ISCCP high-level clouds, Part II: Locating cloud tops. *J. Geophys. Res.*, **100**, 1137-1147.

- London, J.R., B.D. Bojkov, S. Oltmans, and J.F. Kelly, 1976: Atlas of the Global Distribution of Total Ozone, July 1957-July 1967. *NCAR Tech. Note 113 + STR*, Nat. Cent. for Atmos. Res., Boulder, Colo., 276 pp., National Center for Atmospheric Research, Boulder, CO.
- Ma, Q., and R.H. Tipping, 1991: A far wing line shape theory and its application to the water continuum absorption in the infrared region, I. *J. Chem. Phys.*, **95**, 6290-6301.
- Ma, Q., and R.H. Tipping, 1992: A far wing line shape theory and its application to the foreign-broadened water continuum absorption, II. *J. Chem. Phys.*, **95**, 818-828.
- Ma, Q., and R.H. Tipping, 1994: The detailed balance requirement and general empirical formalisms for continuum absorption. *J. Quant. Spectr. Radiat. Trans.*, **51**, 751-757.
- Macke, A., 1994: Scattering of light by irregular ice crystals in three-dimensional inhomogeneous cirrus clouds, in *Eighth Conference on Atmospheric Radiation*, Nashville, Tennessee, January 23-28, pp. 304-306.
- Masaki, G.T., 1972 (rev., 1976): The Wolf Plotting and Contouring Package. GSFC Computer Program Lib. # A00227, Computer Sciences Corporation, Goddard Space Flight Center, Greenbelt, MD, 187 pp. .
- Matthews, E., 1983: Global vegetation and land use: New high-resolution data bases for climate studies. *J. Clim. Appl. Meteor.*, **22**, 474-487.
- Matthews, E., and W.B. Rossow, 1987: Global, seasonal maps of surface visible reflectivity from satellite observations. *J. Clim. Appl. Meteor.*, **26**, 170-202.
- McMillin, L.M., and C. Dean, 1982: Evaluation of a new operational technique for producing clear radiances. *J. Appl. Meteor.*, **21**, 1005-1014.
- Minnis, P., and E.F. Harrison, 1984: Diurnal variability of regional cloud and clear sky radiative parameters derived from GOES data, 3, November 1978 radiative parameters. *J. Clim. Appl. Meteor.*, **23**, 1032-1051.
- Minnis, P., P.W. Heck, and D.F. Young, 1993: Inference of cirrus cloud properties from satellite-observed visible and infrared radiances, 2, Verification of theoretical cirrus radiative properties. *J. Atmos. Sci.*, **50**, 1305-1322.
- Mishchenko, M.I., W.B. Rossow, A. Macke, and A.A. Lacis, 1996: Sensitivity of cirrus cloud albedo, bidirectional reflectance, and optical thickness retrieval accuracy to ice-particle shape. *J. Geophys. Res.*, (submitted).
- Oort, A.H., 1983: Global Atmospheric Circulation Statistics, 1958-1973. NOAA Professional Paper 14, NOAA Geophysical Fluid Dynamics Laboratory, U.S. Dept. of Commerce, Rockville, MD, 180 pp. .
- Roberts, R.E., J.E.A. Selby, and L.M. Biberman, 1976: Infrared continuum absorption by atmospheric

water vapor in the 8-12  $\mu\text{m}$  window. *Appl. Opt.*, **15**, 2085-2090.

- Rossow, W.B., and L. Garder, 1984: Selection of a map grid for data analysis and archival. *J. Clim. Appl. Meteor.*, **23**, 1253-1257.
- Rossow, W.B., and L.C. Garder, 1993a: Cloud detection using satellite measurements of infrared and visible radiances for ISCCP. *J. Climate*, **6**, 2370-2393.
- Rossow, W.B., and L.C. Garder, 1993b: Validation of ISCCP cloud detections. *J. Climate*, **6**, 2370-2393.
- Rossow, W.B., and R.A. Schiffer, 1991: ISCCP cloud data products. *Bull. Amer. Meteor. Soc.*, **72**, 2-20.
- Rossow, W.B., and Y.-C. Zhang, 1995: Calculation of surface and top of atmosphere radiative fluxes from physical quantities based on ISCCP datasets, 2, Validation and first results. *J. Geophys. Res.*, **100**, 1167-1197
- Rossow, W.B., F. Moshier, E. Kinsella, A. Arking, M. Desbois, E. Harrison, P. Minnis, E. Ruprecht, G. Seze, C. Simmer, and E. Smith, 1985: ISCCP cloud algorithm intercomparison. *J. Climate App. Meteor.*, **24**, 877-903.
- Rossow, W.B., E. Kinsella, A. Wolf, and L. Garder, 1987: International Satellite Cloud Climatology Project (ISCCP) Description of Reduced Resolution Radiance Data. In, *WMO/TD No. 58*. (eds.), World Meteorological Organization, Geneva, 143 pp.
- Rossow, W.B., L.C. Garder, and A.A. Lacis, 1989: Global, seasonal cloud variations from satellite radiance measurements. Part I: Sensitivity of analysis. *J. Climate*, **2**, 419-458.
- Rossow, W.B., L.C. Garder, P.J. Lu, and A.W. Walker, 1991: International Satellite Cloud Climatology Project (ISCCP) Documentation of Cloud Data. *WMO/TD-266*, World Climate Research Programme (ICSU and WMO), Geneva, March, (revised), 76 pp. plus three appendices.
- Rossow, W.B., Y. Desormeaux, C.L. Brest, and A.W. Walker, 1992: International Satellite Cloud Climatology Project (ISCCP) Radiance Calibration Report. *WMO/TD-No. 520*, *WCRP-77*, 104 pp.
- Rossow, W.B., A.W. Walker, and L.C. Garder, 1993: Comparison of ISCCP and other cloud amounts. *J. Climate*, **6**, 2394-2418.
- Rossow, W.B., C.L. Brest, and M. Roiter, 1996: International Satellite Cloud Climatology Project (ISCCP) Radiance Calibration Report-Update. *WMO/TD-No. XXX*, World Climate Research Programme (ICSU and WMO), Geneva, 71 pp.
- Rothman, L.S., R.R. Gamache, A. Barbe, A. Goldman, J.R. Gille, L.R. Brown, R.A. Toth, J.M. Flaud, and C. Camy-Peyret, 1983: AFGL atmospheric absorption line parameters compilation: 1982 edition. *Appl. Opt.*, **22**, 2247-2256.

- Schiffer, R.A., and W.B. Rossow, 1983: The International Satellite Cloud Climatology Project (ISCCP): The first project of the World Climate Research Program. *Bull. Amer. Meteor. Soc.*, **64**, 779-784.
- Schiffer, R.A., and W.B. Rossow, 1985: ISCCP global radiance data set: A new resource for climate research. *Bull. Amer. Meteor. Soc.*, **66**, 1498-1505.
- Seze, G., and W.B. Rossow, 1991a: Time-cumulated visible and infrared radiance histograms used as descriptors of surface and cloud variations. *Int. J. Remote Sensing*, **12**, 877-920.
- Seze, G., and W.B. Rossow, 1991b: Effects of satellite data resolution on measuring the space-time variations of surfaces and clouds. *Int. J. Remote Sensing*, **12**, 921-952.
- Smith, W.L., H.M. Woolf, C.M. Hayden, D.Q. Wark, and L.M. McMillin, 1979: The TIROS-N Operational Vertical Sounder. *Bull. Amer. Meteor. Soc.*, **60**, 117-118.
- Warren, S.G., 1984: Optical constants of ice from the ultraviolet to the microwave. *Appl. Opt.*, **23**, 1206-1225.
- Werbowetzki, A., (editor), 1981: Atmospheric Sounding User's Guide. NOAA, U.S. Dept. of Commerce, Washington, D.C. .
- Wielicki, B.A., and L. Parker, 1992: On the determination of cloud cover from satellite sensors: The effect of sensor spatial resolution. *J. Geophys. Res.*, **97**, 12,799-12,823.
- Zhang, Y.-C., W.B. Rossow, and A.A. Lacis, 1995: Calculation of surface and top of atmosphere radiative fluxes from physical quantities based on ISCCP datasets, 1, Method and sensitivity to input data uncertainties. *J. Geophys. Res.*, **100**, 1149-1165

## **5.2. PROJECT DOCUMENTS**

- WCP-6: The International Satellite Cloud Climatology Project, January 1981, World Meteorological Organization, Geneva.
- WCP-73: The International Satellite Cloud Climatology Project (ISCCP) Cloud Analysis Algorithm Intercomparison, March 1984, World Meteorological Organization, Geneva.
- WMO/TD-No. 58: The International Satellite Cloud Climatology Project (ISCCP) Description of Reduced Resolution Radiance Data, July 1985 (Revised August 1987), World Meteorological Organization, Geneva.
- WMS/TD-No. 88: The International Satellite Cloud Climatology Project (ISCCP) Research Plan and Validation Strategy, January 1986, World Meteorological Organization, Geneva.
- WMO/TD-No. 266: International Satellite Cloud Climatology Project (ISCCP) Documentation of Cloud Data, December 1988 (Revised April 1991), World Meteorological Organization, Geneva.
- WMO/TD-No. 520: International Satellite Cloud Climatology Project (ISCCP) Radiance Calibration Report, (WCRP-77), December 1992, World Meteorological Organization, Geneva, 104 pp.
- WMO/TD-No. XXX: International Satellite Cloud Climatology Project (ISCCP) Radiance Calibration Report - Update, World Meteorological Organization, Geneva, 71 pp.



## 6. APPENDICES

### 6.1. TOVS ATMOSPHERE GRIDDED DATA PRODUCT (TV)

#### 6.1.1. OVERVIEW

As part of the ISCCP cloud analysis, information concerning the atmospheric temperature and humidity profiles and the ozone column abundances are used in the radiative model to account for atmospheric effects on the satellite radiances. Although these data are also available from the original sources, the version used in the ISCCP processing (called TV data) is archived with the cloud climatology to document the ISCCP data analysis procedure and to provide these data in a more convenient format especially suited to satellite data processing. A subset of the TV data is also included in the Stage D1 cloud product and summarized in the Stage D2 cloud product.

The **original atmospheric dataset** is obtained from the TIROS Operational Vertical Sounder (TOVS) System, flown on the NOAA Operational Polar Orbiting Satellite series since 1978 (Werbowetzki 1981). These data are supplied by and can be obtained from

ISCCP Central Archives  
NOAA/NESDIS/NCDC  
Climate Services Division/Satellite Services Branch  
FOB3, Room G233  
Suitland, MD 20233

Phone: 704-271-4800 (option #5)  
FAX: 704-271-4876  
e-mail: [satorder@ncdc.noaa.gov](mailto:satorder@ncdc.noaa.gov)

The TOVS system consists of three instruments (Kidwell 1995): the High Resolution Infrared Radiation Sounder (HIRS/2), the Stratospheric Sounding Unit (SSU, supplied by the United Kingdom), and the Microwave Sounding Unit (MSU). The measurements from these three instruments are processed by NOAA to produce the TOVS Sounding Product, which includes 15 layer-mean temperatures (from the surface to the stratosphere), precipitable water amounts for three layers (middle and lower troposphere), estimated surface pressure, tropopause temperature and pressure, ozone column abundance, and clear sky radiances. Although the original sounding measurements are often available from two polar orbiters that could be used to produce soundings for the whole globe up to four times daily, only about one sounding per day is available that contains complete (temperature and humidity) information.

To provide complete global coverage at all times, the TOVS dataset is **supplemented by two climatologies**: the NOAA GFDL temperature/humidity climatology from a global collection of rawinsonde balloon measurements (Oort 1983) and the ozone climatology from the NIMBUS 4 BUV data (Hilsenrath and Schlesinger 1981). The NOAA GFDL climatology, using data from 1958 to 1973, provides 15-year averages for each month of the year interpolated onto a regular map grid with an approximate resolution of 430 km. The climatology provides profiles of temperature and absolute humidity at 11 standard pressure levels with surface temperatures reduced to sea level according to standard practice. The NIMBUS 4 BUV ozone climatology, averaging satellite measurements from 1970 to 1977, gives the zonal mean total ozone column abundances at latitude increments of 10 degrees for each month of the year. Since there are no satellite data poleward of 81°, due to the orbit of NIMBUS 4, and no data poleward of 67° in the winter, due to the lack of sunlight, values from the London *et al.* (1976) climatology are substituted at these high latitudes. These datasets are combined with topographic height data from the National Center for Atmospheric Research to produce the CLIM MONTHLY dataset that contains the same type of information provided by the TOVS product.

### 6.1.2. ARCHIVE TAPE LAYOUT

Each TV data archive tape has four header files, 12 climatological data files, 12 TOVS monthly data files, and up to 366 TOVS daily data files arranged chronologically. The total number of files on a tape depends on the number of years of data reported. If more than one year of data is present on a tape, then the sequence of TOVS MONTHLY data files and DAILY data files is repeated for each additional year.

**Table 6.1.1. TV Archive Tape Layout.**

FILE	CONTENTS	FORMAT	RECORD LENGTH (BYTES)
1	README file	ASCII	80
2	Table of Contents	ASCII	80
3	Read Software	ASCII	80
4	Ancillary Data Table	ASCII	80
5-16	CLIM MONTHLY Data	Binary	16530
17-28	TOVS MONTHLY Data	Binary	16530
29-394	TOVS DAILY Data	Binary	16530

*Note: The GPC produces archive tapes using IBM standard label format which means that there are label records written before and after each file on the tape. On IBM systems, these labels provide information to the operating system about the name and format of the file and will appear transparent to the user. On non-IBM systems these label records will appear as extra short files surrounding each file listed above and should be skipped by the user. The presence or absence of these files depends on which archive supplies tape copies to the user, as they may either provide an exact copy (labels present) or a modified copy (labels absent).*

### 6.1.3. HEADER FILE CONTENTS

**File 1** is the **README** file that contains ASCII text providing descriptive information about the tape format and contents, similar to what is in this section. The first line of text (80 bytes) gives the ISCCP tape designator code that identifies the contents and version (Table 2.5.12).

**File 2** is the **Table of Contents** file that lists the date or date range of each data file on the tape in ASCII columns defined in Table 6.1.2.

**Table 6.1.2. Table of Contents layout.**

COLUMN	DESCRIPTION
1	File number
2	Data set name
3	Date range (YYMMDD - YYMMDD)

*Note: For CLIM MONTHLY files, the dates are given as 000000; for TOVS MONTHLY files, the beginning and ending dates are given. For TOVS DAILY files, a single date is given.*

**File 3** contains **FORTRAN subroutines** for reading, decoding (see section 2.1.4), and using the

atmospheric data as follows:

Program SAMPLE: Example of how to use these subroutines  
Subroutine TVOPEN: Open a TV file and initialize  
Subroutine TVREAD: Unpack TV data for one latitude band  
Subroutine RDANC: Read ancillary data file  
Subroutine EQ2SQ: Convert equal-area map to equal-angle map

**File 4** contains the **Ancillary Data Table** that lists characteristics of each map grid cell in ASCII columns defined in Table 6.1.3.

**Table 6.1.3. Ancillary Data Table Layout.**

COLUMN	DESCRIPTION
1	ISCCP map grid cell number (1 - 6596)
2	Equal-area latitude index (south-to-north = 1 - 72)
3	Equal-area longitude index (1 - 144)
4	Western-most equal-angle longitude index
5	Eastern-most equal-angle longitude index
6	Map grid cell center latitude in degrees
7	Map grid cell center longitude in degrees
8	Map grid cell area (km <sup>2</sup> )
9	Land cover fraction (%)
10	Topographic altitude (m)
11	Vegetation type (Table 2.5.3)

### 6.1.4. DATA FILE CONTENTS

Each data file contains 12 records of 16530 bytes each, representing complete global coverage. Each record contains a 30 byte prefix followed by data for 550 map grid cells. The last record has the last 120 bytes filled with values = 255 (Figure 6.1). Each map grid cell contains 30 variables (Figure 6.1). See Section 6.1.5. for definitions of the variables. Each variable is coded as a single binary byte with a value from 0 to 255. The value 255 is reserved to represent missing data. Conversion tables are provided in the READ program (Header file 3) to convert these into physical values.

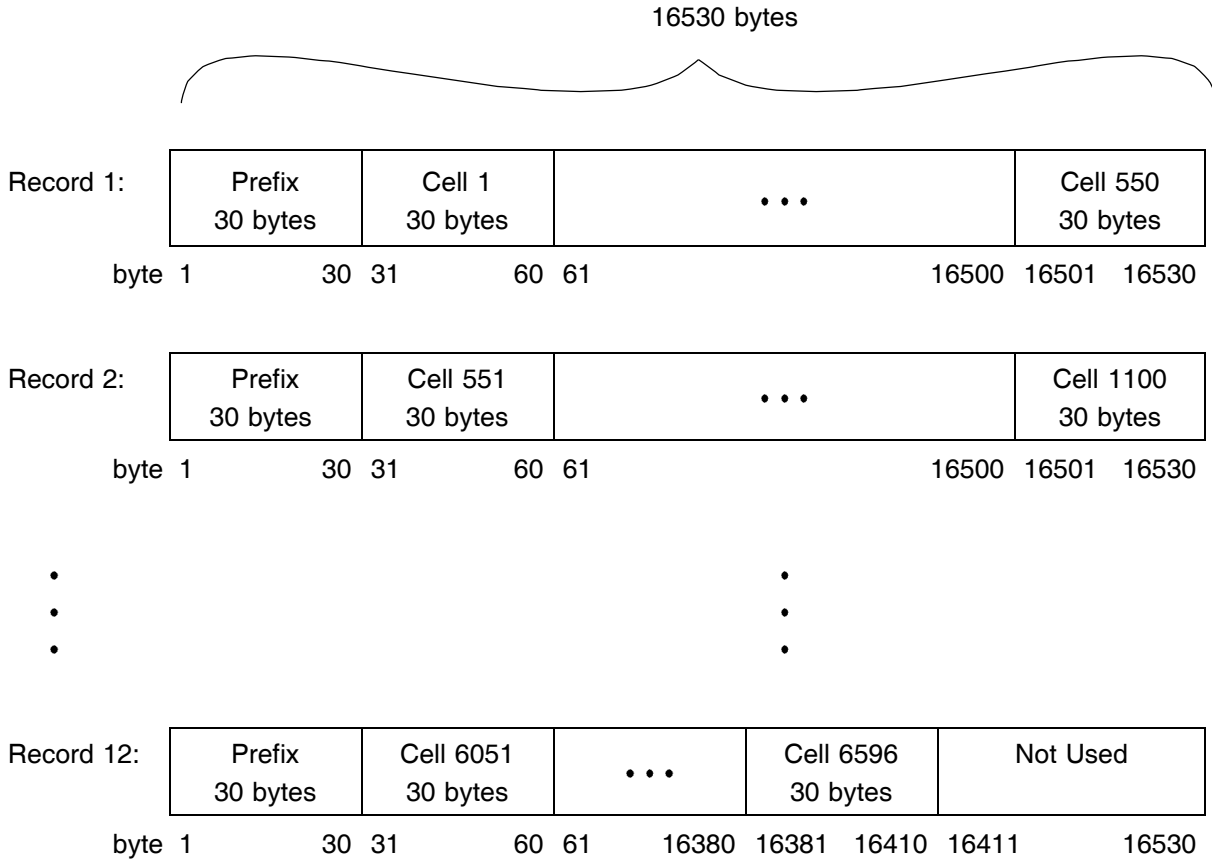


**Figure 6.1.** TV Data File Layout.

**Table 6.1.4. TV Data Record Prefix Layout.**

BYTE No.	DESCRIPTION
1	File number on tape (5-394)
2	Record number in file (1-12)
3	Data type (1 = TOVS DAILY, 3 = TOVS MONTHLY, 4 = CLIM MONTHLY)
4	Year of data (YY = 00 for CLIM MONTHLY)
5	Month of data (MM = 01 - 12)
6	Day of data (DD = 01 - 31; = 00 for CLIM and TOVS MONTHLY)
7	First latitude index in record
8	Last latitude index in record
9-30	255 (no data)

**Table 6.1.5. TV Data Map Grid Cell Layout. Note: Bytes 4-11 are not used (= 255) in the TOVS MONTHLY and the CLIM MONTHLY datasets.**

BYTE No.	DESCRIPTION
1	Latitude Index (1-72)
2	Longitude Index (1-144)
3	Origin Code (0-5) (Table 2.5.8)
4	Original Latitude Index
5	Original Longitude Index
6	Hour of Sounding UTC (0-23)
7	Minute of Sounding UTC (0-59)
8	Quality Code from NOAA TOVS data (Table 6.1.6)
9	Cloud top pressure (PC)
10	Cloud amount (CA)
11	Topographic height (ZS, sea level = 0, 23m interval)
12	Surface temperature (TS)
13	Surface pressure (PS)
14	Tropopause temperature (TT)
15	Tropopause pressure (PT)
16	Precipitable water (PW) for 800 - 1000 mb
17	PW for 680 - 800 mb
18	PW for 560 - 680 mb
19	PW for 440 - 560 mb
20	PW for 310 - 440 mb
21	Atmospheric temperature (T) at 900 mb
22	T at 740 mb
23	T at 620 mb
24	T at 500 mb
25	T at 375 mb
26	T at 245 mb
27	T at 115 mb
28	T at 50 mb
29	T at 15 mb
30	Ozone column abundance

### 6.1.5. VARIABLE DEFINITIONS

The three atmosphere datasets, CLIM MONTHLY, TOVS MONTHLY, and TOVS DAILY, have the same contents except that some variables are not used in the two MONTHLY datasets. Each map grid cell has 30 quantities, each coded as a single byte COUNT value. The READ program contains look-up tables used to convert these count values to physical units. Pressures (P, PS, PT) are given in millibars, temperatures (T, TS, TT) are given in Kelvins, precipitable water (PW) is given in centimeters, total ozone abundance (O3) is given in Dobson units, cloud amount (CA) is given directly in percent, and surface topographic height above mean sea level (ZS) is given in intervals of 23 m. Negative values of ZS are set to zero to be consistent with the TOVS convention. The temperature table is non-linear in a way that resembles the sensitivity of satellite radiometers; i.e., lower temperatures are less precisely specified than higher temperatures. Observation origin codes are given in Table 2.5.8.

The NOAA Code from the TOVS data (Table 6.1.6) indicates the combination of instruments and retrieval algorithm used to obtain the temperature profile and the water and ozone abundances. One of seven possible combinations of instruments is indicated by the first digit of the two digit code number in Byte 8; one of three retrieval algorithms is indicated by the second digit. Since complete temperature and water profiles are required for the ISCCP analysis, only those observations that have this information are retained in the ISCCP dataset. In particular, the microwave-based retrieval used in cloudy locations does not contain water vapor information. If the tropopause parameters are missing, then the profile temperature minimum and corresponding pressure are used. If no minimum is found at pressures  $\geq 30$  mb, then the 30 mb values are used. Also, climatological values of ozone are substituted for missing ozone values in otherwise complete observations.

**Table 6.1.6. NOAA Code Values in TV Data Record.**

CODE	DESCRIPTION
33	all instruments (HIRS/2, MSU, SSU) used, tropopause parameters retrieved, clear observation available, statistical retrieval used
34	all instruments (HIRS/2, MSU, SSU) used, tropopause parameters retrieved, partially cloudy observation available, minimum information retrieval used
43	HIRS/2 and MSU used, no tropopause parameters retrieved, clear observation available, minimum information retrieval used
44	HIRS/2 and MSU used, no tropopause parameters retrieved, partially cloudy observation available, minimum information retrieval used
51	all instruments (HIRS/2, MSU, SSU) used, tropopause parameters retrieved, clear observation available, statistical retrieval used
52	all instruments (HIRS/2, MSU, SSU) used, tropopause parameters retrieved, partially cloudy observation available, statistical retrieval used
61	HIRS/2 and MSU used, tropopause parameters retrieved, clear observation available, statistical retrieval used
62	HIRS/2 and MSU used, tropopause parameters retrieved, partially cloudy observation available, statistical retrieval used
71	No MSU data used, no tropopause parameters retrieved, clear observation available, statistical retrieval used
72	No MSU data used, no tropopause parameters retrieved, partially cloudy observation available, statistical retrieval used
74	No MSU data used, no tropopause parameters retrieved, clear observation available, minimum information retrieval used

### 6.1.6. SPATIAL RESOLUTION AND COVERAGE

To produce the ISCCP version of the TOVS atmosphere data, single soundings are collected into the EQUAL-AREA map grid described in Section 3.1.1; there are 6596 cells in this grid. The TVREAD program supplied with the data can re-map the data into the EQUAL-ANGLE map, also described in Section 3.1.1.

The NOAA TOVS Product has a resolution of  $\approx 2.5^\circ$  latitude-longitude, the NOAA GFDL data have a resolution of  $2.5^\circ$  latitude and  $5.0^\circ$  longitude, and the ozone climatology has  $10^\circ$  latitude resolution. Each TOVS sounding is mapped to the ISCCP Equal-Area grid cell that contains the coordinates of the sounding. If more than one observation is available in a cell, the one closest to the cell-center coordinates is used. The NOAA GFDL and ozone data, having lower resolutions than the ISCCP grid, are mapped such that all ISCCP grid cells with centers within the range of the original data grid cells are filled with the same value. Estimated error of the temperature retrievals is  $\approx 2\text{-}3$  K (McMillin and Dean 1982) and  $\approx 25\text{-}30\%$  for water vapor retrievals (Smith *et al.* 1979).

The typical fractional coverage of the globe provided by TOVS on a given day within a three hour interval is 27%. (Note that observations at 0000 UTC are collected over the time period from 2230 UTC the previous day through 0130 UTC. The last time period for each day extends from 1930 UTC to 2230 UTC.) Although results from two polar orbiters can provide four samples per day, over the first ten years of ISCCP operations only about one quarter of the soundings were processed by NOAA and only half of those have both temperature and humidity information, so that the practical sampling frequency is once per day (the frequency has occasionally fallen as low as 0.7 per day averaged over the globe). With such sparse coverage, no attempt was made to retain information on the diurnal variability of temperature and humidity. All observations for a given day are composited into a DAILY map without regard to time of day. Tests of the variability of temperatures in the first layer show that the error associated with neglecting time-of-day is about 2-4 K, somewhat larger over land. The typical global coverage of the daily composites is about 67%. Original observations are indicated by Origin Code = 1.

Daily map grid cells lacking an observation are filled from nearby original values, as long as the two locations have the same surface types (land, water, coast) and their topographic heights differ by < 500 m. Based on the results of tests that simulate missing data by removing actual data, missing values are filled by nearby observations that are within two grid cells to the east or west (within  $\pm 500$  km). The average error grows with increasing distance and grows more rapidly in the north-south direction than the east-west direction. For  $\pm 500$  km distance, the estimated errors are  $\approx 2$ -3 K in temperature, < 15% for precipitable water and  $\approx 10\%$  for ozone. After nearest-neighbor replication, typical global daily coverage is  $\approx 85\%$ . Replicated observations are indicated by Origin Code = 2.

If no observation is available for a particular location and day and no observation is near enough on that day, then the monthly TOVS values are used if available for that location. The monthly TOVS values are calculated from the daily TOVS data with spatial replications performed where needed; no value is reported if less than five observations are available during the month. The distribution of differences between daily and monthly mean TOVS values of layer one temperatures and humidities and the ozone abundances shows rms errors of  $\lesssim 2$  K,  $\lesssim 0.3$  cm and  $\lesssim 10$  Dobson units, respectively. By filling with the monthly mean values, the daily global coverage is  $\approx 95\%$ ; TOVS Monthly values are indicated by Origin Code = 3.

If no TOVS monthly value is available for a particular location, then the CLIM Monthly values are used, indicated by Origin Code = 4. The distribution of differences between the TOVS daily temperatures, humidities and ozone abundances and the combined NOAA GFDL and ozone climatologies for the same locations and months indicate errors  $\lesssim 5$  K for temperatures,  $\approx 25\%$  for water abundances, and  $\approx 15\%$  for ozone abundances. This last step brings global coverage for each day to 100%.

The differences between the TOVS DAILY and MONTHLY water abundances in layer one include a few larger departures from the monthly mean values. The distribution of these differences with latitude and season reveals a small population (about 2-4% of the total) with values much larger than three standard deviations from the local monthly mean value. Other parameters in the original dataset do not exhibit this behavior. These "anomalous" values are removed with the following procedure: (1) distributions of differences between daily and monthly mean water abundance values for the first three layers in each grid cell are collected for eight latitude zones for each month, (2) a range of variations with respect to the monthly mean is determined by the width of these distributions defined by the differences within  $\pm 5\%$  of the mode frequency (approximately equivalent to three standard deviations), (3) daily values outside the range defined by zonal difference distributions and the local monthly mean are set equal to the nearest value within the range. Observations which have been changed in this way are indicated by Origin Code = 5.



### 6.1.7. VERTICAL PROFILES

In the collection of observations from the NOAA TOVS Product, several criteria are used to check the quality of profiles. Individual values in each profile are checked to see if they are in the allowed range: surface and tropopause pressures ( $\geq 0$  and  $\leq 1200$  mb), temperatures ( $\geq 160$  K and  $\leq 360$  K), precipitable water ( $\geq 0$  and  $\leq 10$  cm), and ozone ( $\geq 0$  and  $\leq 600$  Dobsons). Entire profiles are discarded if (1) the surface and first layer temperatures are missing or out of range, (2) more than two layer temperatures are missing or out of range, (3) a precipitable water value is missing or out of range, (4) surface pressure is out of range, (5) bad header information, (6) out of range latitudes or longitudes, and (7) any profiles that retrieved only stratospheric temperatures. If a profile is retained that has missing values, these values are interpolated from the available values.

The standard pressure levels of the original TOVS product define the 15 temperature layers: 1000, 850, 700, 500, 400, 300, 200, 100, 70, 50, 30, 10, 5, 2, 1, 0.4 mb. The standard pressure levels that define the three water abundance layers are 1000, 700, 500, 300 mb. The surface pressure is calculated from the topographic height above mean sea level and the estimated surface temperature. The ocean surface and all locations with heights at or below mean sea level are assumed to have a surface pressure of 1000 mb; if the height is above mean sea level, then the lower layers are truncated at the surface pressure. In addition to the standard layer temperatures, a surface temperature estimated from a combination of the Channel 8 ( $\approx 11 \mu\text{m}$  wavelength) brightness temperature and the NMC forecast model is also reported; in some datasets, the tropopause temperature is also reported.

The ISCCP version of the atmosphere data is interpolated to two fixed stratospheric layers and up to seven layers in the troposphere that vary at each location and time according to the specific values of the surface and tropopause pressures. The temperature values for the new layers are obtained by linear interpolation in pressure coordinates of the original TOVS values (interpolation in  $\ln P$  over these small pressure intervals does not change the results by more than about 1 K). The two stratosphere layers are fixed regardless of the location of the tropopause and defined by pressures of 70, 30 and 0 mb. The standard boundary pressures defining the tropospheric layers are 1000, 800, 680, 560, 440, 310, 180 and 30 mb. The surface and tropopause pressures modify the actual extent of the lower and higher layers in the troposphere. For example, if the surface pressure is 900 mb, then the first layer extends from 800 to 900 mb; if the tropopause pressure is 100 mb, then the seventh layer extends from 180 to 100 mb with a center at 140 mb. The tropopause temperature and pressure in each profile are taken to be either the originally reported values or the actual minimum temperature and corresponding pressure, whichever has the smaller pressure and temperature. If the tropopause pressure is  $< 30$  mb, the tropopause temperature and pressure are taken from the 30 mb values. The layer-mean temperatures are taken to represent temperatures at the center pressures of each layer.

Interpolation of layer values of precipitable water begins by subdividing each layer into very small layers (2 mb thick) using the formula

$$PW = (g)^{-1} \int Q \, dP$$

where  $Q = RH \times Q_s$  and the relative humidity, RH, for each original layer is assumed to be constant.  $g$  is acceleration of gravity.  $Q_s$  is the saturation specific humidity calculated for the smaller layers with center temperatures interpolated linearly in pressure from the temperature profile.

For temperatures  $\geq 273$  K,

$$Q_s = 0.622 e_0 \times \exp [ ( 2500 / 0.461 ) ( 1 / 273 - 1 / T ) ] / P;$$

for temperatures  $< 273$  K, the ratio in the brackets is (2834 / 0.461).  $e_0$  is the triple point vapor pressure of water. The final values at 2 mb intervals are adjusted so that their sum is equal to the original TOVS layer-mean water amount. Then, the values of PW for the new layers are obtained by summing over the appropriate 2 mb layer values.

The NOAA GFDL climatology reports temperatures on standard pressure levels, regardless of the location of the actual surface in pressure coordinates. To make the form of these temperature profiles compatible with the ISCCP version of the TOVS Product, the surface pressure and temperature for each location are calculated using the hydrostatic formula and the NCAR topographic height above mean sea level (taken to be at a pressure of 1000 mb):

$$PS = P_0 \exp [ - g ZS / (R T_0) ]$$

$$TS = T_1 - (T_1 - T_2) (P_1 - PS) / (P_1 - P_2)$$

where  $R$  is the atmospheric gas constant per unit mass,  $ZS$  is the surface height above mean sea level,  $P_0 = 1000$  mb,  $T_0$  is the temperature at mean sea level,  $P_1$  and  $P_2$  are two adjacent pressure levels, and  $T_1$  and  $T_2$  are their respective temperature values.  $P_1$ ,  $P_2$ ,  $T_1$  and  $T_2$  are selected such that  $P_1 \leq PS \leq P_2$ .

The absolute humidities given in the NOAA GFDL climatology are converted to precipitable water amount using

$$PW = (g)^{-1} \int Q dP$$

where vertical profiles of  $Q$  are first linearly interpolated to much finer pressure resolution and the integral calculated over the ISCCP pressure intervals.

### 6.1.8. TIME AVERAGING

Since the pressures at the surface (PS) and tropopause (PT) vary with time, monthly mean profiles are calculated by projecting each profile onto a standard profile extending from 1000 to 30 mb and then averaging over the month. Monthly averages are calculated for each quantity at each pressure level separately. The column total PW for each day is also averaged and used to adjust the monthly mean column total to insure conservation of total water amount. The average profile is then projected onto a profile that extends from the monthly mean value of PS to the monthly mean value of PT.

## 6.2. ICE/SNOW DATA PRODUCT (IS)

### 6.2.1. OVERVIEW

As part of the ISCCP cloud analysis, information concerning the presence of sea ice and snow aids in separating clear and cloudy scenes (Rossow and Garder 1993a). Although these data are also available from the original sources, the version used in the ISCCP processing (called IS data) is archived with the cloud climatology to document the complete ISCCP data analysis procedure and to provide these data in a more convenient format especially suited to satellite data processing. IS data are also included in the Stage D1 cloud product and summarized in the Stage D2 cloud product.

The **original sea ice dataset** used by ISCCP through 1991 is a digital version of the weekly analyses prepared by the U.S. Navy as paper maps since 1972 and is obtained from the Navy/National Oceanic and Atmospheric Administration Joint Ice Center:

NAVY/NOAA Joint Ice Center  
4301 Suitland Road  
Washington, DC 20390  
USA

The weekly sea ice analyses combine data from shore station reports, ship reports, aerial reconnaissance and satellite image analysis. The satellite-based information constitutes 90-98% of the total and comes from visible/infrared imagery from the operational weather satellites and microwave imagery from experimental and operational satellites (when available). If new data do not arrive during the analysis cycle, older values are retained.

In 1993, NOAA ceased preparation of the digital sea ice cover dataset for an indefinite period; the last year of data available is 1991. The **new sea ice dataset** is based solely on a daily analysis of microwave measurements from the SSM/I on U.S. Air Force DMSP weather satellites using the "NASA Team" algorithm (Cavalieri et al. 1984). These data are prepared by and available from

National Snow and Ice Data Center  
Cooperative Institute for Research in Environmental Sciences  
Campus Box 449  
University of Colorado  
Boulder, CO 80309-0449

The **original snow dataset** is the digital version of the Northern Hemisphere Weekly Snow and Ice Cover Charts prepared by the Synoptic Analysis Branch at National Oceanic and Atmospheric Administration since 1966 (Dewey 1987). These data may be obtained from

NOAA/NESDIS  
Washington, DC 20233  
USA

Snow cover is estimated by daily visual inspection of all available visible band satellite imagery; the presence of snow at a particular location represents the latest cloud-free observation of that site available within the week. Unilluminated portions of the polar regions are assumed to be completely snow-covered; Greenland is always reported as snow-covered. In the ISCCP version, Antarctica is also assumed to be permanently snow-covered; all other Southern Hemisphere land is assumed to be snow-free since there is no information available.

The ISCCP version of the snow/ice data is a merger of the separate snow and sea ice datasets and reports only fractional coverage.

### 6.2.2. ARCHIVE TAPE LAYOUT

Each IS data archive tape has four header files, followed by 73 data files for each year arranged chronologically. The total number of data files depends on the number of years reported. Each data file represents a 5-day period.

**Table 6.2.1. IS Archive Tape Layout.**

FILE	CONTENTS	FORMAT	RECORD LENGTH (BYTES)
1	README file	ASCII	80
2	Table of Contents	ASCII	80
3	Read Software	ASCII	80
4	Ancillary Data Table	ASCII	80
5-77	IS Data	Binary	10400

*Note: The GPC produces archive tapes using IBM standard label format which means that there are label records written before and after each file on the tape. On IBM systems, these labels provide information to the operating system about the name and format of the file and will appear transparent to the user. On non-IBM systems these label records will appear as extra short files surrounding each file listed above and should be skipped by the user. The presence or absence of these files depends on which archive supplies tape copies to the user, as they may either provide an exact copy (labels present) or a modified copy (labels absent).*

### 6.2.3. HEADER FILE CONTENTS

**File 1** is the **README** file that contains ASCII text providing descriptive information about the tape format and contents, similar to what is in this section. The first line of text (80 bytes) gives the ISCCP tape designator code that identifies the contents (Table 2.5.12).

**File 2** is the **Table of Contents** file that lists the center dates of the 5-day intervals for the ISCCP data, the sources of the data and the center dates of the time intervals for the original datasets in ASCII columns defined in Table 6.2.2.

**Table 6.2.2. Table of Contents Layout.**

COLUMN	DESCRIPTION
1	File number on archive tape
2	Data set name
3	Center date of file (YYMMDD)
4	Source of sea ice data
5	Original date of East Sector - Navy Northern Sea Ice data or Start date of NSIDC Northern Sea Ice data (YYMMDD)
6	Original date of West Sector - Navy Northern Sea Ice data or End date of NSIDC Northern Sea Ice data (YYMMDD)
7	Original date of Navy Southern Sea Ice data or Start date of NSIDC Southern Sea Ice data (YYMMDD)
8	000000 or End date of NSIDC Southern Sea Ice data (YYMMDD)
9	Source of Snow data
10	Original date of Snow data (YYMMDD)

**File 3** contains **FORTTRAN programs** and subroutines for reading, decoding (see Section 2.1.4), and using the snow/ice data as follows:

Program SAMPLE	Example of how to use the subroutines
Subroutine ISOPEN	Open an IS file and initialize
Subroutine ISREAD	Unpack IS data for one latitude band
Subroutine RDANC	Read ancillary data file
Subroutine EQ2SQ	Convert equal-area map to equal-angle map

**File 4** contains the **Ancillary Data Table** that lists characteristics of each map grid cell in ASCII columns defined in Table 6.2.3.

**Table 6.2.3. Ancillary Data Table Layout.**

COLUMN	DESCRIPTION
1	ISCCP map grid cell number (1 - 41252)
2	Equal-area latitude index (south-to-north = 1 - 180)
3	Equal-area longitude index
4	Western-most equal-angle longitude index
5	Eastern-most equal-angle longitude index
6	Map grid cell center latitude in degrees
7	Map grid cell center longitude in degrees
8	Map grid cell area (km <sup>2</sup> )
9	Land cover fraction (%)

## 6.2.4. DATA FILE CONTENTS

Each IS data file contains 4 records of 10400 bytes each, presenting one global map of ice and snow cover. Each data record has an 87 byte prefix (Table 6.2.4) followed by data for 10313 map grid cells (Figure 6.2). See Section 6.2.5 for definitions of map grids used. Each map grid cell has one variable represented by a single byte code value (Table 6.2.5).

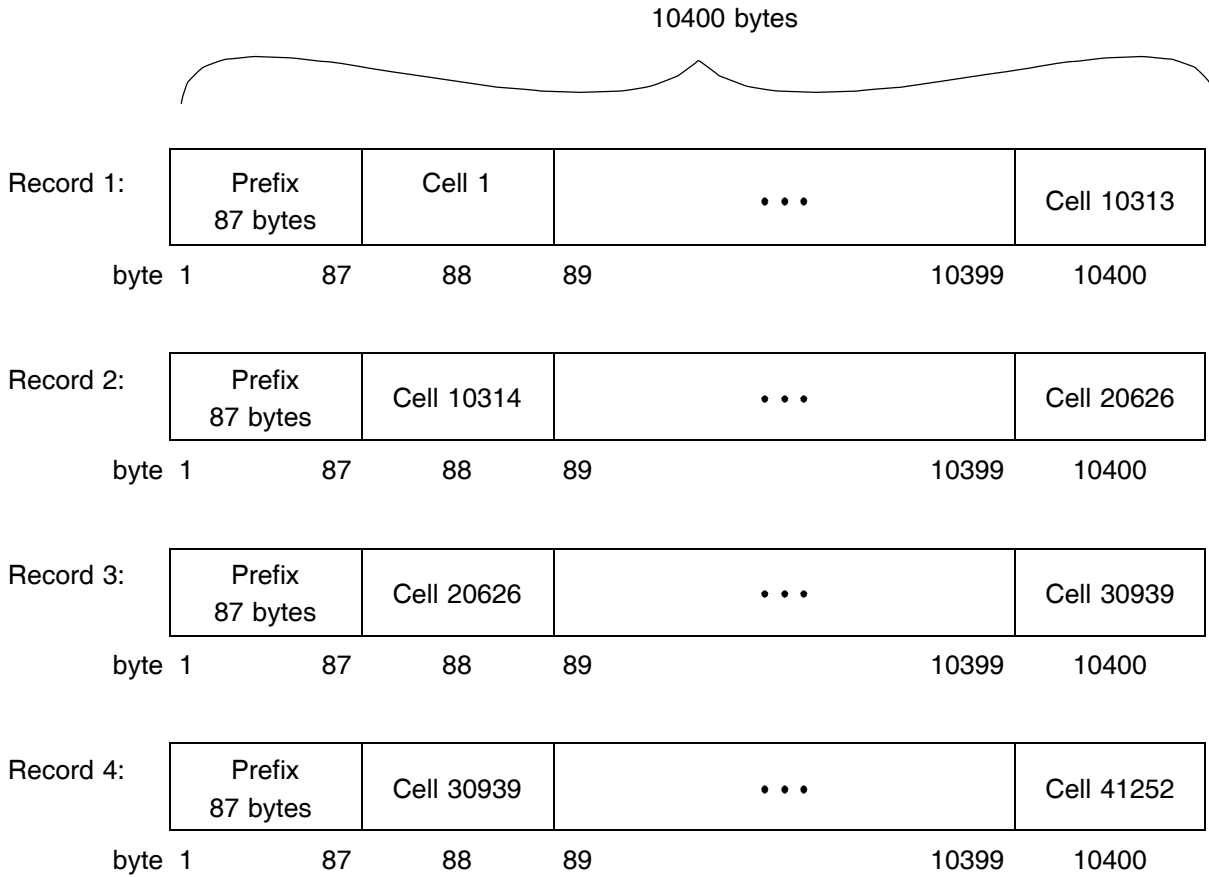


**Figure 6.2.** IS Data File Layout.

**Table 6.2.4. IS Data Record Prefix Layout.**

BYTE #	DESCRIPTION
1	File number on archive tape (5-77)
2	Record number in file (1-5)
3	Data type (ice/snow = 0)
4	First latitude index in record
5	Last latitude index in record
6	Year of dataset (YY)
7	Month of dataset (MM = 1 - 12)
8	Day of dataset (DD = 01 - 31)
9	Sea ice data source code (see Table 2.5.10)
10 - 12	Year, Month, Day of Navy Northern Hemisphere (East) sea ice data or Start Date of NSIDC Northern sea ice data
13 - 15	Year, Month, Day of Northern Hemisphere (West) sea ice data or End Date of NSIDC Southern sea ice data
16 - 18	Year, Month, Day of Southern Hemisphere sea ice data or Start Date of NSIDC Southern sea ice data
19 - 21	All zeros or End Date of NSIDC Southern sea ice data
22	Snow data source code (see Table 2.5.10)
23 - 25	Year, Month, Day of Northern Hemisphere snow data
26 - 87	255 (not used)

*Note:* A value of zero for the three bytes representing the date indicates that no data are available; to date there have been no Southern Hemisphere snow data.

### 6.2.5. MAP GRID DEFINITIONS

The ISCCP ice/snow data are collected into a global EQUAL-AREA map grid with a cell area equal to a 1° latitude/longitude cell at the equator. The cells are formed by equal increments in latitude and variable longitude increments selected to preserve, approximately, the area of the cell and to provide an integer number of cells in a latitude zone. There are 41252 cells in this grid. The position (Greenwich, equator) is a cell corner.

The ISCCP ice/snow data can be converted to a global EQUAL-ANGLE map with 1° increments in latitude and longitude by the Subroutine EQ2SQ contained in ISREAD. There are 64800 map cells in this grid. The position (Greenwich, equator) is a cell corner. The EQUAL-ANGLE version of the data is created by replicating the EQUAL-AREA values within a latitude zone.

## 6.2.6. VARIABLE DEFINITIONS

The ice/snow cover for each map grid cell is given by a one byte classification code (Table 6.2.5):

**Table 6.2.5. Ice/Snow Cover Classification Codes.** All fractions are given in 10% increments.

INTEGER VALUE	DEFINITION
0 - 10	Sea ice fraction for all water cells
20 - 30	Sea ice fraction for water mixed with snow-free land
40 - 50	Sea ice fraction for water mixed with snow-covered land
60	No snow (either snow-free land or water with no sea ice data)
70	Snow-covered land cell (no water)
255	No data

For example, codes 3, 23, and 43 represent 30% sea ice coverage for an all water cell, 30% for a mixed land/water cell with snow-free land, and 30% for a mixed land/water cell with snow-covered land. All land cells over Antarctica are set to code 70.

## 6.2.7. TIME RESOLUTION AND COVERAGE

The ISCCP snow/ice data are presented as a series of datasets representing 5-day intervals and labeled by the center date. Thus, the first dataset, covering the period from 1 - 5 July 1983, is labelled by the date 3 July 1983. The data reported come from the original NOAA snow and Navy/NOAA sea ice datasets, representing 7-day time intervals, with center dates closest to the center of the 5-day interval. The original NSIDC sea ice dataset has daily resolution, so 5-day composites are formed for each 5-day time interval (see Section 6.2.8). The sea ice datasets cover both hemispheres, but the snow data are only for the Northern Hemisphere. In the ISCCP dataset, Antarctica is labelled as permanently snow covered; however, occasional snow cover over the Andes and in southern-most Chile/Argentina are not reported.

## 6.2.8. MERGING ICE AND SNOW DATASETS

The ISCCP version of these two datasets is produced by re-gridding them to a common grid compatible with the ISCCP analysis grids and merging the sea ice and snow information. In addition all land south of 60°S (Antarctica) is labelled as permanently snow covered. The sea ice and snow datasets are mapped to an equal-area grid, equal to 1° latitude/longitude at the equator. The ISCCP grid is lower resolution than the original sea ice grid, so an average fractional cover is calculated from all original sea ice grid cells included within each ISCCP grid cell. The ISCCP grid is approximately the same resolution as the original snow grid, so reported values are either 0 (no snow) or 1 (snow) according to the nearest value in the original grid.

The NSIDC sea ice dataset differs from the Navy analysis (four overlapping years of data, 1988 - 1991, have been examined) in three notable ways: generally lower ice fractions, particularly over the summer Arctic, much more ice along all coastlines, even in summer and at low latitudes, scattered areas of low ice concentration in open ocean even at low latitudes. The first difference is presumably associated with the assumed relation of ice concentration with microwave brightness temperature in the analysis algorithm. The second difference is associated with "side lobe" contamination in coastal scenes where



the much higher emissions from land may produce spurious ice signals. The third difference is the result of surface wind, cloud and precipitation effects on the microwave radiances that have not been completely removed by the "weather" filter. To adjust the NSIDC characteristics to resemble the Navy analysis (we do not know which is more accurate), five tests are applied to produce 5-day composites.

1. To raise the overall concentrations, the maximum value for 5 days is used. In addition, if the maximum concentration is < 75%, it is re-set to 50% and if the maximum is > 75%, it is re-set to 100%.
2. To eliminate spurious low ice concentrations, the maximum value is set to 0 if the **average** value is < 20%.
3. If the number of water grid points is < 65% of the total, the grid cell is changed to "all land" (i.e., sea ice cover is zero).
4. If an ice concentration value is isolated (ie, no nearest neighbors with non-zero concentration), then it is set to 0.
5. If no observations are available in a 5-day period, the average of any available observations in the nearest map grid cells is substituted. If more than 30 map grid cells still lack observations, then the compositing period is extended until all grid cells are filled (the longest extension to date has been to 9 days).

Figures 6.3 and 6.4 illustrate two comparisons of the sea ice cover from the adjusted NSIDC dataset and the Navy analyses. Almost all of the difference between the two datasets in Figure 6.3 occurs in coastal regions, which were not used in the cloud analysis anyway. This is shown by the agreement of the number of map grid cells **totally** covered by sea ice from the two datasets (Figure 6.4).

Finally, the snow and sea ice information are merged. Most locations are either completely land-covered or ocean-covered, so that a single snow or sea ice value can be reported in the merged dataset. To report both snow and sea ice with a single code value in map grid cells with a mixture of land and water, special code values were devised to indicate all combinations of snow/land and ice/ocean cover (Table 6.2.5).

The ISCCP version of these data is arranged in uniform time intervals of 5 days. The original datasets represent different weekly time intervals, each identified by its center date. The merged data are created by reporting the values from the dataset with the center date closest to the center of each 5-day interval. The original time intervals of each data set merged into the ISCCP version are indicated in the prefix of each data record.

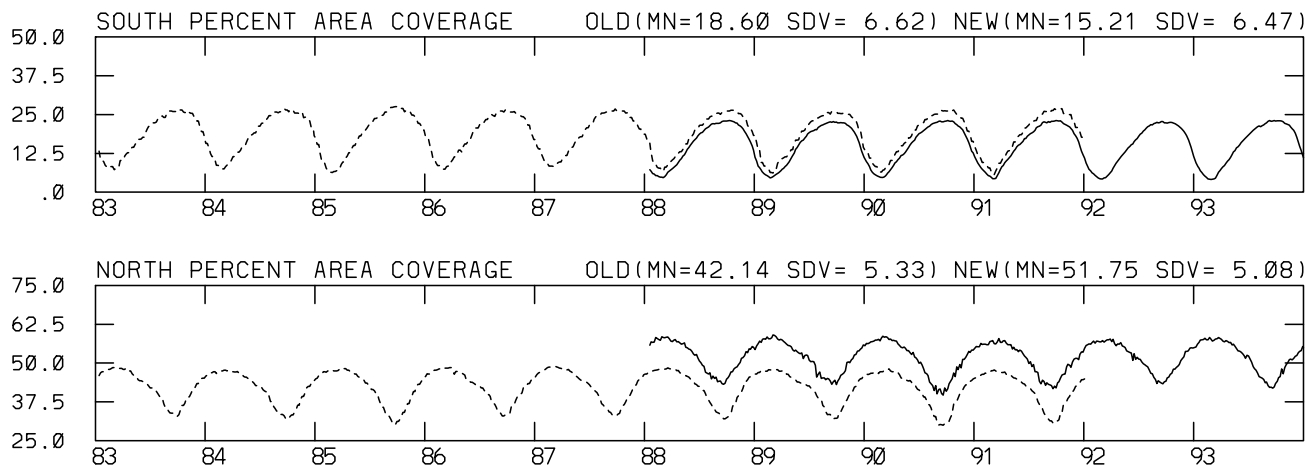


**Figure 6.3.** Monthly mean sea ice cover in the Southern and Northern hemispheres (as fraction of hemispheric area) from the Navy analysis (old, dashed) and the adjusted NSIDC (new, solid) datasets used in the ISCCP cloud analysis.

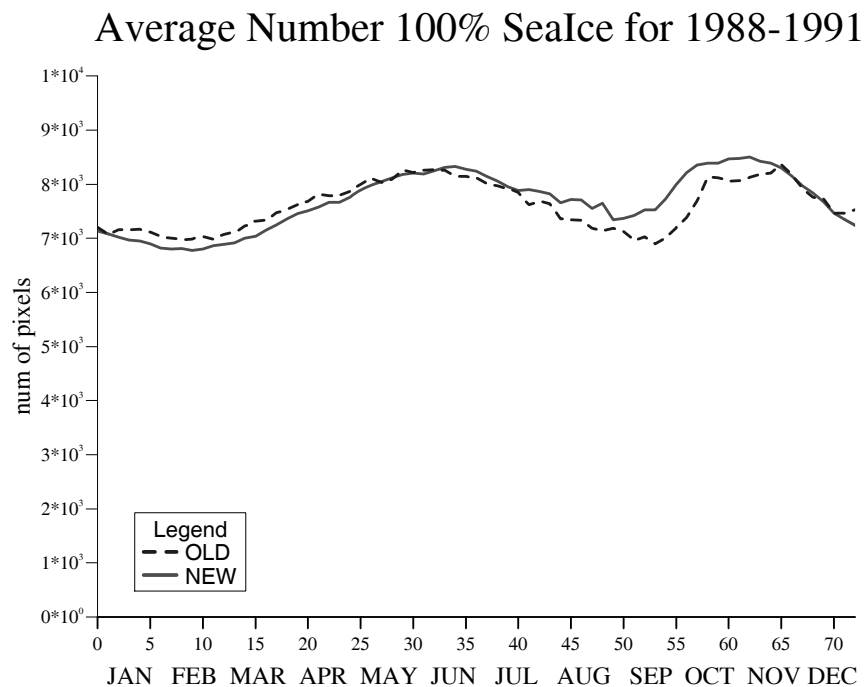


**Figure 6.4.** Average annual cycle of the number of 1° map grid cells totally covered by sea ice in 5-day intervals from the Navy analysis (old, dashed) and adjusted NSIDC (new, solid) datasets used in the ISCCP cloud analysis.